



Norwegian University of
Science and Technology

Surge Tank Atlas for Hydropower Plants

Simon Utseth Sandvåg

Civil and Environmental Engineering

Submission date: June 2016

Supervisor: Leif Lia, IVM

Co-supervisor: Kaspar Vereide, IVM

Norwegian University of Science and Technology
Department of Hydraulic and Environmental Engineering

M.Sc. THESIS IN HYDRAULIC ENGINEERING

Candidate: Mr. Simon Utseth Sandvåg

Title: Surge Tank Atlas for Hydropower Plants

1. Background

Surge tanks are applied in hydropower plants to reduce the pressure forces during acceleration of the water, and to enable speed governing of the turbines. There are two main types of surge tanks; the open surge tank connected to atmospheric air, and the closed surge tank constructed as a closed volume filled with pressurized air. However, numerous variants exist within the two main types. The different variant have different benefits and challenges, and selection of design is dependent on site and project-specific factors. A surge tank atlas, with presentation and comparison of all the different types and variants of surge tanks, would enable hydropower engineers to make easier and improved selection for new hydropower projects.

2. Main questions for the thesis

The thesis shall cover, but is not limited to the main questions listed below.

2.1 Literature and desk study

The candidate shall carry out a literature study of surge tank design and relevant theory.

2.2 Main tasks

The candidate must find available background material such as former studies, textbooks and surge tank design for recent hydropower projects. Related to this material the following must be carried out:

- 1 Systematization and presentation of the different surge tank variants.
- 2 Describe benefits and challenges.
- 3 Description of a method for comparison.
- 4 Comparison of the different surge tank variants.
- 5 Present a case-study selection of the surge tank design.
- 6 Describe additional improvements such as throttles.
- 7 Proposals for future work

3 Supervision and data input

Professor Leif Lia and PhD candidate Kaspar Vereide will supervise and assist the candidate, and make relevant information available.

Discussion with and input from colleagues and other research or engineering staff at NTNU is recommended. Significant inputs from other shall be referenced in a convenient manner.

The research and engineering work carried out by the candidate in connection with this thesis shall remain within an educational context. The candidate and the supervisors are therefore free to introduce assumptions and limitations which may be considered unrealistic or inappropriate in a contract research or a professional context.

4 Report format, references and contract

The master contract must be signed not later than 15. January. The report should be written with a text editing software, and figures, tables, photos etc. should be of good quality. The report should contain an executive summary, a table of content, a list of figures and tables, a list of references and information about other relevant sources. The report should be submitted electronically in B5-format .pdf-file in DAIM, and three paper copies should be handed in to the institute.

The executive summary should not exceed 450 words, and should be suitable for electronic reporting.

The Master's thesis should be submitted within 10th of June 2015.

Trondheim 14. January 2015

Leif Lia
Professor
Department of Hydraulic and Environmental Engineering
NTNU

Abstract

The objective of this master's thesis is to describe the existing surge tank solutions and additional improvements, and to simulate the hydraulic behavior of the surge tanks and how it affects the hydropower plant. The high head hydropower plant Torpa and the low head hydropower plant Åna-Sira are used for the case study, thus the surge tanks can be simulated under different hydraulic conditions. Turbine pressures and mass oscillations after a complete turbine shutdown and turbine regulation parameters from operating the hydropower plant are simulated in the LVTrans software.

The result is a *Surge Tank Atlas*, where the surge tank solutions are described with conceptual drawings, advantages and disadvantages, and documentation from the simulations. This Surge Tank Atlas provides a useful tool to compare different surge tank solutions for both a high head and low head hydropower plant.

Some of the conclusions are valid for both hydropower plants and all the surge tank solutions. Increasing the distance from surge tank to turbine, decreasing the surge tank volume or a strong throttling of the surge tank will increase the water hammer significantly, and to some extent reduce the mass oscillations. An optimal throttling of the surge tank will stabilize the running of the hydropower plant, reduce the surge tank mass oscillations and hence the necessary height and volume of the surge tank.

Other conclusions vary between the open and the closed surge tank, and the high and low head hydropower plant. The closed surge tank shows a better dampening of the water hammer than the open surge tank for both hydropower plant, the closed surge tank can be throttled stronger than the open surge tanks, and the surge tanks at the low head hydropower plant requires more volume than for the high head plant, even though the hydraulic head is one tenth of the high head hydropower plant. Hence there are some significant differences in the hydraulic behavior between the surge tank solutions and the high head and the low head hydropower plant, that will be presented and discussed in the Surge Tank Atlas.

Sammendrag

Hensikten med denne masteroppgaven er å beskrive eksisterende svingesjakter og tilhørende løsninger, og å simulere hydraulikken i svingesjacketten og hvordan den påvirker et vannkraftverk. Høytrykksanlegget Torpa og lavtrykksanlegget Åna-Sira er brukt i et case-studie, slik at svingesjaktløsningene kan simuleres under forskjellige hydrauliske forhold. Turbintrykk etter et fullt turbinavslag og parametre for turbinregulering er simulert i programmet LVTrans.

Resultatet er et *Surge Tank Atlas*, hvor svingesjaktløsningene er beskrevet med konseptuelle tegninger, fordeler og ulemper, og dokumentasjon fra simuleringene. Atlaset gir et nyttig verkty for å sammenligne ulike svingesjaktløsninger, både for et høytrykk- og lavtrykksanlegg.

Noen av konklusjonene er gyldige for alle svingesjaktløsninger, både for høytrykk- og lavtrykksanlegget. Lengre avstand mellom svingesjakt og turbin, mindre svingesjaktvolum eller sterkt strupning av svingesjacketten vil øke turbintrykket fra trykkstøtet, og i litt mindre grad redusere massesvinget. En optimal strupning av svingesjacketten vil stabilisere kjøringen av vannkraftverket, redusere massesvinget og det nødvendige volumet av svingesjacketten.

Andre konklusjoner avhenger av type svingesjakt og om det er et høytrykk- eller lavtrykksanlegg. Et luftputekammer har en mer effektiv demping av trykkstøtet for både høytrykk- og lavtrykksanlegg, luftputekammeret kan strupes sterkere enn de åpne svingesjaktløsningene, og svingesjaktene for lavtrykksanlegget krever større volum enn for høytrykksanlegget, selv om trykket er nesten en tiendedel av høytrykksanlegget. Det er derfor tydelige forskjeller mellom de forskjellige svingesjaktløsningene og mellom høytrykk- og lavtrykksanlegget, som vil bli beskrevet og presentert i atlaset.

Preface

This master's thesis is a part of a master's degree in Hydraulic Engineering at the Department of Hydraulic and Environmental Engineering at NTNU, supervised by professor Leif Lia and Ph.D. Kaspar Vereide. Through the work in my project thesis I was introduced to the surge tank, and how hydraulic transients can be simulated in the LVTrans software, hence it became natural to continue this work in my master's thesis. The work with the thesis has been inspiring, and the process of writing a thesis has been a useful experience. My improved understanding of the hydropower plant, both considering the surge tank design as well as the turbine regulation, would not have been possible without the continuous guidance from both Leif and Kaspar.

To Wolfgang Richter and his colleagues at the Institute of Hydraulic Engineering and Water Resources Management at TU Graz, I am grateful for the good guidance throughout our visit in Graz in February 2016, thanks to the support from my department at NTNU. This week gave me the opportunity to discuss important aspects of my thesis with other professors, Ph.D. students and master students, and I realized that this field of research goes wider than I thought when I started my thesis. The visits to the laboratory at the institute, where we could operate a mini surge tank model and see the Krespa surge tank model during operation, gave a useful understanding of how a complex surge tank works.

I would also thank Bjørnar Svingen for developing and providing the LVTrans software and for answering questions when needed, and co-student Eirik Leknes for day-to-day discussions and critical review on my work with the surge tanks.

Trondheim, June 9, 2016

Simon Utseth Sandvåg

Table of Contents

| | |
|---|-----|
| Abstract | i |
| Sammendrag | ii |
| Preface | iii |
| List of Tables | vii |
| List of Figures | x |
| Abbreviations | xi |
| Symbols | xii |
| 1 Introduction | 1 |
| 1.1 The Surge Tank | 1 |
| 1.2 The Surge Tank Atlas | 2 |
| 2 Theory | 5 |
| 2.1 Basis differential equations for transient flow | 5 |
| 2.2 Water hammer and water column separation | 12 |
| 2.3 Regulation stability | 26 |
| 3 Surge Tank Design | 31 |
| 3.1 The Surge Tank solutions | 35 |
| 3.2 Additional improvements to the Surge Tanks | 43 |
| 4 Method | 49 |
| 4.1 The LVTrans software | 49 |
| 4.2 Hydropower plants for case study | 57 |
| 4.3 Modification of the hydropower plants | 60 |

| | |
|---|------------|
| 5 Surge Tank Atlas | 63 |
| 5.1 The Simple Surge Tank | 65 |
| 5.2 The Two Chamber Surge Tank | 70 |
| 5.3 The Air Cushion Surge Tank | 75 |
| 5.4 The Differential Surge Tank | 80 |
| 5.5 The Throttled Surge Tank | 85 |
| 5.6 The Surge Tank with long chambers | 93 |
| 5.7 The Surge Tank with a "shower head" | 94 |
| 5.8 Parameter vulnerability analysis | 95 |
| 5.9 Comparison and discussion of results | 101 |
| 6 Conclusion and suggestions for future work | 109 |
| 6.1 Conclusion | 109 |
| 6.2 Suggestions for future work | 112 |
| A Construction drawings | A1 |
| B LVTrans script for differential surge tank | B1 |
| C Design and parameters in LVTrans | C1 |

List of Tables

| | | |
|------|---|------|
| 1 | Abbreviations | xi |
| 2 | Symbols, names and units used - part 1 | xii |
| 3 | Symbols, names and units used - part 2 | xiii |
| 3.1 | Comparison of a simulated open and closed surge tank (Sandvåg, 2015). | 33 |
| 3.2 | Key data from selected ACST (Hu et al., 2007). | 39 |
| 4.1 | Key parameters for Torpa and Åna-Sira hydropower plants. . | 58 |
| 5.1 | Simulated and calculated values for the SST at Torpa HPP. . | 67 |
| 5.2 | Simulated and calculated values for the SST at Åna-Sira HPP. | 67 |
| 5.3 | Simulated and calculated values for the 2CST at Torpa HPP. | 72 |
| 5.4 | Simulated and calculated values for the 2CST at Åna-Sira HPP. | 72 |
| 5.5 | Simulated and calculated values for the ACST at Torpa HPP. | 77 |
| 5.6 | Simulated and calculated values for the ACST at Åna-Sira HPP. | 77 |
| 5.7 | Simulated and calculated values for the DST at Torpa HPP. . | 82 |
| 5.8 | Simulated and calculated values for the DST at Åna-Sira HPP. | 82 |
| 5.9 | Values for the singular losses for throttling of the 2CST and the ACST at Torpa and Åna-Sira HPP. | 86 |
| 5.10 | Simulated values for throttling of the 2CST at Torpa HPP. . | 87 |
| 5.11 | Simulated values for throttling of the ACST at Torpa HPP . | 87 |
| 5.12 | Simulated values for throttling of the 2CST at Åna-Sira HPP. | 88 |
| 5.13 | Simulated values for throttling of the ACST at Åna-Sira HPP. | 88 |
| 5.14 | Values for the simulation in the parameter vulnerability analysis. | 97 |
| 5.15 | Simulated regulation parameters for the surge tank solutions at Torpa HPP. | 104 |
| 5.16 | Simulated regulation parameters for the surge tank solutions at Åna-Sira. | 104 |

| | | |
|-----|--|----|
| C.1 | LVTrans data for the SST at Torpa HPP. | C2 |
| C.2 | LVTrans data for the 2CST at Torpa HPP. | C3 |
| C.3 | LVTrans data for the DST at Torpa HPP. | C4 |
| C.4 | LVTrans data for the ACST at Torpa HPP. | C5 |
| C.5 | LVTrans data for the SST at Åna-Sira HPP. | C6 |
| C.6 | LVTrans data for the 2CST at Åna-Sira HPP. | C7 |
| C.7 | LVTrans data for the DST at Åna-Sira HPP. | C8 |
| C.8 | LVTrans data for the ACST at Åna-Sira HPP. | C9 |

List of Figures

| | | |
|------|--|----|
| 1.1 | Turbine pressure amplitudes after a complete shutdown of the turbine. | 2 |
| 1.2 | Sketch of the surges in a upstream and downstream surge tank after a turbine shutdown. | 3 |
| 1.3 | Conceptual design of four basic surge tank solutions. | 3 |
| 2.1 | Free-body diagram for application of the equation of motion. | 6 |
| 2.2 | Control volume for the continuity equation. | 9 |
| 2.3 | Surges and turbine pressure during one period after a turbine shutdown. | 15 |
| 2.4 | Time interval for a water hammer and water wave in a pipeline. | 16 |
| 2.5 | Control volume for finding the change of pressure. | 17 |
| 2.6 | U-tube oscillations. | 20 |
| 2.7 | Conventional tunnel cross section. | 25 |
| 2.8 | Block diagram for a speed feedback governor system. | 27 |
| 2.9 | Results from a Frequency-Response test plotted in a Bode-plot. | 29 |
| 2.10 | Produced power and turbine pressure from a Step-Response test. | 30 |
| 3.1 | Conceptual hydropower plant with upstream and downstream surge tank. | 31 |
| 3.2 | Conceptual designs of open and closed surge tank. | 34 |
| 3.3 | Conceptual design of the SST. | 35 |
| 3.4 | Inclined downstream access tunnel constructed as a SST. | 36 |
| 3.5 | Conceptual designs of the 1CST and 2CST with additional improvements. | 37 |
| 3.6 | Conceptual design of the ACST. | 39 |
| 3.7 | Conceptual design of the water curtain in the ACST. | 41 |
| 3.8 | Conceptual designs the DST. | 42 |
| 3.9 | Conceptual design of a cylindrical DST with inner and outer chamber and a throttle to enhance the differential effect. | 43 |
| 3.10 | Different types of throttles for the surge tank. | 44 |

| | | |
|------|--|----|
| 3.11 | The 4CST surge tank with long chambers at Atdorf PSP. | 46 |
| 3.12 | Two types of 2CST with long lower and upper chambers. | 46 |
| 3.13 | Connection to the upper long chamber at the Krespa surge tank. | 47 |
| 4.1 | Grid for solving single-pipe problems in the MOC. | 52 |
| 4.2 | Unthrottled and optimized throttling of a surge tank. | 54 |
| 4.3 | Hydropower scheme of the Torpa HPP. | 59 |
| 4.4 | Hydropower scheme of the Åna-Sira HPP. | 60 |
| 4.5 | New conceptual design for Torpa HPP. | 61 |
| 4.6 | New conceptual design for Åna-Sira HPP. | 62 |
| 5.1 | Conceptual design of the SST | 65 |
| 5.2 | LVTrans simulations for the SST at Torpa HPP. | 68 |
| 5.3 | LVTrans simulations for the SST at Åna-Sira HPP. | 69 |
| 5.4 | Conceptual design of the 2CST. | 70 |
| 5.5 | LVTrans simulations for the 2CST at Torpa HPP. | 73 |
| 5.6 | LVTrans simulations for the 2CST at Åna-Sira HPP. | 74 |
| 5.7 | Conceptual design of the ACST. | 75 |
| 5.8 | LVTrans simulations for the ACST at Torpa HPP. | 78 |
| 5.9 | LVTrans simulations for the ACST at Åna-Sira HPP. | 79 |
| 5.10 | Conceptual design of the DST. | 80 |
| 5.11 | LVTrans simulations for the DST at Torpa HPP. | 83 |
| 5.12 | LVTrans simulations for the DST at Åna-Sira HPP. | 84 |
| 5.13 | Conceptual throttling of surge tanks. | 85 |
| 5.14 | LVTrans simulations for the throttling of the 2CST at Torpa HPP. | 89 |
| 5.15 | LVTrans simulations for the throttling of the ACST at Torpa HPP. | 90 |
| 5.16 | LVTrans simulations for the throttling of the 2CST at Åna-Sira HPP. | 91 |
| 5.17 | LVTrans simulations for the throttling of the ACST at Åna-Sira HPP. | 92 |
| 5.18 | Different design of long chambers in surge tanks. | 93 |
| 5.19 | Conceptual throttling of surge tanks. | 94 |
| 5.20 | Complete shutdown simulation to investigate of how the placement of a 2CST affects the turbine pressure at Torpa and Åna-Sira. | 96 |
| 5.21 | Worst case scenario simulation of how the mass oscillations change with the volume of the ACST at Torpa and Åna-Sira. | 96 |

| | | |
|------|--|-----|
| 5.22 | Complete shutdown simulation to investigate of how the volume of an ACST affects the turbine pressure at Torpa and Åna-Sira. | 98 |
| 5.23 | Step-Response test to investigate how the produced power changes with PID-parameters for the ACST at Torpa and Åna-Sira. | 98 |
| 5.24 | Step-Response test to investigate how the turbine pressure changes with PID-parameters for the ACST at Torpa and Åna-Sira. | 98 |
| 5.25 | Complete shutdown to investigate how the turbine pressure changes with throttling, and worst case scenario simulation to investigate the mass oscillations with throttling of the SST at Åna-Sira. | 99 |
| 5.26 | Calculation of excavated volume with throttling of the SST at Åna-Sira. | 99 |
| 5.27 | Complete shutdown simulated for very strong throttling of the 2CST at Torpa and Åna-Sira. | 99 |
| 5.28 | Step-Response test to investigate how the produced power changes with very strong throttling of the 2CST at Torpa and Åna-Sira. | 100 |
| 5.29 | Step-Response test to investigate how the turbine pressure changes with very strong throttling of the 2CST at Torpa and Åna-Sira. | 100 |
| 5.30 | Comparison of turbine pressure after turbine shutdown. | 102 |
| 5.31 | Comparison of water levels in the surge tanks. | 103 |
| 5.32 | Comparison of Bode plots. | 105 |
| 5.33 | Comparison of power Step-Response. | 106 |
| 5.34 | Comparison of pressure Step-Response. | 106 |
| 5.35 | Excavation volumes of the tunnels at Torpa and Åna-Sira. | 107 |
| 5.36 | Excavation volumes of the surge tanks at Torpa and Åna-Sira. | 107 |
| C.1 | LVTrans designs for the surge tanks at Torpa HPP. | C10 |
| C.2 | LVTrans designs for the surge tanks at Åna-Sira HPP. | C11 |

Abbreviations

| | |
|-----------------|-------------------------------------|
| HPP | Hydropower plant |
| PSP | Pumped storage plant |
| SST | Simple surge tank |
| 1CST | One chamber surge tank |
| 2CST | Two chamber surge tank |
| 4CST | Four chamber surge tank |
| DST | Differential surge tank |
| 2CDST | Two chamber differential surge tank |
| ACST | Air cushion surge tank |
| mWC | Meter water column |
| m.a.s.l. | Meter above sea level |
| MOC | Method of characteristics |
| PID | Proportional-Integral-Derivative |
| SP | Set point |
| PV | Process variable |

Table 1: Abbreviations

Symbols

| Symbol | Name | Unit |
|---------------|-----------------------------------|-------------------------|
| A_S | Area of pressure shaft | [m^2] |
| A_T | Area of tunnel | [m^2] |
| A_{pipe} | Area of pipe | [m^2] |
| $A_{Chamber}$ | Area of chamber | [m^2] |
| A_{Th} | Thoma area | [m^2] |
| c_w | Velocity of the pressure wave | [$\frac{m}{s}$] |
| v | Velocity of the water wave | [$\frac{m}{s}$] |
| D | Effective diameter | [m] |
| R_H | Hydraulic radius | [m] |
| h_f | Friction loss | [m] |
| f | Darcy-Weissbach's friction factor | [$-$] |
| M | Manning's friction factor | [$\frac{m^{1/3}}{s}$] |
| α_f | Constant in head loss equations | [$-$] |
| h_s | Singular loss | [m] |
| k_i | Singular loss coefficient | [$-$] |
| g | Gravitational acceleration | [$\frac{m}{s^2}$] |
| H | Water head | [mWC] |
| L | Tunnel length | [m] |
| p | Pressure | [mWC] |
| h_{ATM} | Atmospheric pressure | [mWC] |
| Q | Water discharge | [$\frac{m^3}{s}$] |
| V | Volume | [m^3] |

Table 2: Symbols, names and units used - part 1

| Symbol | Name | Unit |
|----------------|--|----------------------|
| t | Time | [s] |
| t_a | Mass inertia time constant | [s] |
| t_r | Reflection time | [s] |
| t_v | Valve closing time | [s] |
| T | Period of harmonic motion | [s] |
| f | Frequency of harmonic motion | [$\frac{1}{s}$] |
| ω | Angular frequency of harmonic motion | [$\frac{rad}{s}$] |
| k | Mass spring constant | [$-$] |
| ρ_w | Mass density of water | [$\frac{kg}{m^3}$] |
| γ_w | Specific weight of water | [$\frac{N}{m^3}$] |
| F | Force | [N] |
| z | Up- and downsurge | [m] |
| m | Mass | [kg] |
| E_W | Water elasticity module | [$\frac{N}{m^2}$] |
| F_{cr}^{air} | Critical area of a air cushion surge tank | [m^2] |
| F^* | Thoma-area in air cushion surge tank | [m^2] |
| n | Polytropic exponent factor | [$-$] |
| V_{AC} | Volume of air cushion surge tank | [m^3] |
| $h_{p,0}$ | Initial pressure in air cushion surge tank | [mWC] |
| σ_3 | Minimum principle rock stress | [MPa] |
| H_2 | Pressure in front of turbine | [mWC] |
| τ_0 | Shear stress | [N/m^2] |
| ξ | Singular loss coefficient | [$-$] |
| C_v | Singular loss coefficient in LVTrans | [$-$] |
| α | Inclination | [m/m] |

Table 3: Symbols, names and units used - part 2

Chapter 1

Introduction

This chapter will introduce the surge tank and some basic surge tank solutions, some central hydraulic aspects of the surge tank and the hydropower plant, and the idea of the Surge Tank Atlas will be presented.

1.1 The Surge Tank

More than 100 years ago solutions and discussions of a possible surge tank solution came up when Raymond D. Johnson (1908) described the first known surge tank in a hydropower plant. Before this time, the problem of large turbine pressure, for example due to high water hammer pressure amplitudes after a turbine shutdown, was solved by a by-pass valve, leading the water in a pipe around the turbine to avoid the possible dangers from high water pressure. This solution is effective in the way that it leads the water away, thus reducing the pressure, but it is not efficient as all of the energy in the water gets lost. Therefore the search began to find a more efficient solution, also able to maintain the head in the water. Especially in hydropower plants with a long tunnel system, this could save a significant amount of time before the turbine can produce energy at maximum water discharge after a shutdown. The main focus in this master's thesis will be the upstream surge tanks, but aspects for the downstream surge tanks will also be mentioned.

The surge tank is a combination of technologies from hydraulic engineering, civil engineering, electrical engineering and mechanical engineering, making them complex solutions that have to be reviewed and planned by engineers from several disciplines to give sufficient control on the water masses to avoid damages on the tunnel system and the electrical and mechanical equipment.

The most interesting case to investigate to understand the hydraulic behavior of a hydropower plant, and the influence of the surge tank, is what happens after a total shutdown of the turbine, where the turbine pressure

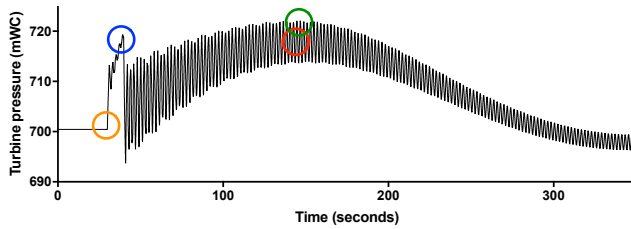


Figure 1.1: Turbine pressure amplitudes after a complete shutdown of the turbine. Orange circle = moment of shutdown. Blue circle = water hammer pressure amplitude. Red circle = mass oscillation pressure amplitude. Green circle = maximum turbine pressure.

- defined as the pressure in front of the turbine valve - suddenly increases. Two main effects affect the turbine pressure - the water hammer and the mass oscillations, and the configuration of the water way and the surge tank decides whether the water hammer or the mass oscillation pressure amplitude has the dominating effect on the turbine pressure. Figure 1.1 shows the turbine pressure after a shutdown. The orange circle marks the moment of the shutdown, the blue circle marks the water hammer pressure amplitude, the red circle marks the mass oscillation pressure amplitude, and the green circle marks the highest pressure, which is a combination of the pressure from the mass oscillation and the water hammer.

1.2 The Surge Tank Atlas

A *Surge Tank Atlas* could provide an overview over the existing surge tank solutions, some additional improvements, and show how different surge tank solutions affect the hydropower plant under different conditions. As an introduction to the surge tank, the concept and placement in a hydropower plant are shown in Figure 1.2, where the surges in the upper and lower surge tank are shown after a complete turbine shutdown, and conceptual designs of the four basic surge tank solutions are shown in Figure 1.3. In the Surge Tank Atlas the four basic surge tank solutions will be simulated for two different hydropower plants, the high head hydropower plant Torpa, and the low head hydropower plant Åna-Sira, both in Norway.

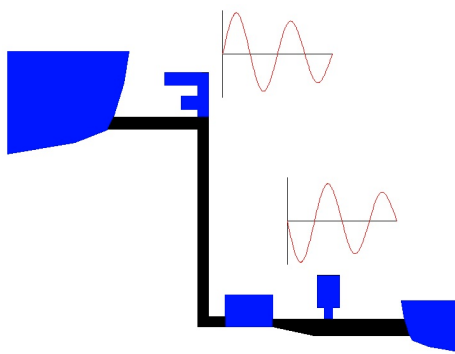


Figure 1.2: Sketch of the surges in a upstream and downstream surge tank after a turbine shutdown.

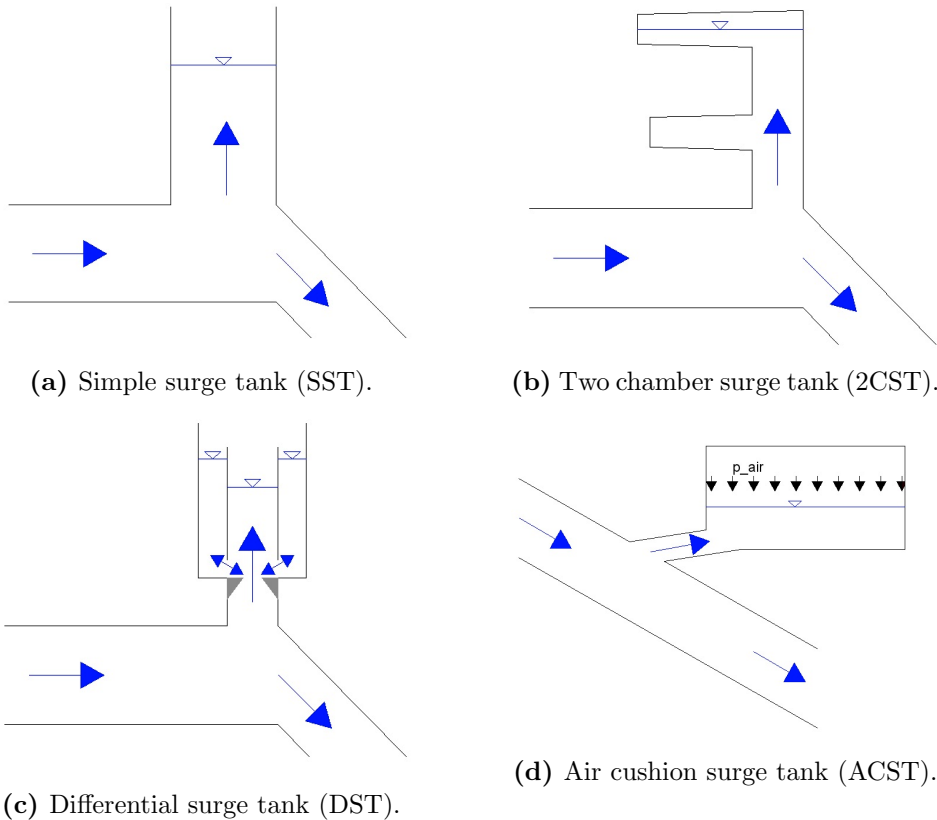


Figure 1.3: Conceptual design of four basic surge tank solutions.

Chapter 2

Theory

This chapter will describe some basic differential equations for the understanding of the water hammer and the mass oscillations that occur in a hydropower plant, and some regulation theory to better understand how the surge tank affects the regulation of the hydropower plant.

2.1 Basis differential equations for transient flow

Transient flow is unsteady flow in a pipeline that is changing over time. To do calculations on the transient flow, for example as it is done in the LVTrans software (Svingen, 2015), the method of characteristics (MOC) is used to solve the equation of motion and the continuity equation at both ends of a pipe section with a given time step dx . The smaller the step is, the more precise and demanding are the calculations.

2.1.1 The equation of motion

The free-body diagram used by Wylie and Streeter (1993) to derive the equation of motion is shown in Figure 2.1. This shows a conical tube filled with a fluid of mass with density ρ . In this thesis the fluid will always be water with the known density ρ_w . The tube has an inclination α , the independent variables are the distance x and the time t , and the other parameters are the velocity v , the pressure p , the cross sectional area A , the shear stress τ_0 and the volume V .

As the forces are shown on the figure, Newton's 2nd law states that the summation of the forces is equal to the mass times the acceleration, as shown in (2.1), where the mass $m = \rho A dx$ and the acceleration $a = dv/dt$.

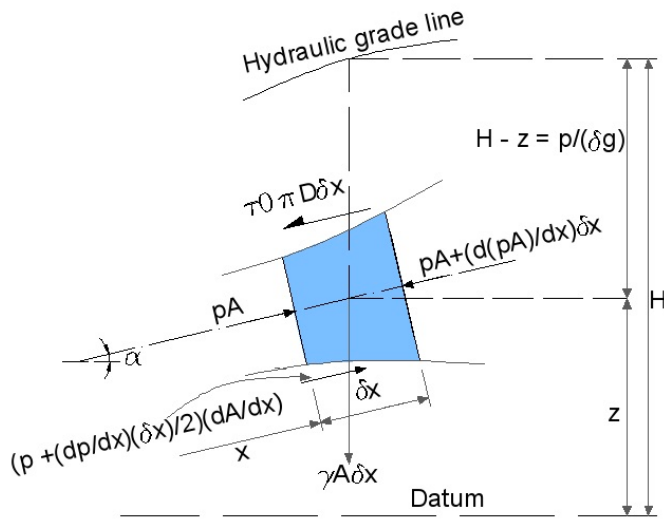


Figure 2.1: Free-body diagram for application of the equation of motion.

$$\begin{aligned}
 pA - \left[pA + \frac{\partial(pA)}{\partial x} dx \right] + \left(p + \frac{\partial p}{\partial x} \frac{dx}{2} \right) \frac{\partial A}{\partial x} dx \\
 - \tau_0 \pi D dx - \rho g A dx \sin a = \rho A dx \frac{dv}{dt} \quad (2.1)
 \end{aligned}$$

By removing the parts of higher order and by simplifying, the following are obtained:

$$\frac{\partial(pA)}{\partial x} + \tau_0 \pi D + \rho g A \sin a + \rho A \frac{dv}{dt} = 0 \quad (2.2)$$

The term dv/dt in Equation (2.2) is the total derivative with respect to the time, that can be described with the partial derivatives as

$$\frac{dv}{dt} = v \frac{\partial v}{\partial x} + \frac{\partial v}{\partial t} \quad (2.3)$$

The shear stress τ_0 is considered to be the same as if the transient flow were unsteady. The value of τ_0 is developed from the Darcy-Weisbach equation as shown in Equation (2.4), where Δp is the friction head loss. The force

balance on the pipe in steady flow is the change in pressure multiplied with the cross-sectional area of the pipe, equal to the shear force, as shown in (2.5). Combining these equations give the τ_0 as shown in Equation (2.7). To ensure that the shear stress always goes the opposite direction of the flow, as the transient flow in a system flows in both directions, an absolute sign is used.

$$\Delta p = f \frac{\rho L v^2}{2D} \quad (2.4)$$

$$\Delta p \frac{\pi D^2}{4} = \tau_0 \pi D L \rightarrow \Delta p = \frac{4\tau_0 L}{D} \quad (2.5)$$

$$\Delta p = \frac{4\tau_0 L}{D} = f \frac{\rho L v^2}{2D} \quad (2.6)$$

$$\tau_0 = f \frac{\rho L v |v|}{8} \quad (2.7)$$

Then, including Equation (2.7) and Equation (2.3) in Equation (2.2), the following is obtained:

$$\frac{\partial(pA)}{\partial x} + f \frac{\rho L v |v|}{8} \pi D + \rho g A \sin a + \rho A \left(v \frac{\partial v}{\partial x} + \frac{\partial v}{\partial t} \right) = 0 \quad (2.8)$$

The cross-sectional area of the pipe is given by $\frac{\pi D^2}{4}$, hence the second term in Equation (2.8) can be given as $f A \frac{v |v|}{2D}$. Then the area A is part of all the terms and can be removed. By dividing all the terms on the density ρ , the equation becomes

$$\frac{\partial p}{\partial x} \frac{1}{\rho} + f \frac{v |v|}{2D} + g \sin a + v \frac{\partial v}{\partial x} + \frac{\partial v}{\partial t} = 0 \quad (2.9)$$

For unsteady flows with low Mach-number (where the Mach-number is the object's speed divided by the speed of sound), the term $\partial v / \partial x$ can be excluded, which is the case for the unsteady flow in a pipe, hence

$$\frac{\partial p}{\partial x} \frac{1}{\rho} + f \frac{v|v|}{2D} + g \sin a + \frac{\partial v}{\partial t} = 0 \quad (2.10)$$

The pressure in a given point in the pipe is given by the difference of the height from the hydraulic grade line to an arbitrary datum H , and the height from the point in the pipe to the same datum z , multiplied with the density and the mass acceleration, hence

$$p = \rho g(H - z) \quad (2.11)$$

The density is assumed constant, hence $\frac{\partial \rho}{\partial x} = \rho$. $\frac{\partial z}{\partial x}$ is equal to the inclination of the pipe, given by $\frac{\partial z}{\partial x} = \sin \alpha$. Including these changes, the final equation of motion is with some simplifications as shown in Equation (2.14).

$$\frac{\partial (\rho g(H - z))}{\partial x} \frac{1}{\rho} + f \frac{v|v|}{2D} + g \sin a + \frac{\partial v}{\partial t} = 0 \quad (2.12)$$

$$g \left(\frac{\partial H}{\partial x} - \sin \alpha \right) + f \frac{v|v|}{2D} + g \sin a + \frac{dv}{dt} = 0 \quad (2.13)$$

$$g \frac{\partial H}{\partial x} + f \frac{v|v|}{2D} + \frac{dv}{dt} = 0 \quad (2.14)$$

2.1.2 The continuity equation

The control volume used by Wylie and Streeter (1993) to derive the continuity equation is shown in Figure 2.2, that shows a moving control volume of length dx . This control volume moves and stretches with the velocity u as the inside surface of the pipe moves and stretches, where v is the velocity of the flow in the pipe. To derive the continuity equation one can start with the principle of conservation of mass, by stating that the rate of mass inflow into the control volume is just equal to the time rate of increase of mass within the control volume, as shown in Equation (2.15).

$$-\left[\frac{\partial \rho A(v - u)}{\partial x} \right] dx = \frac{d'}{dt}(\rho Adx) \quad (2.15)$$

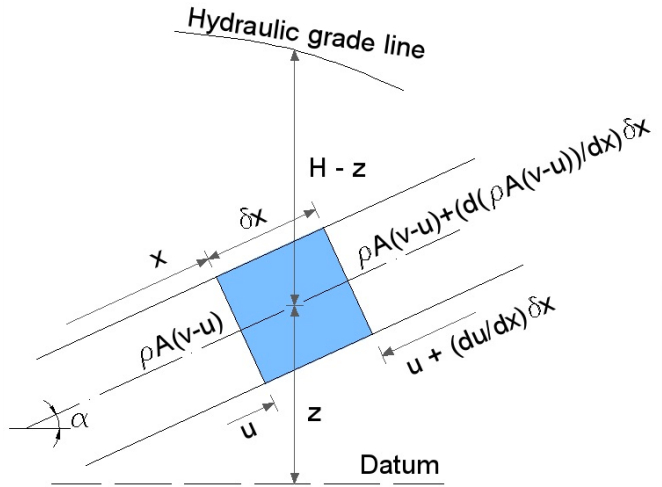


Figure 2.2: Control volume for the continuity equation.

The total derivative with respect to this axial motion of the pipe is given by

$$\frac{d'}{dt} = u \frac{\partial}{\partial x} + \frac{\partial}{\partial t} \quad (2.16)$$

with the time rate of increase of the length dx given as

$$\frac{d'}{dt} dx = \frac{\partial u}{\partial x} dx \quad (2.17)$$

The term $\frac{d'}{dt}(\rho Adx)$ on the right side of Equation (2.15) can be written as $\frac{d'}{dt}(dx)\rho A + \frac{d'}{dt}(\rho A)dx$. By using Equation (2.17), the first term $\frac{d'}{dt}(dx)\rho A$ can be written as $\rho A \frac{\partial u}{\partial x} dx$, and the second term $\frac{d'}{dt}(\rho A)dx$ can be written as $u \frac{\partial(\rho A)}{\partial x} + \frac{\partial(\rho A)}{\partial t}$ by using Equation (2.16).

Including the expansion of the first two terms on the left side of Equation (2.15), so that $\frac{\partial(\rho AV)}{\partial x} = \rho A \frac{\partial v}{\partial x} + v \frac{\partial(\rho A)}{\partial x}$ and $\frac{\partial(\rho Au)}{\partial x} = \rho A \frac{\partial u}{\partial x} + u \frac{\partial(\rho A)}{\partial x}$, Equation (2.15) can be written as

$$\begin{aligned} \rho A \frac{\partial v}{\partial x} + v \frac{\partial(\rho A)}{\partial x} - \rho A \frac{\partial u}{\partial x} - u \frac{\partial(\rho A)}{\partial x} + \\ \rho A \frac{\partial u}{\partial x} + u \frac{\partial(\rho A)}{\partial x} + \frac{\partial(\rho A)}{\partial t} = 0 \end{aligned} \quad (2.18)$$

and by removing equal terms

$$\rho A \frac{\partial v}{\partial x} + v \frac{\partial(\rho A)}{\partial x} + \frac{\partial(\rho A)}{\partial t} = 0 \quad (2.19)$$

The two last terms of the equation above is the total derivative of the density and the area of a pipe with respect to motion of a mass particle, $\frac{d(\rho A)}{dt}$. Then the equation becomes

$$\frac{1}{\rho A} \frac{d(\rho A)}{dt} + \frac{\partial v}{\partial x} \quad (2.20)$$

The term $\frac{d(\rho A)}{dt}$ can be written as $A \frac{d\rho}{dt} + \rho \frac{dA}{dt}$ so that

$$\frac{A \frac{d\rho}{dt} + \rho \frac{dA}{dt}}{\rho A} + \frac{\partial v}{\partial x} = 0 \rightarrow \frac{\frac{dA}{dt}}{A} + \frac{\frac{d\rho}{dt}}{\rho} + \frac{\partial v}{\partial x} = 0 \quad (2.21)$$

For prismatic conduits, meaning that the tube has constant dimensions along its length, some adjustments are made to the equation above. The bulk modulus of elasticity K of a fluid is described in Equation (2.22), with $\Delta = \frac{d}{dt}$. The deformation of the area, that is a function of the pressure, is described in Equation (2.23).

$$K = \frac{\Delta p}{\Delta \rho / \rho} \rightarrow \frac{\frac{d\rho}{dt}}{\rho} = \frac{\frac{dp}{dt}}{K} \quad (2.22)$$

$$\frac{dA}{dt} = \frac{dA}{dp} * \frac{dp}{dt} \quad (2.23)$$

These equations combined put into Equation (2.21) give

$$\frac{\partial v}{\partial x} + \frac{\frac{dp}{dt}}{K} \left(1 + \frac{K}{A} \frac{dA}{dP} \right) = 0 \quad (2.24)$$

This equation can also be written as Equation (2.25), which is the one-dimensional conservation of mass equation for slightly compressible fluids in a prismatic tube of any slope.

$$\rho a^2 \frac{\partial v}{\partial x} + \frac{dp}{dt} = 0 \quad (2.25)$$

where a^2 allows elastic changes in the unsteady equation. a^2 is given as

$$a^2 = \frac{K/\rho}{1 + (K/A)(\Delta A/\Delta p)} \quad (2.26)$$

Equation (2.25) is general for unsteady flow, but it also has to describe steady flow, in this case considered as a special condition of unsteady flow. The steady flow is not changing over time, hence the term $\frac{\partial p}{\partial t}$ in the total derivative $\frac{dp}{dt}$ is equal to zero, leaving the remaining term $v \frac{\partial p}{\partial x}$ from the total derivative, hence

$$\rho a^2 \frac{\partial v}{\partial x} + v \frac{\partial p}{\partial x} = 0 \quad (2.27)$$

In steady flow, one does not consider variations in the area or the density, hence $\frac{\partial v}{\partial x}$ is also equal to zero, meaning that to fulfill Equation (2.29), also $\frac{\partial p}{\partial x}$ must equal zero, which can not be true because the pressure has to increase or decrease with the length in an inclined tube. While the expression with a^2 allows elastic changes in the unsteady equation, it does not admit fluid density or conduit cross-sectional area changes in steady state, giving this inconsistency. The way of solving this is by combining Equations (2.25) and (2.9). Equation (2.9), derived for the equation of motion, is given as

$$\frac{\partial p}{\partial x} \frac{1}{\rho} + f \frac{v|v|}{2D} + g \sin a + v \frac{\partial v}{\partial x} + \frac{\partial v}{\partial t} = 0 \quad (2.9)$$

Equation (2.25) is arranged with respect to $\frac{\partial v}{\partial x}$

$$\frac{\partial v}{\partial x} = -\frac{1}{\rho a^2} \frac{dp}{dt} = -\frac{1}{\rho a^2} \left(v \frac{\partial p}{\partial x} + \frac{\partial p}{\partial t} \right) \quad (2.28)$$

Replacing $\frac{\partial v}{\partial x}$ in (2.9) gives

$$\frac{\partial p}{\partial x} \left(1 - \left(\frac{v}{a} \right)^2 \right) - \frac{v}{a^2} \frac{\partial p}{\partial t} + \rho \frac{dv}{dt} + \rho g \sin \alpha + \rho \frac{fv^2}{2D} = 0 \quad (2.29)$$

With small Mach numbers, $v/a \ll 1$, the term $(v/a)^2$ can be dropped in both steady and unsteady flow. The transport term $v \frac{\partial p}{\partial x}$ is also negligible compared to the other terms, meaning that $\frac{\partial p}{\partial t}$ is also equal to zero. By simplifying, Equation (2.26) becomes

$$\rho a^2 \frac{dv}{dx} + \frac{dp}{dt} = 0 \quad (2.30)$$

To get to the final expression for the continuity equation it can be stated that

$$\frac{dp}{dt} = \rho g \frac{dH}{dt} \quad (2.31)$$

hence the equation can be written as

$$\frac{a^2}{g} \frac{dv}{dx} + \frac{\partial H}{\partial t} = 0 \quad (2.32)$$

The derivation above gives several expressions for the continuity equation, but Equation (2.32) is the one that Wylie and Streeter (1993) use as a simplified equation for the method of characteristics, along with the simplified equation of motion in Equation (2.14).

2.2 Water hammer and water column separation

The water hammer is an elastic wave with a short period of only a few seconds, occurring in a closed system. Though water in general is considered

to be an incompressible fluid, the water will be compressed when it is under very high pressure. In a big water volume, for example a large magazine, the pressure wave from the water hammer propagates through the water with a velocity of $c_w = 1430m/s$ (Guttermesen, 2006), equal to the speed of sound in water. This value is slower in a pipe due to disturbances and transients in the pipe, hence $c_w = 1200m/s$ will be used in this thesis. This is also the value that is being used in LVTrans software. The energy in the water hammer is potentially dangerous if the pressure goes above the designed pressure limit, hence this problem has to be considered as a crucial part of a hydropower plant.

The water hammer can be avoided or drastically reduced by slow regulation of the turbines, but this is not a preferable way to run a hydropower plant, as the plant usually requires a more stable and efficient operation. The preferable solution is a surge tank, constructed close to the junction between the horizontal inlet tunnel and the pressure shaft, so that when the water masses are rejected during a turbine shutdown, the water masses will go straight towards the free water surface in the surge tank, thus protecting the long inlet tunnel and reducing the water hammer. The surge tank also works as a reservoir, shortening the distance the water has to travel when the turbine starts up again. Using the head in the surge tank to accelerate the water masses, the surge tank shortens the water inertia time constant, t_a , significantly improving the turbine regulation. This effect is very important as the hydropower plant, more than just producing the energy, can work as a regulating unit in the power grid when the load can be increased or decreased more rapidly compared to a solution without the surge tank. As described in the author's project thesis (Sandvåg, 2015) this effect gets even more important when considering a hydropower pumped storage, where rapid changes between production and pumping mode require a larger surge tank capacity.

Another problem is the water column separation. This problem is of special interest in hydropower plants where there is a long pressure tunnel downstream the turbine. When the turbine regulator reduces the discharge of the turbine or shuts down the turbine completely, the water is on its way through the outlet tunnel, and a sudden shutdown will create areas under pressure that can cause instabilities in the waterway and damages to the tunnel. To solve this problem a surge tank downstream the turbine can be constructed. Then the surge tank can supply water rapidly to the water flow after a turbine shutdown. This will make the surges in the surge

tank go the opposite way compared to the upstream surge tank. The hydropower scheme of the actual hydropower plant decides whether it has to be constructed an upstream or downstream surge tank, both of them, or no surge tank at all. This will be described more in detail in Chapter 3.

To derive the equation for the water hammer and the reflection time of the water hammer, the situation of a water hammer in an inelastic pipeline, as described in the book *Vassdragsteknikk II* (Guttormsen, 2006) will be used. The evolution of the pressure p through the pipeline, using five different time intervals will be described, shown in Figure 2.4. Figure 2.3 shows how the surges and the pressure evolves during the period. The positive direction is from the magazine towards the turbine.

The different processes occur because of the differences in the water velocity and the pressure wave velocity, as the pressure wave velocity is much faster than the water velocity, $c_w \gg v$. During one period of the surge, one upsurge and one downsurge has occurred, and the pressure wave has travelled twice back and forth between the closing valve and free water surface in the surge tank.

1. $t < 0$ - see Figure 2.4a

The water is flowing through the turbine with a discharge Q and velocity v_w , as during normal running of the power plant.

2. $0 < t < L/c_w$ - see Figure 2.4b

The turbine closes rapidly, and a pressure wave of speed $-c_w$ will be sent the opposite direction as the water velocity v . There is still water entering the pipeline from upstream side. At the end of the this interval the pressure wave reaches the upper magazine. The water stops at the turbine, and starts flowing in the opposite direction.

3. $L/c_w < t < 2L/c_w$ - see Figure 2.4c

The pressure wave is reflected by the magazine, now going towards against the turbine. When the pressure wave again hits the closing valve by the end of this interval, the water hammer is reflected and the reflection time of the water hammer, t_r is reached. The water is flowing towards the magazine in the start of the interval, and the magazine reaches its highest water level, before the water wave starts to travel towards the turbine.

4. $2L/c_w < t < 3L/c_w$ - see Figure 2.4d

The valve reflects the pressure wave, that again starts propagating towards the magazine.

5. $3L/c_w < t < 4L/c_w$ - see Figure 2.4e

When the pressure wave is reflected by the magazine the second time, and starts traveling back towards the valve, so does the water wave. At the end of this interval one period is over, and one upsurge and downsurge have occurred in the magazine, and for the power plant case in the surge tank. This process then continues until the pressure wave is damped, and the mass oscillations will be damped.

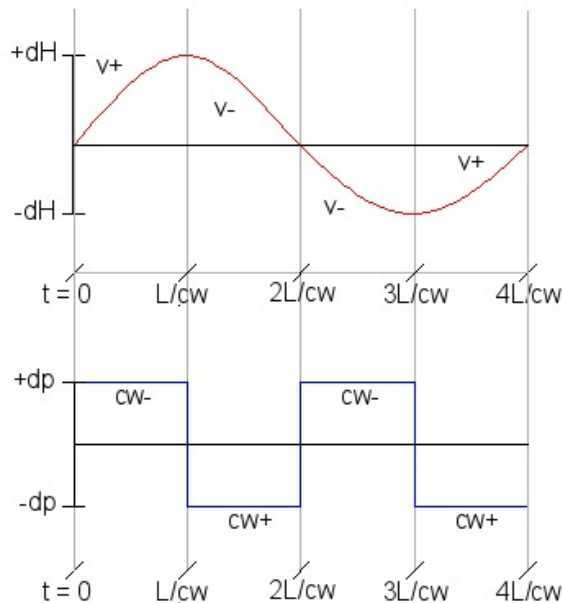
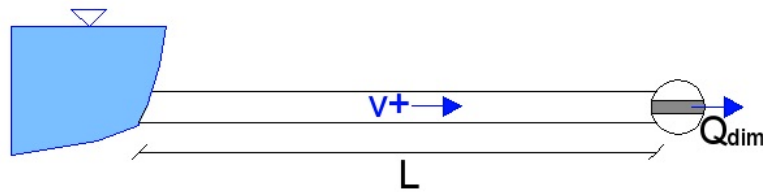
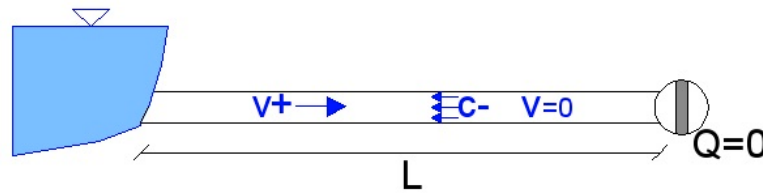


Figure 2.3: Surges (red curve) and turbine pressure (blue curve) during one period after a turbine shutdown.

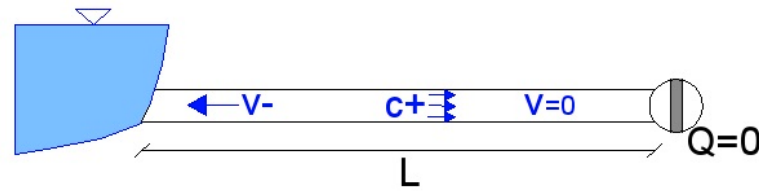
In a pipe that is considered as inelastic, Δp can be found by studying the impulse, which is the force F times the time t , watching an area of the pipe where the pressure wave moves during the time Δt . This control volume is shown in Figure 2.5. To find the pressure increase, measured in meter water column (mWC), the value of Δh will be found. Equation (2.33) gives Δp as function of Δh . The density remains constant, hence the change in pressure is a result of the change in head, Δh



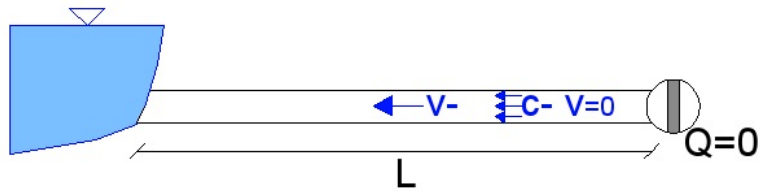
(a) Time interval 2: $t < 0$



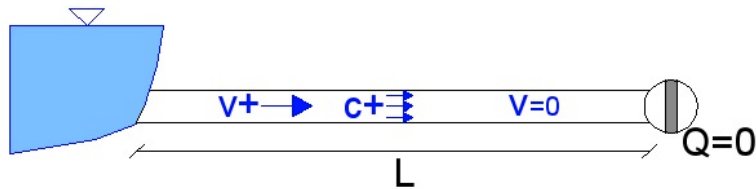
(b) Time interval 2: $0 < t < L/c_w$



(c) Time interval 3: $L/c_w < t < 2L/c_w$



(d) Time interval 4: $2L/c_w < t < 3L/c_w$



(e) Time interval 5: $3L/c_w < t < 4L/c_w$

Figure 2.4: Time interval for a water hammer and water wave in a pipeline.

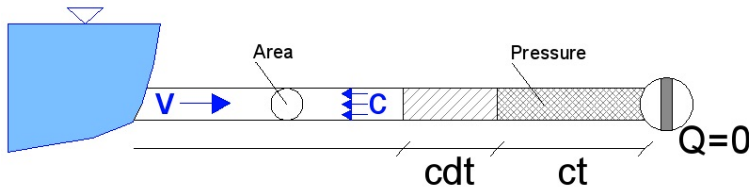


Figure 2.5: Control volume for finding the change of pressure.

$$\Delta p = \rho g \Delta h \rightarrow \Delta h = \frac{\Delta p}{\rho g} \quad (2.33)$$

The above mentioned impulse, Ft , is then equal to the change of momentum, which is mass times the change in velocity, $m\Delta v$, and in this case also the velocity v times the change in mass Δm , $v\Delta m$. This is because the water is considered elastic and its mass can then be compressed during high pressure due to the density changes. Newton's second law states that change in impulse equals the change in momentum, as shown in Equation (2.34).

$$F\Delta t = m\Delta v + v\Delta m \quad (2.34)$$

In the given control volume the force $F = \Delta p A_{pipe}$, the mass $m = \rho A_{pipe} c \Delta t$, and the change in mass $\Delta m = \rho A_{pipe} v \Delta t$ are of interest. Combining these equations with Equation (2.34) above, and then removing A_{pipe} and Δt from both sides, give Equations (2.35), that can be simplified into Equation (2.36).

$$\Delta p A_{pipe} \Delta t = \rho A_{pipe} c_w \Delta t \Delta v + v \rho A_{pipe} v \Delta t \quad (2.35)$$

$$\Delta p = \rho c_w \Delta v + \rho v^2 \quad (2.36)$$

The last expression, ρv^2 , is negligible because the wave velocity $c_w \gg v$. When the shutdown is total, meaning that the turbine closes rapidly, $\Delta v = v$, making the expression $\Delta p = \rho c_w v$. This can then be put this into Equation (2.33), giving the final equation for the pressure increase in mWC as shown in Equation (2.37). This is also known as the Joukowsky pressure (Nielsen, 2015).

$$\Delta h = \frac{\rho c_w v}{\rho g} = \frac{c_w v}{g} \quad (2.37)$$

The velocity of the pressure wave can be written as in Equation (2.38), as a function of the water elasticity module E_w and the density ρ . The velocity is equal to the speed of sound in the liquid.

$$c_w = \pm \sqrt{\frac{E_w}{\rho}} \quad (2.38)$$

2.2.1 Reflection time of water hammer, t_r

The reflection time of the water hammer, t_r , is half the time of a total surge period t . The surge period T is the total time of an upsurge and a downsurge, until the water reaches the initial water level in the surge tank for the second time. During this time the water hammer has traveled two times between the turbine and the surge shaft water surface, with the reflection time as shown in Equation (2.39).

$$t_r = \frac{2L}{c_w} \quad (2.39)$$

The reflection time depends on whether the closing of the turbine is considered as quick or slow, compared with the turbine valve closing time, t_v . When $t_r > t_v$, the closing is considered quick. In this case, the pressure increase is as in Equation (2.37).

When the closing is considered slow, the closing time is longer than the reflection time, $t_r < t_v$. Then, multiplying Equation (2.37) with t_r/t_v , the pressure increase is given as Equation (2.40).

$$\Delta h = \frac{c_w v}{g} \frac{t_r}{t_v} \quad (2.40)$$

This is a simplified equation, but it serves as a useful formula to evaluate how the turbine closing time affects the pressure increase.

2.2.2 Mass oscillations

The surge tank is an excellent technology when it comes to efficiently reducing the water hammer or the water column separation, but at the same time it introduces another problem - the mass oscillations. Differences in water levels between connected free water surfaces - the surge tank and the magazine - make the water flow as a pendulum between the water surfaces until the friction forces in the tunnels dampen the oscillations. With an upstream surge tank these oscillations will go from the upper magazine and the water surface in the upstream surge tank, and for a downstream surge tank the oscillations will go between the lower magazine and the downstream surge tank. The changes in the magazine water level is negligible as the water surface areas and the volumes of the magazines are several orders bigger than in the surge tanks.

During standstill of the turbine, the water level in the surge tank will be equal to the upper magazine level. During normal operation this water level will be equal to the upper magazine level minus the head losses in the inlet tunnel.

The main reason for the construction of the surge tanks is reduction of the water hammer, but the design criteria for the surge tanks is mainly the mass oscillations. The surge tank has to be designed with limits for the surges, defined by construction criteria and maximum allowed water pressure in the system. The worst case scenario for the downsurge is after the shutdown, when the turbine is started up again at the worst possible moment. This is used to design the lower limit of the upstream surge tank.

The pressure created from the surge acts on the water in the inlet tunnel, so the magazine, the inlet tunnel and the surge shaft will work as a U-tube-system. Formulas to be used for the mass oscillations in the hydropower plant tunnel system are then equivalent to the formulas for a U-tube oscillation, where the water flows between the two free water surfaces, as shown in Figure 2.6. If the system has no friction losses, this water pendulum will continue forever, but because of head and friction losses in the tube, the oscillation will be damped and the surges will decrease in a stable system. An oscillation starts when the water level increases or decreases the height z in the surge tank. This force is shown in Equation (2.41). The mass this force has to accelerate is given by Equation (2.42).

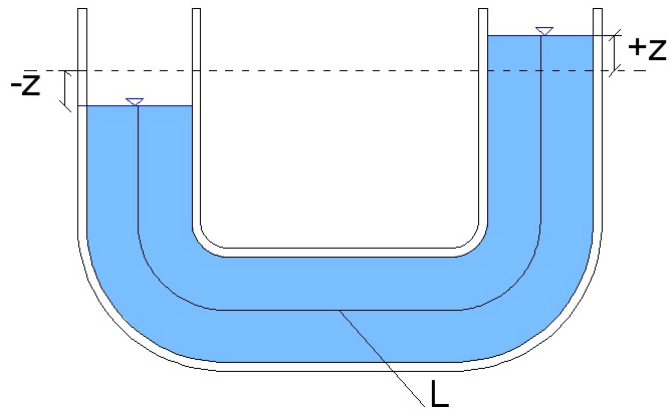


Figure 2.6: U-tube oscillations.

$$F = \rho g A_{pipe} 2z \quad (2.41)$$

$$m = \rho A_{pipe} L \quad (2.42)$$

where L is the tube length between the two water surfaces. Using Newton's second law, equaling the forces $F = ma$, where $a = dv/dt$ and $v = -dz/dt$, the equations above can be combined to the differential equation as shown in Equation (2.43) and Equation (2.44), which is the differential equation for a simple harmonic motion. In addition to using Newton's second law, Hooke's law for a mass on a spring is used to derive the function. One of the easiest ways of describing what happens with the surges in a surge tank is to consider the water string in the surge tank as the spring, and the water flowing out of the surge tank as the mass that drags the water downwards against the turbine. Thus, comparing these equations with the analogy of the simple harmonic motion, the expression multiplied with z , $\frac{2g}{L}$ will be analogue to the spring constant k divided by the mass m . The angular frequency of the harmonic motion is then described as shown in Equation (2.45), analogue to this situation as shown in Equation (2.46).

$$\frac{d^2 z}{dt^2} + \frac{2g}{L} z = 0 \quad (2.43)$$

$$F = m \frac{d^2z}{dt^2} = -kz \rightarrow \frac{d^2z}{dt^2} + \frac{k}{m}z = 0 \quad (2.44)$$

$$\omega = \sqrt{\frac{k}{m}} \quad (2.45)$$

$$\omega = \sqrt{\frac{2g}{L}} \quad (2.46)$$

The frequency $f = \frac{\omega}{2\pi}$, and the time period $T = 1/f$, so the time period can be written as

$$T = 2\pi \sqrt{\frac{L}{2g}} \quad (2.47)$$

As mentioned above, the mass oscillations between the free water surfaces work based on the same concept, but they are more complex, involving the friction in the system, in comparison with the analogous purely mathematical U-Tube solution where the gravity is the only driving force and the damping occurs because the water loses some head for every pendulum. This loss will be stronger in the hydropower plant. To do these calculations and simulations of the mass oscillations in the tunnel system, some assumptions have to be made, all of them considered acceptable through research and experience (Guttorpsen, 2006).

- The changes in the water discharge are considered to be momentary.
- The head losses are considered to be the same for non-stationary as for stationary water flow, which makes the head losses easier to calculate.
- The head loss due to velocity, $\frac{v^2}{2g}$, is considered negligible compared to the friction loss in the inlet tunnel.
- The mass inertia of the water is negligible.
- The water level in the upper magazine is considered constant.

Analogous to Equation (2.41), Equation (2.48) shows the driving force in the oscillation, and as mentioned the friction force R is introduced as shown in Equation (2.49), where α_f is the constant in either Manning's equation ($\alpha_f = \frac{L}{M^2 R_h^{4/3}}$) or Darcy-Weissbach's equation ($\alpha_f = f \frac{L}{2gD}$) where the head loss is calculated.

$$F = \rho g A_T z \quad (2.48)$$

$$R = g A_T h_f = \rho g A_T \alpha_f v |v| \quad (2.49)$$

The mass that travels through the inlet tunnel is given by $m = \rho A_T L$, the resultant of the forces is the driving force F minus the friction force R , and Newton's second law states that $F = ma$, where $a = dv/dt$ is the acceleration. Hence

$$\rho g A_T z - \rho g A_T \alpha_f v |v| = \rho g L \frac{dv}{dt} \quad (2.50)$$

Removing ρA_T from both sides of the equation, and solving with respect to dv/dt this gives

$$\frac{dv}{dt} = \frac{g}{L} (z - \alpha_f v |v|) \quad (2.51)$$

Then the continuity equation can be used, which says that $Q_{TOT} = Q_T + Q_S$, indexed T for tunnel and S for surge tank, giving Equation (2.52). Here the velocity of the surge tank inflow is defined as how fast the water level, dz , rises during a given time interval dt , while the velocity in the tunnel is the inflow velocity v .

$$Q = Q_T + Q_S = v A_T + \frac{dz}{dt} A_S \quad (2.52)$$

Solving Equation (2.52) with respect to v , and then derivating dv/dt , the following are obtained

$$v = \frac{Q}{A_T} - \frac{A_S}{A_T} \frac{dz}{dt} \quad (2.53)$$

$$\frac{dv}{dt} = 0 - \frac{A_S}{A_T} \frac{d^2z}{dt^2} \quad (2.54)$$

Then, combining Equation (2.51) with Equation (2.54) the differential equation for the mass oscillations are obtained, analogue to the one for the U-tube.

$$\frac{dv}{dt} = -\frac{A_S}{A_T} \frac{d^2z}{dt^2} = \frac{g}{L} (z - \alpha_f v |v|) \quad (2.55)$$

$$\frac{d^2z}{dt^2} + \frac{A_T}{A_S} * \frac{g}{L} z - \frac{A_T}{A_S} \alpha_f v |v| = 0 \quad (2.56)$$

This can be solved by partly integration, as it is impossible to solve it as done for the harmonic motion for the U-tube oscillation in the pipe without the friction force. If Equation (2.51) is solved with regards to Δv and Equation (2.53) is solved with regards to Δz , it is possible to find the water levels in the surge tank for given time intervals. The smaller the time step, the more precise the calculations, so it is a matter of computational capacity to make the calculations precise and efficient.

To simplify the calculations of the maximum upsurge and downsurge, Equation (2.57) is useful, for example to design the upper and lower limits of a surge tank. A_S is the area of the surge shaft, $\sum(L/A_T)$ is the inertia of the water masses flowing through the shafts and tunnels, where L is the length and A_T is the tunnel area. Logically a smaller area of the tunnels and the surge shaft, will give bigger up- and downsurge, and longer tunnels will create more inertia that will also give bigger up- and downsurge.

$$\Delta z = \Delta Q \sqrt{\frac{\sum L/A_T}{g A_S}} \quad (2.57)$$

2.2.3 The water inertia time constant, t_a

The mass inertia is a phenomena first stated in Newton's first law, which states that objects, in this case the water masses, tend to keep on doing what they are doing, so the force acting on the water masses needs some time to create the changes in motion of the water masses. The bigger the water masses inertia, the longer will it take to accelerate the water. This time of accelerating the water has its own time constant, called the water inertia time constant, t_a , defined as in Equation (2.58) (Guttorpsen, 2006), where the the water mass inertia is decided based on the tunnels between the closest free water surface upstream and downstream the turbine. Therefore, the installation of the surge tank in a hydropower plant shortens t_a significantly. A design criteria for the time constant is that $t_a < 1$ second.

$$t_a = \frac{Q}{gH_e} \sum (L/A_T) \quad (2.58)$$

2.2.4 Stability of water surface in a surge tank

To ensure that the mass oscillations are stable, it is important that the area in the surge tank is bigger than a given minimum. There exist several definitions of this area and the stability criteria, among others the one defined by Svee (1972), but the common used stability criteria is the one of Thoma (1910), as shown in Equation (2.59).

$$A_{Th} = \frac{LA_T}{2\alpha_f g H_e} \quad (2.59)$$

Here the α is the friction loss coefficient, which give the friction loss h_f when multiplied by the velocity v^2 and divided on twice the gravitational acceleration, $h_f = \alpha_f * \frac{v^2}{2g}$. This friction loss coefficient can be found using both Manning's equation ($\alpha = \frac{L}{M^2 R_h^{4/3}}$) and Darcy-Weissbach's equation ($\alpha_f = f \frac{L}{2gD}$). Using the friction coefficient from Manning's equation, and assuming a conventional tunnel cross section with the hydraulic radius given as $R_h = 0,265\sqrt{A_T}$ and a safety factor of 1,5, the minimum area of the surge shaft A_{min} can be written as

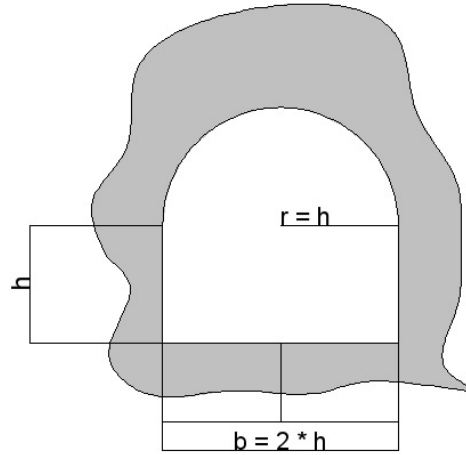


Figure 2.7: Conventional tunnel cross section.

$$A_{min} = 1,5 \frac{LA_T}{2 \frac{L}{M^2 R_h^{4/3}} g H_e} = 0,0125 \frac{M^2 A_T^{5/3}}{H_e} \quad (2.60)$$

In a conventional tunnel cross section the tunnel has the shape and the ratios between lengths and radius as shown in Figure 2.7, where b is the width, and h is half the height, with the same value as the radius r .

If the Thoma-area is not sufficient, the surges could increase uncontrolled and make mass oscillations so big that there will be almost impossible to regulate the system. From now on the Thoma-area is defined as A_{min} in Equation (2.60), including the safety factor 1,5. It is here worth to mention that as far as the author is aware of, there are no scientific reasons for why the safety factor is chosen to 1,5, and that the result might be over dimensioned surge tank as a result of a conservative design criteria.

2.2.5 Stability of water surface in an air cushion surge tank

In an air cushion surge tank (ACST), the design process is different compared to the other solutions of the surge tank. Roald Svee (1972) described a way of calculating the critical area of a surge tank with a compressed air cushion, F_{cr}^{air} to be

$$F_{cr}^{air} = F^* \left(1 + n \frac{P_{z,0}}{\gamma a_0} \right) \quad (2.61)$$

Where F^* is equivalent to the Thoma-area A_{Th} , $P_{z,0}$ is the pressure of the air cushion, a_0 is distance between the surge tank roof and the water level in the surge tank, and γ is the specific weight of the water. n is the polytropic exponent for air, which for an air cushion chamber usually has the value $n = 1, 4$, because the process is adiabatic, meaning that the compression of air happens without heat or mass interactions with the environment. This is not valid for all situations for heat transfer in closed volumes, but for normal transients, such as water hammer and mass oscillations in an air cushion surge tank constructed as a underground rock cavern, the thermodynamics can be regarded as adiabatic (Vereide, Tekle and Nielsen, 2015).

Another way of finding the minimum volume in the ACST, as described by Guttormsen (2006), is shown in Equation (2.62).

$$V_{AC,min} = 1,4 h_{p,0} A_{ekv} \quad (2.62)$$

Where $h_{p,0}$ is the pressure in meter water column (mWC), equivalent to $P_{z,0}$ above, A_{ekv} is equivalent to the Thoma-area A_{min} , and $n = 1, 4$ is the polytropic exponent for air as described above, saying that the process is adiabatic. This value can be in the range of $n = 1 - 1,4$.

2.3 Regulation stability

The surge tank serves for two main reasons; to reduce the water hammer, and to improve the regulation of the power plant. Because of the inertia of the water masses, the water will need time to accelerate from the reservoir towards the turbine, which will give a slow regulation of the power plant. When the surge tank is placed closer to the power plant, it creates a shorter distance from the closest free water surface to the turbine, thus reducing the time the water need to accelerate to the turbine, which gives the power plant a more efficient regulation.

In the power grid there is a continuous need for flexibility, capacity and well working power markets. As said by the Norwegian energy system operator Statnett - "The power system is an art of balance" (Statnett, 2016). The

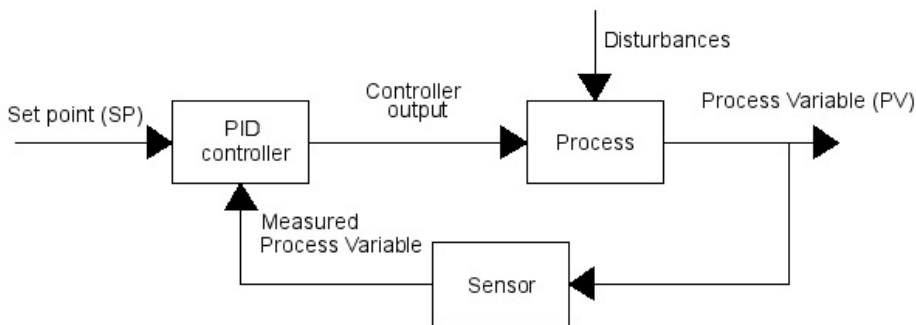


Figure 2.8: Block diagram for a speed feedback governor system.

frequency on the Norwegian power grid is 50 Hz, and the power plants has to deliver a stable frequency that does not oscillate more than 0,1 Hz. Hence a typical Norwegian power plant is then controlled by the need of power to the grid. If the power plant runs with a given discharge and speed, a change of the power need in the grid will give a deficit or a surplus in the actual hydropower plant that will accelerate or decelerate the water masses. This will increase or decrease the rotational speed, thus changing the produced power delivered to the grid from the power plant. The purpose is to maintain the power production at a certain level, decided by the frequency in the power grid. This can be controlled by regulating the discharge to the turbine, maintaining the balance between the produced power and the power need in the grid. The speed is measured by a small electric generator, and this generator communicates through a regulator with a valve in the inlet tunnel, increasing or decreasing the discharge to the turbine. In addition, the generator that delivers power to the grid is equipped with an electrical regulator that measures the voltage on the net, and it is able to regulate the generator (Balchen et al., 2003). A system like this can be shown with the simplified block diagram in Figure 2.8.

The turbine governor measures the rotational speed and/or produced power and closes or opens the guide vanes or nozzles in order to maintain a Set point (SP) (Balchen et al., 2003). The turbine is governed with a Proportional-Integral-Derivative control, shortened PID, that consist of a proportional, an integral and a derivative coefficient (National Instruments, 2016). The PID can compare the Process variable (PV), as shown in Figure 2.8 against a given Set point, while the system tries to reach a steady state situation. In the LVTrans software the PID is, as it is controlled by three

coefficients, controlled by the values P , T_i and T_d , among others. By increasing the proportional gain P , the system becomes faster, but also more unstable, while the integral term is found by setting T_i to a value to reduce the minimal steady state error. In this thesis the derivative term, that can be tuned by changing the value of T_d , will not be investigated further, and the tuning of the PID will be done based on P and T_i . The process on how to tune these values is described further in Chapter 4.

The regulation stability can be tested and quantified through a Frequency-Response analysis and Step-Response tests.

2.3.1 Frequency-Response analysis

To do a Frequency-Response analysis, an Amplitude-Phase-Frequency-diagram (APF-diagram) can be drawn, where the amplitude and the phase angle can be seen in context (Nielsen, 1990). The Frequency-Response analysis runs on an isolated grid, where the frequency is disturbed, starting with 0,001 Hz and ending with 10 Hz. Then the gain amplitude with and without speed feedback and the phase angle can be plotted, with the frequency disturbance as the x-axis in a plot called a Bode-plot (Bode, 1945). There are several criteria that can help to decide the stability of the governor (Nielsen, 1990):

- The Nyquist stability criterion states that the system is stable if the phase angle ($^\circ$) between the impulse and the response is higher than -180° at the frequency where the gain amplitude (h) first crosses the 0-line (the cross frequency).
- Phase margin $\Psi > 45^\circ$, where the phase margin (Ψ) is the margin between the actual phase and -180° at the cross-frequency.
- Gain margin $\Delta h > 2 = 6dB$, where the gain margin (Δh) is the gain value at the frequency where the phase crosses the -180° line.

A Bode-plot is shown in Figure 2.9. The red circle marks disturbances from a local water hammer due to the mass oscillations, where the red crosses mark at which cross frequency this occurs, the gain amplitude and the phase angle. The blue circle marks the cross-frequency where the gain amplitude with (N) and without (A) feedback cross, and the blue cross at which phase

angle this occurs, as mentioned in the Nyquist stability criterion above. The green circle marks where the phase crosses the line of -180° , and the green cross marks the gain amplitude at this point.

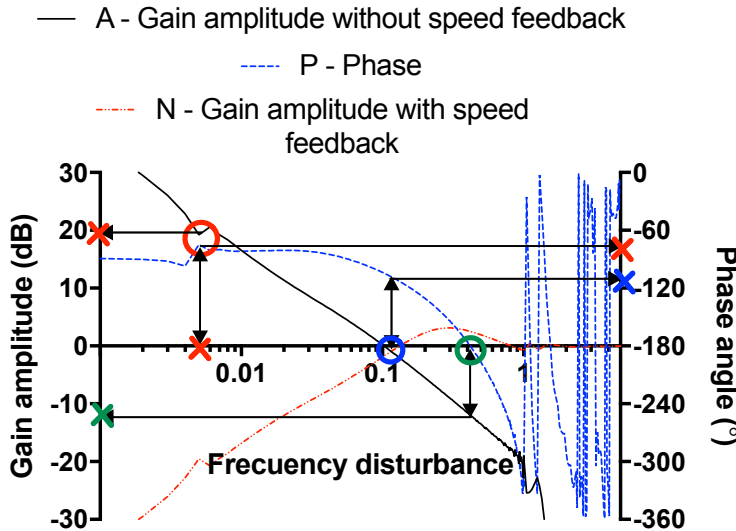
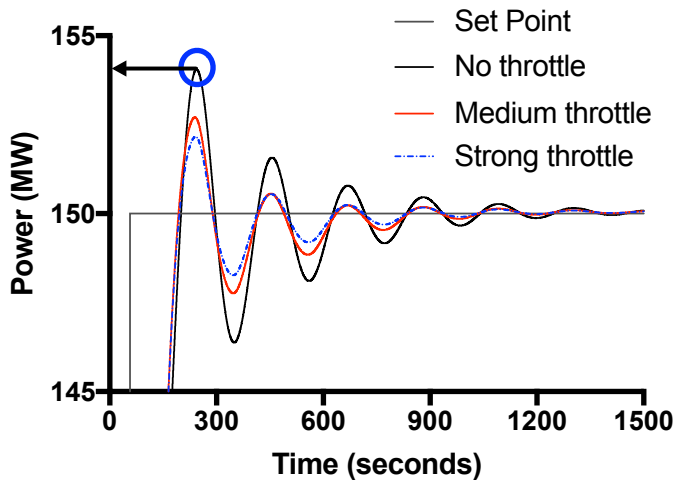


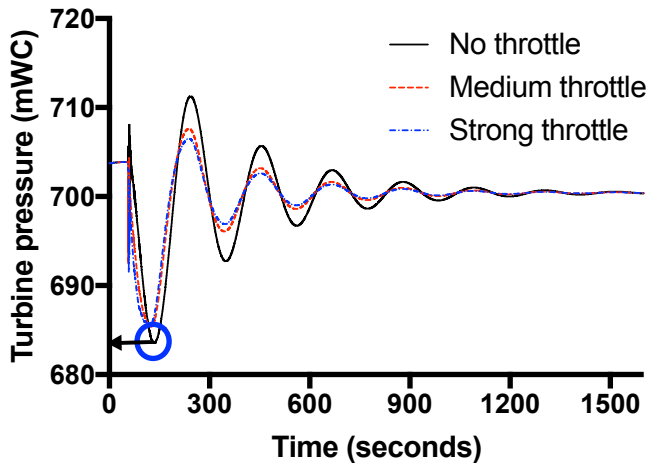
Figure 2.9: Results from a Frequency-Response test plotted in a Bode-plot.

2.3.2 Step-Response test

Governor performance is defined as how accurately the produced power may be controlled and is quantified by how fast the system reaches a steady state after a disturbance (Vereide et al., 2016). With a load acceptance case from 0 to 100 %, two diagrams can be made where one can see how the generated power and the turbine pressure vary, finding the overshoot and undershoot values, and by this evaluate whether the governor performance is sufficient for the demands of the power plant. Figure 2.10 shows the two Step-Response plots for finding the power overshoot and pressure undershoot, zoomed in around the Set point value. Here one can see the Process Variable trying to reach the Set point and a steady state. The blue circles mark the power overshoot and the pressure undershoot. The figures also show how throttling of the surge tank affects the behavior, with reduced over- and undershoot with stronger throttling, until a certain point where the throttling becomes too strong, hence it almost closes the surge tank and removes the function of the surge tank.



(a) Step-Response power plot.



(b) Step-Response pressure plot.

Figure 2.10: Produced power and turbine pressure from a Step-Response test. The blue circles marks the power overshoot and the turbine pressure undershoot.

Chapter 3

Surge Tank Design

This chapter will introduce the concept of the surge tank, and the different surge tank solutions will be described.

The final design of the surge tank depends on several parameters and conditions. For a typical hydropower plant, the optimization process of the surge tank depends on geological and topographical conditions, as well as economic and convenient construction methods, where the main purpose is to create stable hydraulic conditions in the surge tank that ensures a stable and reliable regulation of the power plant, and that requires the least amount of maintenance. The surge tank is constructed to reduce the water hammer, which is its main purpose, but the design criteria for the surge tank is decided by the mass oscillations and how they influence the hydraulic conditions. A conceptual design of a hydropower plant with an upstream and downstream surge tank is shown in Figure 3.1.

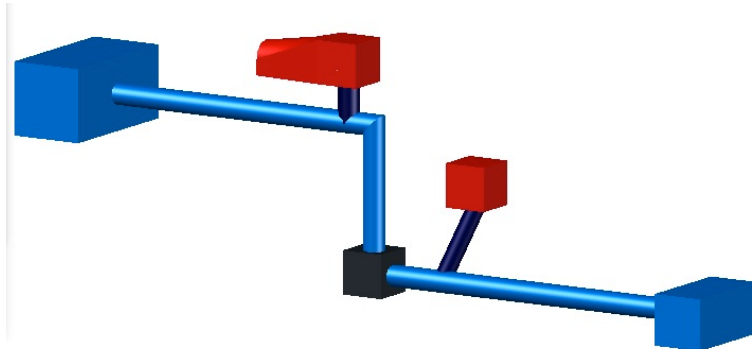


Figure 3.1: Conceptual hydropower plant with upstream and downstream surge tanks.

The topography and the geological conditions are the parameters that decide the water way from the inlet to the outlet and the placement of the power station. Nowadays, especially in hydropower countries like Norway and

Austria, new hydropower projects often consist of improvements of older power plants to improve the capacity or the efficiency, or the construction of new tunnels and power houses constructed close to the existing power plant. Therefore the final design of the surge tank could as well be a result of cost savings during the project, even though the hydraulic conditions will not be optimal.

If an existing tunnel can be used as an access tunnel to the new excavated tunnel, and this access tunnel is placed reasonably close to the power house, this could serve as a surge tank, thus saving costs in excavation works. This is one example where practical conditions give a final design of the surge tank that maybe is not the best when one consider hydraulic conditions, but the most practical solution. The surge tank and the possibility of using additional improvements such as throttles or arrangements to enhance the differential effect, provide a wide option of designs.

In the author's project thesis *Surge Tank Design for Pumped Storage Plants in Norway* (Sandvåg, 2015) the open and the closed surge tank were investigated. In a case study hydropower plant of 10 000 MW, from the Blåsjø reservoir to Jøsenfjorden, with a head of more than 1000 meters, based on the idea from co-supervisor Kaspar Vereide, the results in Table 3.1 were obtained from simulations done in the LVTrans software. The most central results from these simulations is that the time constants are shorter for the ACST, that the total excavated volume is smaller for the ACST, and that there are huge differences in the amplitudes of the water level oscillations in the 2CST and the ACST. In this case the water hammer is bigger for the ACST, but that is more a result of an optimization to find a surge tank solution close to the design pressure, in this case 15 % above the static pressure of 1000 mWc, which equals 1150 mWc, so it is not a conclusion to draw from the project thesis that the water hammer increases with an ACST solution. The big difference in the head loss is a result of a pressure tunnel in the ACST solution with a friction factor that is unnecessary high, in combination with a cross-sectional area of the pressure tunnel that is too small, giving a smaller excavated volume as well.

This chapter will introduce four of the existing surge tank solutions. The surge tanks can be divided into two main categories - the open and the closed surge tank as shown in Figure 3.2. The open surge tank is connected to the atmosphere and therefore usually placed quite close to the surface. The simple surge tank, the two chamber surge tank and the differential surge tank are examples of the open surge tank that will be described. So

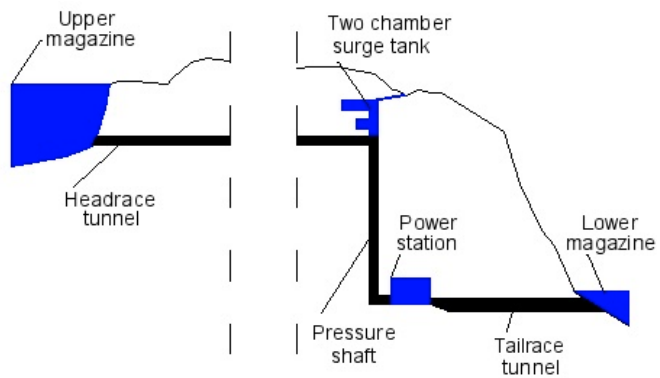
| Parameter | Unit | 2CST | ACST |
|------------------------------------|-------------|-------------|-------------|
| Maximum upsurge | m.a.s.l. | 1045 | 51,2 |
| Maximum downsurge | m.a.s.l. | 818 | 48,6 |
| Maximum turbine pressure | mWC | 1132 | 1150 |
| Reflection time, t_r | s | 1,6 | 0,5 |
| Water inertia time constant, t_a | s | 0,5 | 0,2 |
| Total excavated volume | Mm3 | 4,9 | 1,5 |
| Head loss | m | 12 | 38 |

Table 3.1: Comparison of a simulated open and closed surge tank (Sandvåg, 2015).

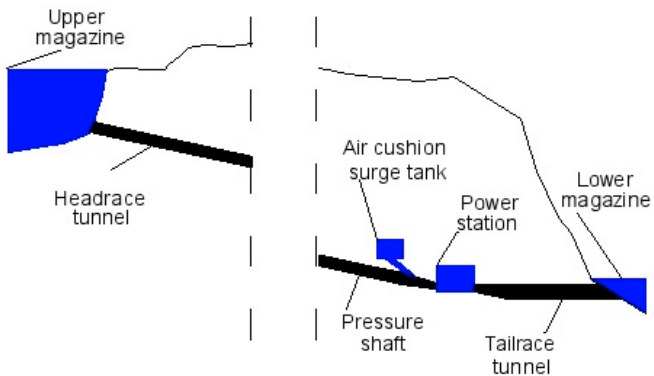
will the closed surge tank, which is a complete different solution that consist of a underground cavern filled with air, creating an air cushion inside the cavern that works as a damping device.

In addition some additional improvements to the surge tank will be described. Throttling of the surge tank, use of a "shower head" solution, and construction of long chambers are the solutions that will be described more in detail.

Finally it is important to mention that complex surge tank solutions may contain elements from all of the above mentioned solutions, and that there exist an unlimited amount of possible solutions in the end. For example the surge tank Krespa in the hydropower plant PSP Obervermunt II in Austria contains a throttle, a long connection shaft leading to three lower chambers, with a riser shaft leading to the upper chamber, that is constructed as a long tunnel to enhance a differential effect from free surface flow, before the flow goes through a "shower head" during outflow to reduce the water fall when the water flows back into the riser shaft.



(a) Open surge tank



(b) Closed surge tank

Figure 3.2: Conceptual designs of open and closed surge tank.

3.1 The Surge Tank solutions

3.1.1 The Simple Surge Tank

The first surge tank made was the simple surge tank (SST) with the purpose of reducing the pressure amplitude from the water hammer and to improve the regulation of the power plant, reducing the distance to the closest free water surface. The SST can be excavated directly as a cylindrical shaft in the rock masses, or it can be built as a steel tank. A conceptual design of the SST is shown in Figure 3.3.

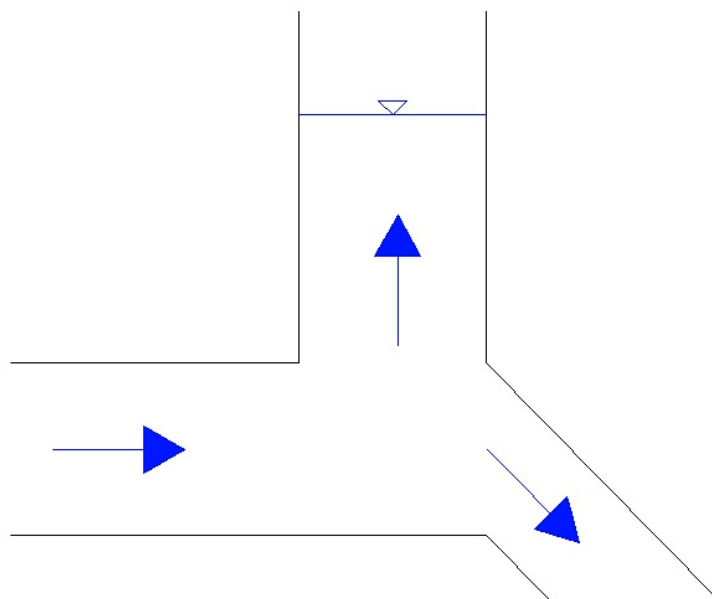


Figure 3.3: Conceptual design of the SST.

The SST is a limited solution, with a damping capacity that will not be sufficient for high head or big discharge, or a combination of the two. If a SST is to be constructed with these conditions, the SST will need to be constructed as a surge tower going far above the surface, or with a very large cross-sectional area, giving very high excavation volumes.

There are though some situations where the SST will be used also for more complex hydropower plants, for example to construct a downstream surge tank. In a typical Norwegian hydropower plant where the power house has a large overburden, there has to be constructed an access tunnel to the power

house, with sufficient area to be able to transport the mechanical equipment into the power house. This access tunnel is then placed as close as possible to the power house, and it may serve as a downstream surge tank. With an inclined surge tank, the water surface area will be bigger, hence the equivalent area A_{ekv} of the SST will be n times bigger if the inclination is $\frac{1}{n}$ in a tunnel with A_T , so $A_{ekv} = n * A_T$. This is illustrated in Figure 3.4.

The downstream surge tank may also be more complex, as for a lot of the Austrian designs, where the headrace tunnel is short compared to the long tailrace tunnel, hence the strongest hydraulic transients occur in the tailrace tunnel.

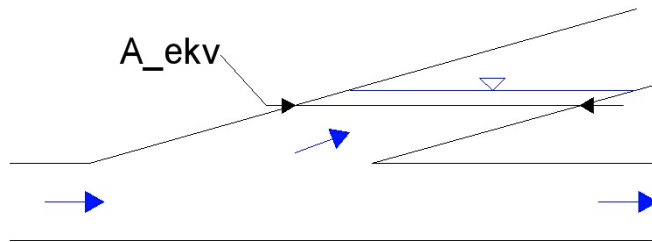


Figure 3.4: Inclined downstream access tunnel constructed as a SST.

3.1.2 The Two Chamber Surge Tank

If the SST is not sufficient, the construction of chambers will improve the damping and reduce water level oscillations. The easiest solution is to construct a single chamber, which is basically a SST with a connection shaft, but this section will mainly focus on the two chamber surge tank (2CST), with both a lower and an upper chamber. A 1CST constructed with a throttle or a solution to enhance the differential effect could therefore be a well suited option to the 2CST, demanding less construction work and excavation volume. Figure 5.19 summarizes some of the conceptual design of the chamber surge tank: The 1CST, the standard 2CST, the 2CST with the lower chamber as part of the inlet tunnel, and a differential 2CST (2CDST).

The 2CST is constructed with a connection shaft with the Thoma-area to ensure stability, a lower chamber designed within the lower surge limit, a riser shaft between the lower and the upper chamber, and the upper chamber designed within the upper surge limit. Then the water level during optimal operation will be in the riser shaft between the chamber, and the oscillations

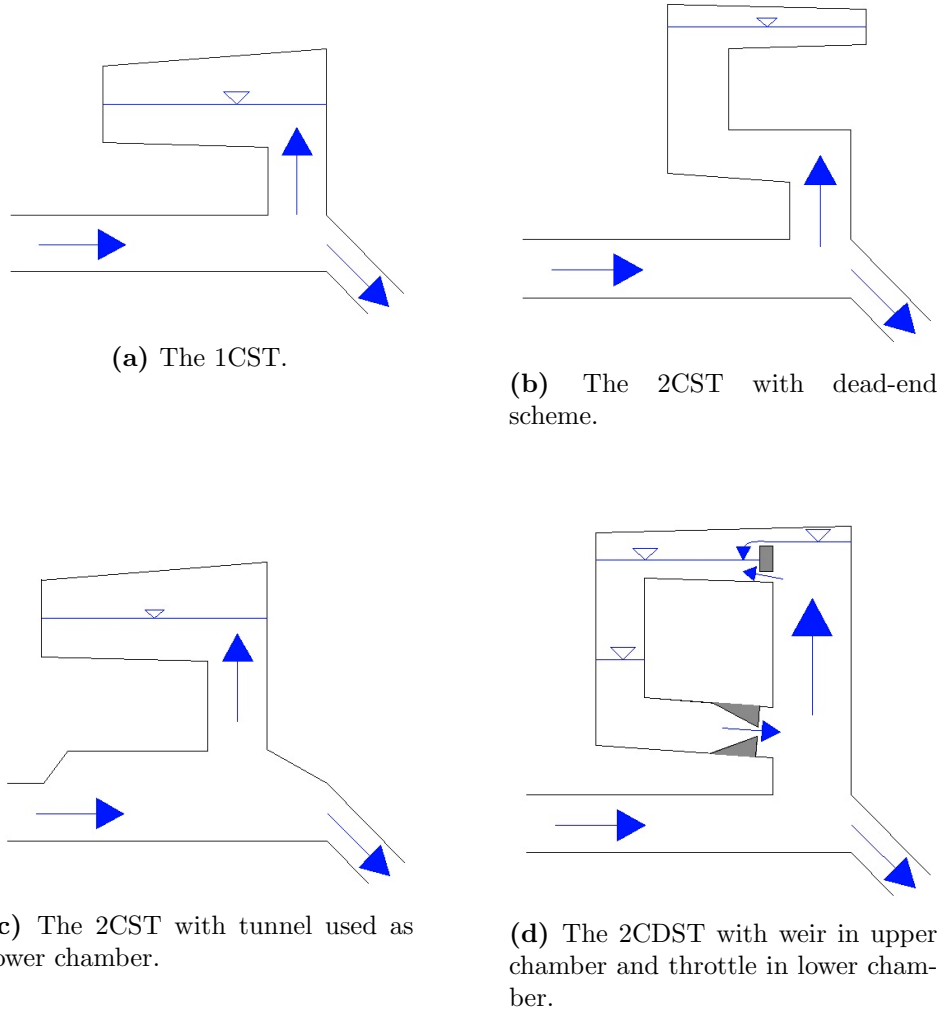


Figure 3.5: Conceptual designs of the 1CST and 2CST with additional improvements.

shall never pass the surge limits during operation of the power plant.

The 2CST provides great flexibility, and therefore there exist a great variety of 2CST designs. As long as the water level oscillations are stable and within the surge limits, the chambers in the 2CST can be constructed in almost any way possible. The easiest way to imagine the 2CST may be that the lower and upper chamber are cylindrical volumes with a larger diameter than the Thoma-area of the connection shaft and the riser shaft. Another way is to image the chambers as tunnels with a large cross-sectional area to ensure a large water surface in the chamber. A slightly different solution is to construct the 2CST with the tunnel working as the lower chamber, increasing the tunnel volume in this part, as shown in Figure 3.5c.

The design of the 2CST is very dependent of the topography. If there is a high overburden the 2CST can be taller, with a smaller cross-sectional area in the chambers, while the cross-sectional area must be bigger if the overburden is lower.

3.1.3 The Air Cushion Surge Tank

In comparison to the open surge tank, the air cushion surge tank (ACST) can be constructed closer to the power house. The construction is done by excavating an underground cavern, and then by filling the cavern with pressurized air. This air cushion works as a damper, limiting the surges down to a magnitude much smaller than in the open surge tank. The total volume of the cavern is normally around 50 % larger than the necessary air volume (Broch, 2000). The ACST is considered the state-of-the-art solution for surge tanks in Norway (Vereide, Lia, Richter and Zenz, 2015), but there exist solutions also in other countries. An overview over some constructed ACSTs is shown in Table 3.2.

The topographical conditions in Norway are favorable for the ACST, and also in general for underground power houses (Broch, 2000). Geological conditions with relatively high horizontal stresses reduces the required overburden. This makes Norwegian conditions more favorable in comparison with conditions in for example the Austrian Alps (Vereide, Lia, Richter and Zenz, 2015). Even though one can talk about high rock strength and quality, the most important parameter is the minimum - not the average - principle stress σ_3 . Hence it is possible to construct an ACST also in weaker geological conditions if the principle stresses are isotropic. The Finite Element

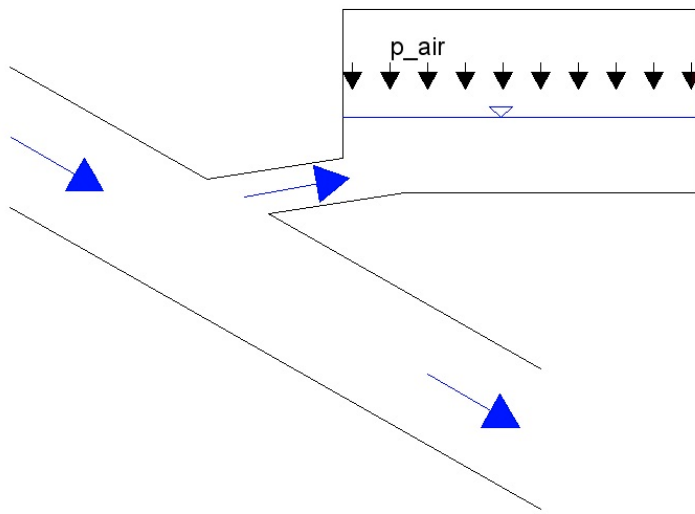


Figure 3.6: Conceptual design of the ACST.

| Project | Year | Capacity (MW) | Head (m) | Discharge (m³/s) | Volume (m³) |
|------------|------|---------------|----------|------------------|-------------|
| Driva | 1973 | 140 | 570 | 38,9 | 6700 |
| Jukla | 1974 | 47 | 180 | 23,5 | 4000 |
| Oksla | 1980 | 200 | 465 | 55,6 | 17000 |
| Sima | 1988 | 520 | 558 | 125 | 6200 |
| Osa | 1981 | 1200 | 200 | 67,5 | 12500 |
| Kvilldal | 1981 | 90 | 537 | 322,6 | 136000 |
| Tafjord | 1982 | 82 | 859 | 13,1 | 2000 |
| Brattset | 1982 | 80 | 272 | 43,5 | 10000 |
| Ulset | 1985 | 37 | 338 | 16,8 | 4800 |
| Torpa | 1979 | 150 | 475 | 48,5 | 12000 |
| Dagangou | 2000 | 20 | 69 | 16 | 4396 |
| Ziyili | 2004 | 130 | 474 | 34 | 11927 |
| Xiaotiandu | 2006 | 240 | 371,4 | 77,7 | 22540 |

Table 3.2: Key data from selected ACST (Hu et al., 2007).

Model (FEM) can be used to map a certain point in the rock cavern, with high precision, given the above mentioned design concept that the internal water pressure does not exceed the minimum principle stress (Edvardsen and Broch, 2002). This requires comprehensive geological studies both before, during and after the construction of the ACST.

For the ACST, a pressure tunnel is constructed from the intake to the power house. Compared to the open surge tank solution, that has a flat or low inclined headrace tunnel, followed by a vertical or steep inclined shaft - usually steel lined due to high internal water pressure - the excavation of the pressure tunnel for the ACST solution requires less excavation volumes as the total water way is shorter. The vertical pressure shaft is a demanding and costly operation, as traditional drill and blast can not perform vertical drilling, and it is therefore preferable from a constructional point of view to construct the tunnel system with an ACST, as long as the inclination of the tunnel is not too steep, making it impossible to excavate with traditional drill and blast. One other consideration is that the life time of a steel shaft is usually lower than the hydropower plant lifetime (Vereide, Lia, Richter and Zenz, 2015), so it can be considered preferable to avoid the steel lined pressure shaft.

When deciding where to excavate the cavern for the ACST, it is important to observe and investigate the zones of water leakage. Openings where water may enter or leave the cavern are also openings where there will be air leakage. The pressurized air cushion will then press the air out of the cavern. To investigate the location of the leakage zones, core drilling and hydraulic jacking tests are normally part of the investigation (Broch, 2000). To reduce the air leakage, a water curtain can be installed. The water curtain is an installation that consists of several bore holes filled with water, raising the pressure around the rock cavern, thus making it harder for the air to leak out of the cavern. Kvilldal was the first power plant to take into use the hydrodynamic control the water curtain gives (Broch, 2000). The water curtain at Kvilldal consisted of 45 bore holes with a 50 mm diameter with a total length of 2,5 kilometers, with about 10 to 20 meters between each bore hole, and a 120 l/min capacity water pump, with a maximum pressure of 5,1 MPa in the water curtain, 1 MPa above the pressure in the ACST. A conceptual design of the water curtain is shown in Figure 3.7.

If the leakage from the ACST is too big, the air cushion has to be refilled more than its planned maintenance. Emptying and refilling the ACST is

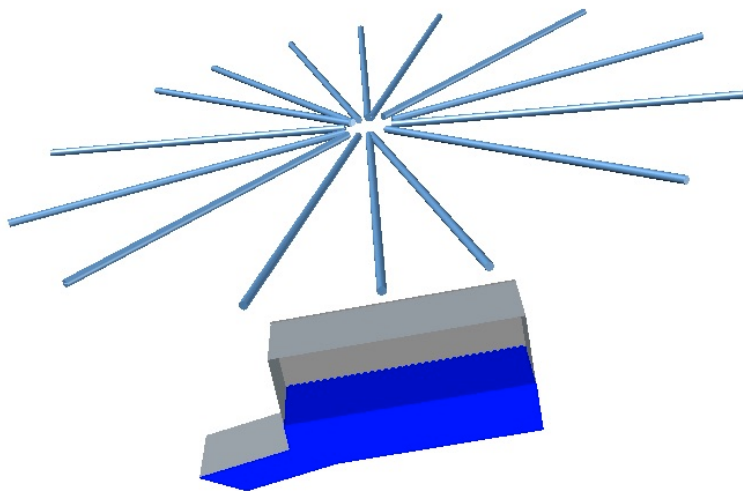


Figure 3.7: Conceptual design of the water curtain in the ACST.

very time demanding. This make take several weeks, and has to be considered when optimizing the surge tank solutions to avoid weeks or months without power production.

To give an idea of the volume of an ACST, the Kvilldal hydropower plant in Norway has a ACST volume of around $110\ 000\ m^3$ (Dahlø, 1988), on a hydropower plant with a capacity of 1240 MW. The shape of the ACST is not that important, and there are a lot of different solutions how to construct the ACST, all from a rectangular cross section to a combination of several cross sections and tunnels combined. The important parameter is the water surface area and wether the air cushion is compressed enough to give the wanted damping effect in the ACST, without too much air leakage. Kvilldal also gives a rough estimate of possible cost reductions in a project when choosing the ACST, and during this project this solution was approximately NOK 30 millions (EUR 3,5 millions) cheaper than a conventional surge tank design (Dahlø, 1988). But one must have in mind the eventual income losses during maintenance of the ACST - at Kvilldal the time of filling the cavern with air was 1 month (Vereide, Tekle and Nielsen, 2015).

3.1.4 The Differential Surge Tank

Charles Jaeger (1954) described various surge tank solutions, among these the differential surge tank (DST). The simplest way of describing the DST is as a combination of a SST with the throttling effect, either combined or separated as shown in Figure 3.8 (Wylie and Streeter, 1993). The focus here will be on the combined solution, with an inner riser that accelerates the water rapidly into a larger outer chamber, thus creating a waterfall from the inner riser with diameter D_2 to the larger chamber with diameter D_1 , limiting the surge in the larger chamber.

In the DST shown in Figure 3.9, the separation of the water masses is done when the water flows from the inner riser to the outer chamber, creating a waterfall that dampens the surge in the outer chamber. In addition, in the lower connection between the inner riser and the outer chamber, a solution is constructed that works as a singular head loss, where the water flows in or out, depending on the water levels in the inner riser and the outer chamber. When the water level in the inner riser is higher than the outer chamber, water flows through the connection into the outer chamber. If the water level is higher in the outer chamber, the opposite happens, and the water flows into the inner riser. After a shut-down the water level in the inner riser and the outer chamber will eventually stabilize.

The DST is in practice any one of the other mentioned open surge tank solutions, where a differential effect is enhanced.

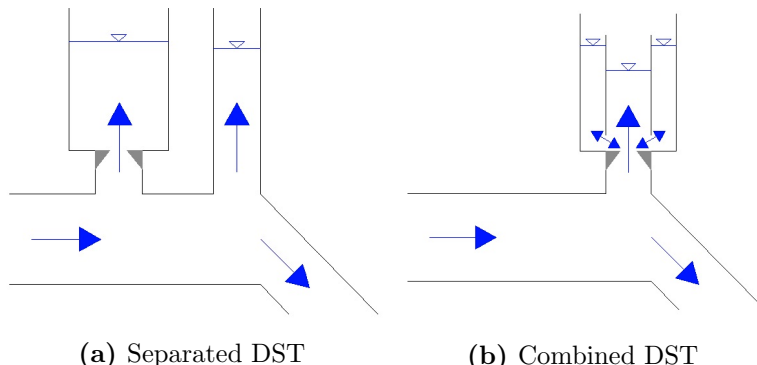


Figure 3.8: Conceptual designs the DST.

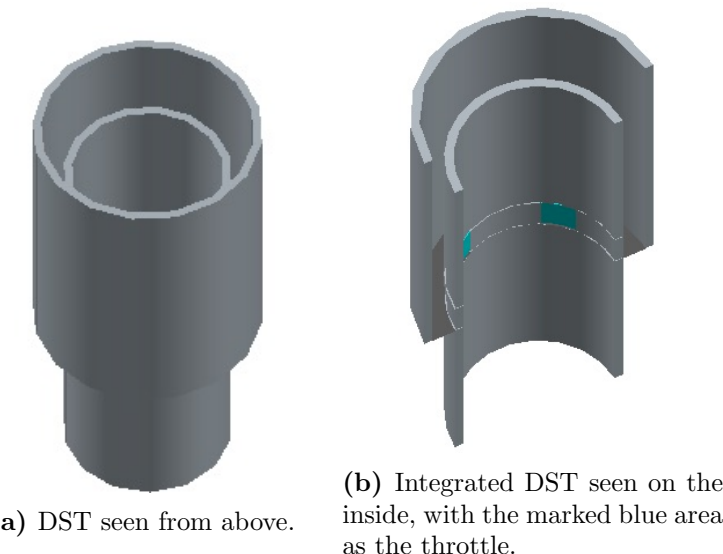


Figure 3.9: Conceptual design of a cylindrical DST with inner and outer chamber and a throttle to enhance the differential effect.

3.2 Additional improvements to the Surge Tanks

A new designed surge tank today will probably consist of additional improvements to the surge tank. They are made to enhance wanted secondary hydraulic effects in the surge tank. In this section different variants of throttling, long chambers and a "shower head" will be described as additional improvements, and relevant examples where the solutions are being used will be shown.

3.2.1 Throttling

Three factors are the most important for the design of the surge tank - the arrangement of the chambers, their geometry, and the design of a possible throttle (Richter et al., 2012). A throttle, or orifice, is a unit to optimize the loss coefficients when the water flows upstream or downstream the surge shaft. It can be connected to the connection tunnel to the chamber, or between chambers, usually it is connected to the connection tunnel. The solution can be a symmetric orifice, an asymmetric orifice or a vortex throttle. Symmetric throttling is a solution with the same intended hydraulic loss in both direction, while asymmetric throttling has different hydraulic

losses during upward and downward flow. The vortex throttle introduces an even bigger hydraulic loss in the outflow direction, and hence it is also called a reverse flow throttle. The flow is forced through a steel torus, and then again through a pipe orthogonally into the lower chamber when emptying the chamber (Gomsrud, 2015). This is a complex construction, and the massive dissipation of energy and the unsteady loss behavior in the throttle makes it difficult to run the hydropower plant smoothly. There were some vortex throttles constructed in Austria in the 1960s, for example the still existing vortex throttle at KW Kaunertal, but because of the complexity and the potential instability of the vortex throttle, the above mentioned orifice throttles are normally being used today (Richter et al., 2012). The design that is shown in Figure 3.10c is inspired by Steyrer (1999).

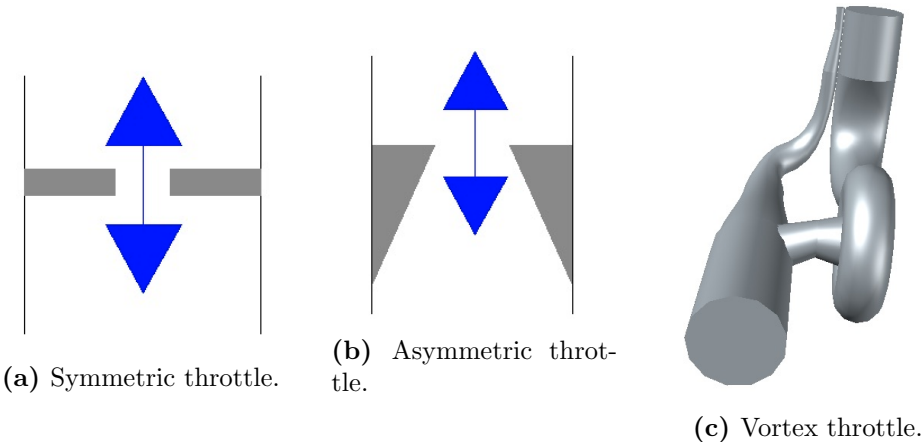


Figure 3.10: Different types of throttles for the surge tank.

As mentioned earlier, the surge tank works as a damping device for the mass oscillations between the surge tank and the reservoir. A throttle could be used to design the upper and lower surge limits, for example to increase the loss coefficient before reaching the upper chamber, thus lowering the area of the upper chamber, but on the other hand this will create a larger water hammer in front of the turbine after a shutdown, as the throttle slows down the water masses. Therefore the throttle has to be optimized to find the optimal ratio between the pressure amplitudes from the water hammer and the mass oscillations, so the throttle does not increase the turbine pressure so that it goes above the design pressure for the water way.

The decision whether it is necessary to install a throttle depends on the costs of the throttle compared to the cost savings of constructing the surge tank.

The throttle limits the water level oscillations in the surge tank, hence it reduces the necessary volume of the surge tank. The cost of the throttle can be divided into the construction of the throttle and the steel and concrete used, in addition to eventual model tests to simulate the hydraulic losses through the throttle, while the geological conditions decide the excavation costs.

3.2.2 Long chambers

A long chamber is a free surface flow tunnel, where the water flows like a wave when entering the chamber, driven by the length and the inclination of the tunnel. This leads to a dampening of the mass flow, thus a significant amount of excavation volume can be saved constructing the chamber as a longer tunnel. But on the same time as dampening the mass flow, a massive waterfall can be generated during outflow, with the danger of air entrainment into the connection shaft and the hydraulic system (Richter et al., 2012). A combination of 1D- and 3D-numerical simulations and physical model testing should be done to investigate the effects of such a waterfall. The eventual inclination of the long upper chamber has to be modified in a way that ensures that the chamber is never completely filled so that pressurized flow occurs, and to optimize the waterfall. An example of a surge tank with long inclined chambers, and a very complex design, is the surge tank at Atdorf PSP in Germany (Richter et al., 2014), as shown in Figure 3.11, which is actually four long chambers, creating a 4CST. There are two connections to the lower chambers from the tailrace tunnel and a connection shaft to the upper chamber. A model of this surge tank were constructed at the Institute of Hydraulic Engineering and Water Resources Management at TU Graz, Austria, where the hydraulic effects and parameters such as the inclination and inside roughness of the longer chambers were investigated to optimize the flow and to avoid pressurized flow in the long chambers (Richter et al., 2014).

As for the lower chamber this can also be constructed as a long chamber. The effect of the long chamber depends on whether the chambers, if the solution is constructed as a two chamber surge tank, is designed as a dead end or a flow through solution. The conceptual difference of the two mentioned solutions is shown in Figure 3.12. The dead-end scheme gives a direct water hammer response of the main shaft, but the disadvantage of this is that there will be no waterfall damping when the water flows from the upper chamber, and there is more likely that air can be entrained into the tunnel system,

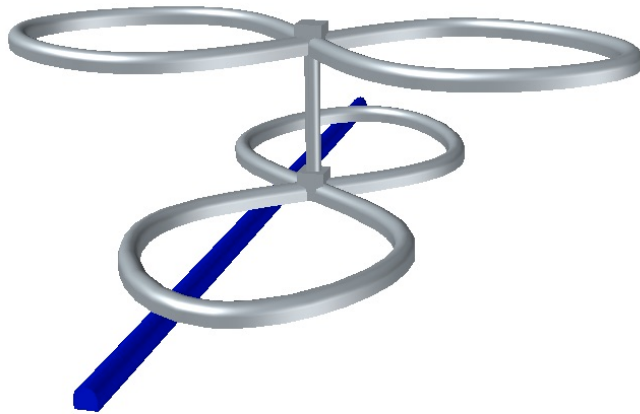


Figure 3.11: The 4CST surge tank with long chambers at Atdorf PSP.

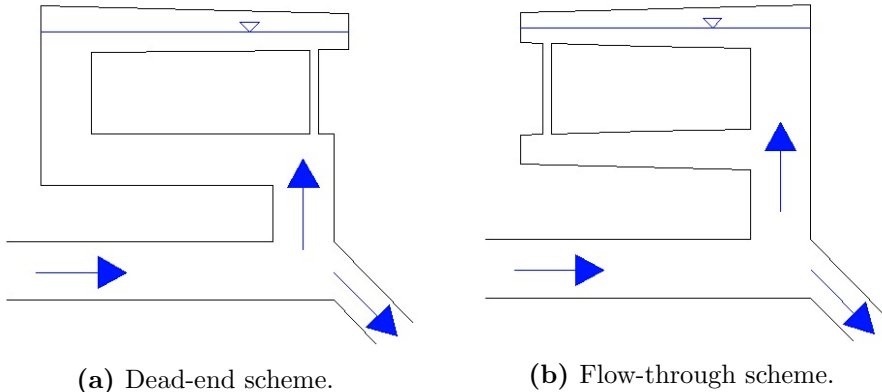


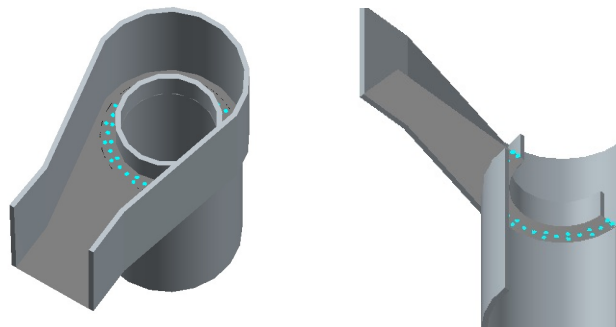
Figure 3.12: Two types of 2CST with long lower and upper chambers.

which by all means should be avoided. The flow-through scheme gives good degassing, but it does not reflect the water hammer as efficiently as the dead-end solution. The filling and emptying of the flow-through scheme is better and more stable, but in a design phase this has to be measured against the increased inertia of the water masses (Richter et al., 2012).

To improve the stability of hydropower schemes with long chambers as part of the surge tank, aeration shafts can be constructed to prevent that cavitation and column separation will occur in the lower chamber (Richter et al., 2014).



(a) The Krespa surge tank at the Obervermunt II PSP.



(b) Krespa shower head seen from above.

(c) Krespa shower head seen from below.

Figure 3.13: Connection to the upper long chamber at the Krespa surge tank. The blue circles show the "shower head" seen from above (b) and from below (c).

3.2.3 "Shower head"

As for the long chamber surge tanks described above, great waterfalls can occur that have to be damped to avoid turbulence and air entrainment into the tunnel system. One way to do this is to introduce several combined singular losses, creating smaller waterfalls instead of the potential big waterfall that may occur without these singular losses. As an example the Krespa surge tank of the PSP Obervermunt II will be used. Figure 3.13b shows the connection from the shaft to the long upper chamber at Krespa, and on Figure 3.13c one can see how the intended singular losses create several smaller waterfalls.

Chapter 4

Method

In this chapter the proposed method for the simulations will be presented, the method of characteristics and how it is used in LabVIEW and LVTrans will be described, and the case study power plants and their redesigns for the simulations will be presented.

4.1 The LVTrans software

The LVTrans software is described in a manual written by its developer Bjørnar Svingen (2015). The software is used to simulate and calculate transient liquids in pipe systems, including open channels and gas filled pipes, with hydropower as the primary field for the program.

LVTrans is programmed in LabVIEW, which is an object based programming language, and the way to build a hydropower plant is to put in objects, for example a pipe, surge tank or a turbine, and to choose the parameters to obtain the hydropower plant. Then one can simulate the hydropower plant, in real time, faster or slower, and one can observe the hydraulics in the hydropower plant, for example what happens with the surges in a surge tank, or how the turbine pressure evolves after a shutdown.

4.1.1 Method of characteristics

The software uses the method of characteristics (MOC), which is a method that solves the partial differential equations for elastic pipe flow. To describe the MOC, the simplified equations of motion (L1) and continuity (L2) will be used, as shown in Equations 4.1 and 4.2. The description is based on Wylie and Streeter (1993), where the most important equations and boundary conditions will be described.

$$L_1 = g \frac{\partial H}{\partial x} + f \frac{v|v|}{2D} + \frac{dv}{dt} = 0 \quad (4.1)$$

$$L_2 = \frac{a^2}{g} \frac{dv}{dx} + \frac{\partial H}{\partial t} = 0 \quad (4.2)$$

These two equations are a pair of quasilinear hyperbolic partial differential equations, in terms of the velocity and the hydraulic grade-line equation as dependent variables, and the time and distance along the pipe as the independent variables. The MOC transforms these equations into four ordinary differential equations. Combining the equations of continuity and motion with an unknown multiplier λ gives

$$L = L_1 + \lambda L_2 = \lambda \left(\frac{\partial H}{\partial x} \frac{g}{\lambda} + \frac{\partial H}{\partial t} \right) + \left(\frac{\partial v}{\partial x} \lambda \frac{a^2}{g} + \frac{\partial v}{\partial t} \right) + \frac{fv|v|}{2D} \quad (4.3)$$

The multiplier λ can be given two particular values to simplify Equation (4.3). After some steps, it can be shown that x and t , the time and the distance along the pipe, have the following relation, that shows the change in position of a wave related to the change in time by the wave propagation velocity a .

$$\frac{dx}{dt} = \pm a \quad (4.4)$$

For the λ value there exist two parallelism for the positive and the negative values, so that the two positive values are identified as a C^+ equation, and the two negative values as C^- equation.

$$C^+ = \begin{cases} \frac{g}{a} \frac{dH}{dt} + \frac{dv}{dt} + \frac{fv|v|}{2D} = 0 \\ \frac{dx}{dt} = +a \end{cases} \quad (4.5)$$

$$(4.6)$$

$$C^- = \begin{cases} -\frac{g}{a} \frac{dH}{dt} + \frac{dv}{dt} + \frac{fv|v|}{2D} = 0 \\ \frac{dx}{dt} = -a \end{cases} \quad (4.7)$$

$$(4.8)$$

The two total differential equations (4.5) and (4.7) are only valid when their respective equations (4.6) and (4.8) are valid. This can be visualized as it develops on the xt-plane, which is the independent variable plane. Then (4.6) and (4.8) are characteristic lines on the xt-plane in different directions depending on whether (4.5) or (4.7) is valid. Because no mathematical approximations have been made in this transformation, the original differential equations (4.1) and (4.2) will be solved by the C^+ and C^- set of equations.

To use these equations for a single pipe, as is done in LVTrans, Figure 4.1 can be used to show how it is done. This xt-grid has an even number of reaches, N , with length Δx and time step $\Delta t = \Delta x/a$, with the time steps along the y-axis and the length steps along the x-axis. As shown in the figure, starting at point A, equation (4.5) is used from A to P along the C^+ line, and equation (4.7) is used from P to B along the C^- line. This process introduces new equations to be solved, so that the head and the discharge can be found in every step. Some approximations are being done in this step, with the objective that a reasonable accuracy is provided in general unsteady flow, that also holds for special conditions during steady flow. A problem in liquid transients, as in a pipe in a hydropower plant scheme, begins where the head H and the discharge Q are known initial values during steady-state conditions at each section for $t = 0$. Then the described process, from point A to P, and then from P to B, is repeated for the next time step $t = n\Delta t$. For a smaller time step Δt more iterations will be done, and for a smaller length step Δx the distance between each C^+ and C^- interval will decrease, also giving more iterations, hence the triangles in Figure 4.1 will decrease in size and increase in quantity. Some simulations in LVTrans, for example the water hammer in front of the turbine, requires small time and length steps to be able to capture the turbine pressure from the water hammer, while others such as the water level oscillations in the surge tank can be simulated with bigger time and length steps.

To be able to control the simulations, boundary conditions are introduced. These boundary conditions are defined by the elements in LVTrans, and this is also why every element in LVTrans has to be connected to another

element by a pipe element. The boundary conditions defined by Wylie and Streeter (1993) are:

- Reservoir at Upstream End with Elevation Specified
- Discharge as a Specified Function of Time at Upstream End
- Centrifugal Pump at the Upstream End with the Head-Discharge Curve Known
- Dead End at the Downstream End of Pipe
- Valve at Downstream End of Pipe
- Orifice at Downstream End of Pipe

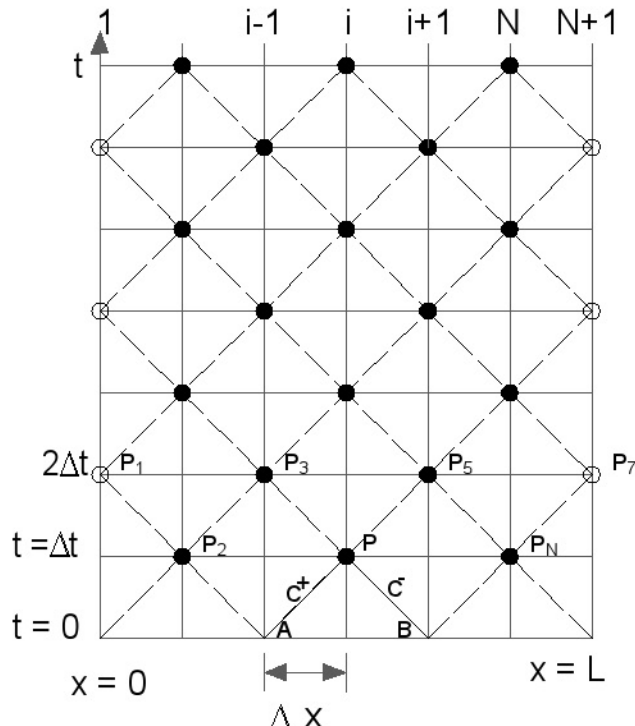


Figure 4.1: Grid for solving single-pipe problems in the MOC.

4.1.2 Elements and method in LVTrans

Pipes and friction losses

All the elements in LVTrans are connected by separate pipes, with length, pipe diameter, friction factor, and starting and ending elevations as input parameters. LVTrans also offers the opportunity to design the pipes as tunnels with a conventional cross-section, but for the simulations done in this thesis every pipe element is simplified as a circular tube with diameter D . The friction factors used are $f = 0,07$ for unlined tunnels, $f = 0,04$ for concrete lined tunnels and $f = 0,015$ for steel lined tunnels.

Singular losses and throttle configuration

To simulate throttling in LVTrans, the singular loss of a throttle configuration has to be calculated or evaluated through modeling, and the throttle is represented in LVTrans as a singular loss. The singular loss is calculated as shown in Equation (4.9). ξ is known as the traditional loss coefficient, while LVTrans uses C_V as input, meaning that a smaller value of C_V will give a bigger singular loss.

$$C_V = \frac{Q_0^2}{2H_0} = \frac{A^2 g}{\xi} \quad (4.9)$$

As mentioned in Chapter 3, the throttling can be symmetric or asymmetric. For symmetric throttling the inflow throttle value C_{Vm} and the outflow value C_{Vp} have the same value, for the asymmetric throttling they have different values, depending on the loss ratio and the wanted hydraulic losses. The throttling in the simulations in this thesis is symmetric for all the simulations, hence the losses are the same in both directions and $C_{Vm} = C_{Vp}$.

To find the optimal throttling in LVTrans, different C_V values are tested until the pressure amplitudes from the water hammer and the mass oscillation have approximately the same value after a complete shutdown of the power plant. An example of the pressure amplitudes of a throttled and unthrottled surge tank are shown in Figure 4.2. Then this is considered as a medium throttle, and the strong throttle is put to 25 % of this C_V value.

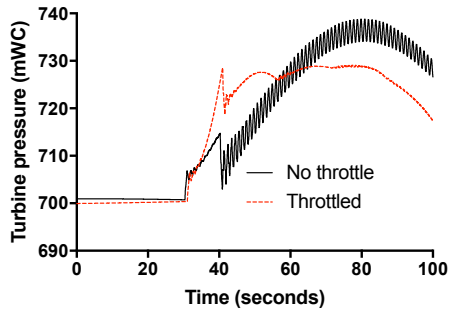


Figure 4.2: Unthrottled and optimized throttling of a surge tank.

Design pressure

To calculate the design pressure, which is the pressure limit in front of the turbine to make sure that the waterway can handle the pressure after a shutdown, a sudden shutdown of the power plant is performed in LVTrans. The way of doing this is by logging the final pipe element before the turbine, and plotting the H_2 value from the logged file. This value is then compared against the design pressure to decide whether the water hammer is within the limits, or if the design of the power plant has to be changed. For all the simulations the design pressure is chosen to be 15 % above the maximum static pressure, as shown in Equation (4.10).

$$p_{Design} = (z_{Magazine} - z_{Turbine}) * 1,15 \quad (4.10)$$

Design of the air cushion surge tank

Important input parameters for the ACST in LVTrans is the initial pressure $h_{p,0}$, the diameter D and the initial volume V_{init} of the cavern and the initial liquid kote $Liqkote,init$.

The initial pressure $h_{p,0}$ is calculated as shown in Equation (4.14). This is the basis for the calculation of the initial volume V_{init} as shown in Equation (4.16), where $n = 1,4$ is the adiabatic constant as described in Section 2.2.4. The diameter of the cavern is then selected mostly based on constructional aspects. The initial liquid kote then has to be in sufficient distance from the tunnel roof, so the water will not entrain air into the waterway.

$$h_{p,0} = z_{Magazine} - z_{Aircushion} + h_{atm} \quad (4.11)$$

$$V_{AC,min} = 1,4h_{p,0}A_{min} \quad (4.12)$$

Design of the two chamber surge tank

To design the 2CST the variable surge tank element in LVTrans is used, where the elevation and the area can be set in intervals from 0 to 9 to decide the design of the surge tank. The connection shaft between the tunnel and the lower chamber, and between the lower and the upper chamber, is set to the area decided by the Thoma stability criteria. Then several designs are tried out until the design criteria for 2CST are met. For the final design the water level during normal operation is in the shaft between the two chambers, the upsurge during shutdown is below a given level in the upper surge tank, and the downsurge are minimum two meters above the tunnel roof, preferably in the lower surge chamber. The upper surge limit depends on the topography.

New design and programming of the differential surge tank

The DST is not programmed in LVTrans, therefore a new solution was tried programmed in LVTrans to be able to simulate the differential effect in the DST. In this attempt the the variable surge tank is used as a basis, adding an outer chamber after a lower boundary L_{Lim} . Above this boundary the differential opening is installed, allowing flow between the inner riser and the outer chamber. The new input parameters are the mentioned lower limit L_{Lim} , the area of the outer chamber A_{Out} , the area of the differential opening A_{Diff} and the singular loss value k_{diff} of the differential opening. The programming did not gave the wanted behavior of the surge tank. The LVTrans code is shown in Appendix B.

Instead the DST is put together in LVTrans as a combination of a SST and a SST with a throttle, with a distance of 50 meters between the two chambers. The proposed methodology for the design of the DST, is to find an optimal throttle of one SST, with a given diameter, and add a SST with half the diameter, and no throttle, as could have been the scenario in a combined DST. Then, through a trial and error process in LVTrans final solutions

are found, and simulated and evaluated against the other solutions. In the graphs the DST is then called *DST* and *Throttled DST*.

Turbine and PID

The LVTrans has pelton turbine, francis turbine and francis pump turbine elements. For the power plants in this thesis the francis turbine is used. The values in LVTrans for the turbine and the PID are calculated using an Excel sheet made for the LVTrans software. The the turbine pressure is measured in LVTrans, the plotted value is the static water height, including the elevation of the turbine, hence for Torpa HPP the actual pressure will be 256 *meters* lower as the turbine is located at 256 *m.a.s.l.*, and for Åna-Sira HPP the actual pressure will be 1 *meter* higher, as the turbine is located at -1 *m.a.s.l.*. This is valid for all the figures where the turbine pressure is plotted.

Frequency-Response testing

To run the Frequency-Response test, a installed program in LVTrans called "AFF control" is used with the PID unit. The PID element comes with several types that can be used, in this case the PID unit "AFF WCC old-style". The Frequency-Response test is performed on an open isolated grid, and the results are plotted in a Bode-plot.

The open and the closed surge tank have a different behavior. Therefore the PID unit has to be tuned to fit the behavior of the hydropower plants. The method below is the "Method 1" described by Bjørnar Svingen (2015).

- The PID is set on Island mode, with "SP P [MW]" = 0, "droop" = 0, and "SP n [0-1]" = 0,9.
- $P = 1$ and $T_i = 10$ are set for the "PID n Island".
- The system is stabilized.
- $T_i = 10^{10}$.
- "SP n" is changed from 0,9 to 1,0 to observe the changes in "PV n".
- The value of P is increased until the "PV n" overshoots "SP n" by 15 %.

- Then T_i is reduced to increase the overshoot until it reaches 30 %.
- The T_d is increased until the overshoot is OK, in this case 15% (this step is skipped in the tuning process in this thesis.).

Step-Response testing

To perform the Step-Response test, the set point is first set to where the produced power is equal to zero. Then this situation is logged for 60 seconds after stabilizing, and then the set point value is increased to the nominal installed effect of the hydropower plant. LVTrans then logs how the produced power and the pressure in front of the turbine varies with time. The governor performance in the system is good if the produced power follows the curve of the specified set point, with a power overshoot below a given value, and if the pressure in front of the turbine is above an undershoot value, and if both of them stabilize within a given time limit when the system reaches steady state (Vereide et al., 2016).

4.2 Hydropower plants for case study

The selected hydropower plants for the case study are the Norwegian hydropower plants Torpa and Åna-Sira. These hydropower plants are selected to be able to simulate the hydraulic behavior in two different hydropower schemes, as Torpa is a high pressure hydropower plant with quite low discharge, while Åna-Sira is a low pressure hydropower plant with a much larger discharge. Using these power plants to test the surge tank solutions, the function of the surge tanks can be investigated under different conditions.

Table 4.1 shows some of the most important parameters of the power plants. The values are based on the technical drawings from both of the projects as shown in Appendix A. Some of the values are read directly from the technical drawings while others are measured by hand from the drawings and can therefore be more inaccurate.

| Parameter | Torpa | Åna-Sira |
|------------------------------|---------------------------------------|---|
| Higher magazine water level | 708 m | 48 m |
| Lower magazine water level | 265 m | 0 m |
| Netto hydraulic head | 430 m | 44 m |
| Nominal discharge | $35m^3/s$ | $375m^3/s$ |
| Maximum discharge | $40m^3/s$ | $390m^3/s$ |
| Turbine | 2 x 75 MW Francis | 3 x 50 MW Francis |
| Turbine kote | 256 m | -1 m |
| Yearly production | 390 GWh | 602 GWh |
| Inlet tunnel length | 9450 m | 1600 m |
| Inlet tunnel area | $35m^2$ | $160m^2$ |
| Pressure tunnel/shaft length | 130 m | 120 m |
| Pressure tunnel/shaft area | $21/17m^2$ | $60/30m^2$ |
| Outlet tunnel length | 10150 m | 150 m |
| Outlet tunnel area | $35m^2$ | $100m^2$ |
| Upstream surge tank | Air cushion | One chamber surge tank with symmetric concrete throttle |
| Downstream surge tank | Access tunnel with additional chamber | None |

Table 4.1: Key parameters for Torpa and Åna-Sira hydropower plants.

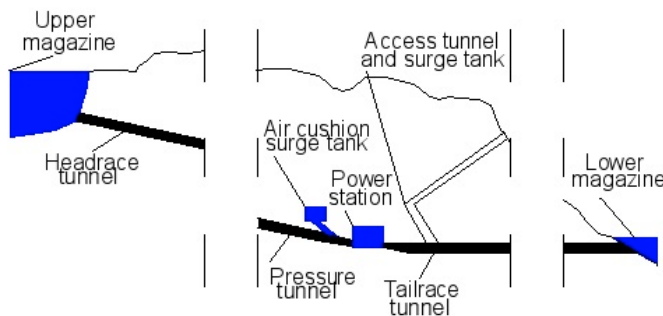


Figure 4.3: Hydropower scheme of the Torpa HPP.

4.2.1 Torpa hydropower plant

The Torpa HPP was constructed in the late 1980's, and is owned by the Norwegian power company Oppland Energi AS. It is located in Åmot, Oppland, and is a part of the Dokka hydropower scheme. The HPP takes advantage of a total head of 470 meters, with two turbines of 75 MW, a turbines head of 430 meters and a discharge of $40m^3/s$, that produces approximately 390 GWh per year. A 9,5 km long inlet tunnel and a 10,5 km long outlet tunnel makes it a large hydropower scheme (Oppland Energi AS, 2016).

An air cushion chamber (ACST) were constructed, mainly because of the topography. With a low overburden a conventional upstream surge tank solution would have been difficult. The chamber is blasted as a conventional tunnel and it has a donut shape with an average cross-section of $94,4 m^2$. The total length of the blasted tunnel is around 230 meters, giving a total volume of $17400 m^3$, with the air cushion volume ranging between 11100 and $12900 m^3$.

In the outlet tunnel there is an access tunnel that are being used as surge tank downstream, with an additional constructed chamber. This works as a simple surge tank, therefore the area and the volume of the surge tank is very large, so that the water surface area is sufficient to prevent air entrainment into the water way.

An overview of the Torpa HPP are shown in Figure 4.3.

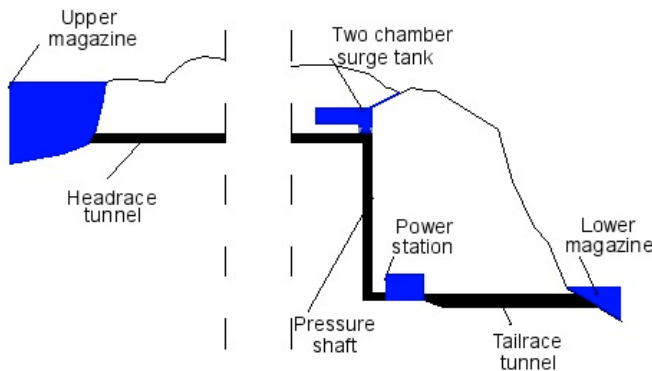


Figure 4.4: Hydropower scheme of the Åna-Sira HPP.

4.2.2 Åna-Sira hydropower plant

The Åna-Sira HPP was first started in 1971 and it was updated in 1989. It is located in Flekkefjord in the Vest-Agder county, and is owned by the Norwegian power company Sira-Kvina Kraftselskap. The HPP has a low head of only 48 meters, but with its massive discharge of $390\text{m}^3/\text{s}$, the HPP produces around 600 GWh per year. The power station houses three Francis turbines of 50 MW each. It has shorter tunnels than the Torpa HPP, with an inlet tunnel of approximately 1600 meters and a short outlet tunnel of 150 meters.

Åna-Sira HPP has a surge tank solution with a single chamber, connected to the inlet tunnel by a concrete throttle. The chamber is constructed with a typical tunnel cross section with a width of 15 meters, a height that varies between 16 and 19 meters, and a total length of 89,5 meters. This gives a volume of the surge tank of approximately 23000 m^3 . Because of the short outlet tunnel there is no need for a downstream surge tank.

An overview and some of the most important details of the Åna-Sira HPP are shown in Figure 4.4.

4.3 Modification of the hydropower plants

The hydropower plants mentioned in the previous section, Torpa and Åna-Sira, will be used further as conceptual hydropower schemes for the Surge

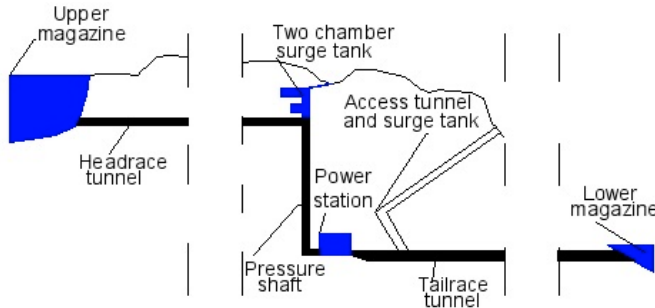


Figure 4.5: New conceptual design for Torpa HPP.

Tank Atlas. All of the simulations done in LVTrans will only be affected of changes upstream the turbine, therefore the outlet tunnels in both hydropower plants and the downstream surge tank in the Torpa HPP will remain unchanged for all the simulations. To be able to compare the surge tank solutions in the redesigned hydropower plants with the original HPPs, the values are modified and adapted to the original solution.

4.3.1 Redesign Torpa HPP

For Torpa HPP, the actual design for the ACST will be changed to a conceptual design that can be used for the other open surge tanks that are connected to atmospheric air, as shown in Figure 4.5. Then the inclined pressure tunnel to the turbine for the ACST is replaced by a horizontal headrace tunnel leading to a pressure shaft to the turbine for the open surge tanks.

For the open surge tank solutions at Torpa HPP, the headrace tunnel has the diameter $D = 6,7m$, giving the area $A_T = 35m^2$. This gives the Thoma-area

$$A_{Th} = 0,0125 \frac{M^2 A_T^{5/3}}{H_e} = 0,0125 \frac{30m^{1/3/s^2} 35m^{25/3}}{430m} = 10m^2 \quad (4.13)$$

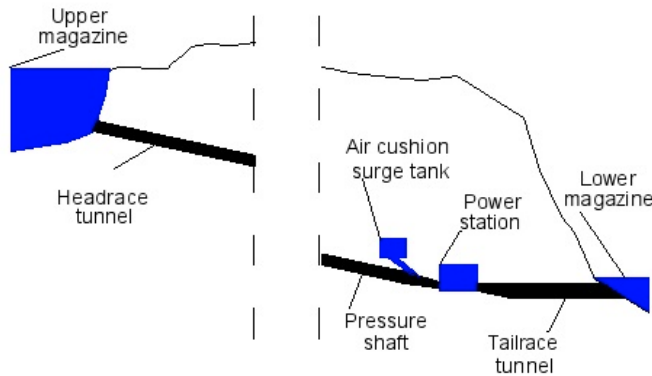


Figure 4.6: New conceptual design for Åna-Sira HPP.

4.3.2 Redesign Åna-Sira HPP

For Åna HPP, the conceptual design for the actual throttled 1CST solution will be kept the same for the other open surge tank solutions, while Figure 4.6 shows the design to be used for the ACST solution. Then the headrace tunnel and the pressure shaft is replaced by an inclined pressure tunnel. The diameter of the inclined tunnel is set to $D = 15m$, giving an area $A_T = 177m^2$. The ACST is placed 350 meters from the power station.

The ACST has the following calculated input parameters in LVTrans:

$$\begin{aligned} h_{p,0,AS} &= z_{Magazine} - z_{Aircushion} + h_{atm} \\ &= 48mWC - 28mWC + 10mWC = 30mWC \end{aligned} \quad (4.14)$$

$$A_{Th} = 0,0125 \frac{M^2 A_T^{5/3}}{H_e} = 0,0125 \frac{30m^{1/3/s^2} 177m^{25/3}}{44m} = 1426m^2 \quad (4.15)$$

$$V_{AC,min,AS} = 1,4 h_{p,0,AS} A_{Th} = 1,4 * 30mWC * 1426m^2 = 60000m^3 \quad (4.16)$$

Chapter 5

Surge Tank Atlas

This chapter will present the Surge Tank Atlas, with a short description of the surge tank solutions, documentation from simulations done in LVTrans, a parameter vulnerability analysis where some of the parameters are changed to investigate how they affect the hydraulic behavior of the hydropower plants for the case study, and a comparison and discussion of the results.

The main purpose of the Surge Tank Atlas is to create an overview of the existing surge tank solutions, their advantages and disadvantages, and to compare the solutions. Given parameters will be investigated, with the purpose that a hydropower engineer could be able to use the Surge Tank Atlas to select the best surge tank solution given some key parameters from the actual hydropower project. The Surge Tank Atlas will contain a "data sheet" for each surge tank solution, with a description of the solution, advantages and disadvantages and documentation from the LVTrans simulations.

A complete turbine shutdown, a shutdown and a start up during the worst time, creating the largest downsurge, a Frequency-Response test and a Step-Response test will be performed in LVTrans for all the solutions, and important values like maximum upsurge and downsurge, turbine pressures and turbine regulation parameters will be plotted. The water inertia time constants and excavated volumes will be calculated and presented for each solution. This should give enough documentation to be able to compare the parameters and to give advices on what will be the best solution.

The design of the hydro power plants are made to represent the reality as good as possible, but there are some limitations and potential sources of error that can affect the results from the simulations, that one has to have in mind when studying the results:

- The power plants are designed with one turbine, instead of two (Torpa HPP) and three (Åna-Sira), leading to some necessary changes in the

water way design to adjust the power plant to make sure that the water inertia time constant, t_a , maintains a value $t_a < 1$, leading to shorter tunnels with larger area, reducing the ratio L/A . This is only a problem for the solutions at Åna-Sira HPP, where the design with one instead of three turbines gave a high value of t_a .

- The tuning of the PID-parameters are performed for the closed surge tank, and for the 2CST at each power plant, then the same PID-parameters are used for the two other open surge tank solutions, the SST and the DST. This is because the water way design are kept the same for all the open surge tank solutions for the same power plants, hence the PID-parameters are not tuned for every power plant.
- For the surge tank designs, the lower surge limit is set to two meters above the tunnel roof, while there is not focused on the upper surge limit, limited by the topography. Hence some of the surge tank solutions, especially the simple surge tank, would probably not be suitable for a topography that sets an upper surge limit.

All of the results are presented in this chapter. The input values for the LVTrans simulations, and the construction drawings used from the power plants, are attached in the appendix. The surge tank with long chambers and the surge tank with a "shower head" are also presented as surge tank solutions, but these solutions are only presented with a description, and without simulations in LVTrans.

5.1 The Simple Surge Tank

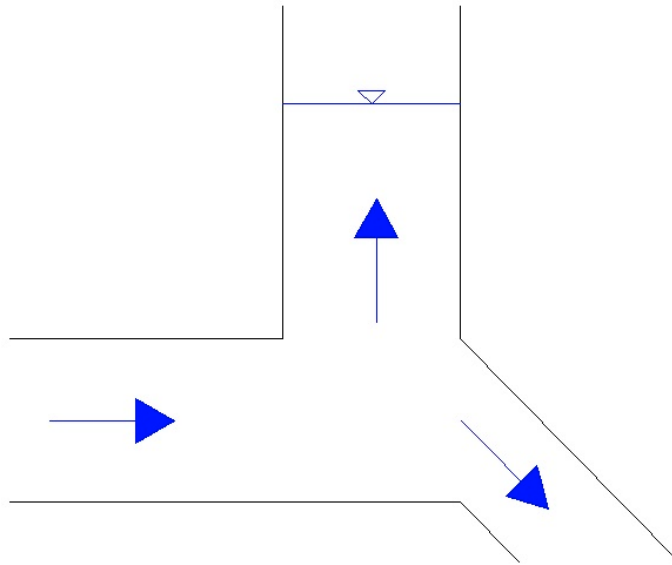


Figure 5.1: Conceptual design of the SST

Description

If the hydropower scheme has a simple design with a short pressure tunnel, there is no need for a surge tank, but if there is a need for a closer placement of a free water surface, the simplest surge tank solution is a simple shaft where the water can oscillate during regulation and shut-down of the power plant - a simple surge tank (SST).

This will give an easy construction, and it is easy to simulate the mass oscillations as there will be practically no secondary hydraulic effects. In addition the maintenance costs will probably be lower compared to a more complex solution. The SST can be constructed as a cylinder as shown in Figure 5.1, or it can be constructed with a connection tunnel leading to a bigger chamber, thus making it a 1CST solution.

One of the situations where the SST can be taken into use today can be

for a downstream surge tank, where an access tunnel can be used as the SST. Maybe the access tunnel itself has a large enough volume to dampen the oscillations, if not an extra cavern can be excavated within the access tunnel, that can save costs compared to planning and constructing a new surge tank solution.

Advantages

- Easy to plan and construct.
- Easy to do calculations and simulations.
- Simple hydraulics - no secondary hydraulic effects.
- Low maintenance costs.
- Downstream access tunnel can be used as SST.

Disadvantages

- The shaft will be very high if the mass oscillations go higher, and there may be a need for constructing a surge tower above the topography surface.
- The SST offers no additional damping compared to the other surge tank solution.

Documentation**SST at Torpa HPP**

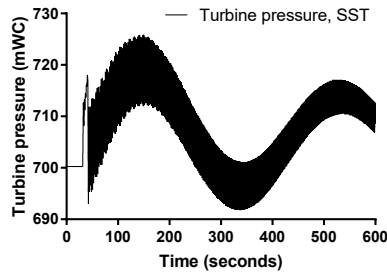
| Parameter | Unit | Value |
|-------------------------------|-----------------|--------------|
| Upsurge and downsurge | <i>m.a.s.l.</i> | 719 - 681 |
| Maximum turbine pressure | <i>mWc</i> | 726 |
| Water hammer amplitude | <i>mWc</i> | 718 |
| Mass oscillation amplitude | <i>mWc</i> | 719 |
| Water inertia time constant | <i>s</i> | 0,24 |
| Excavated volume - tunnels | $1000m^3$ | 710 |
| Excavated volume - surge tank | $1000m^3$ | 5,3 |
| Power overshoot | <i>MW</i> | 150,15 |
| Pressure undershoot | <i>mWc</i> | 693 |
| Cross frequency | <i>Hz</i> | 0,09 |
| Gain margin | <i>dB</i> | 10 |
| Phase margin | $^\circ$ | 81,8 |

Table 5.1: Simulated and calculated values for the SST at Torpa HPP.**SST at Åna-Sira HPP**

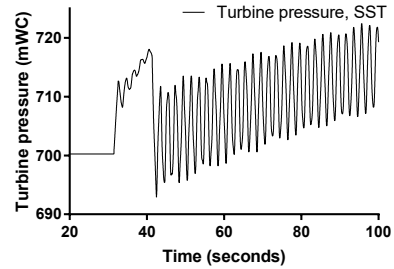
| Parameter | Unit | Value |
|-------------------------------|-----------------|--------------|
| Upsurge and downsurge | <i>m.a.s.l.</i> | 50,7 - 40 |
| Maximum turbine pressure | <i>mWc</i> | 50,7 |
| Water hammer amplitude | <i>mWc</i> | 48,5 |
| Mass oscillation amplitude | <i>mWc</i> | 50,7 |
| Water inertia time constant | <i>s</i> | 0,62 |
| Excavated volume - tunnels | $1000m^3$ | 407 |
| Excavated volume - surge tank | $1000m^3$ | 26,5 |
| Power overshoot | <i>MW</i> | 152,8 |
| Pressure undershoot | <i>mWc</i> | 42,6 |
| Cross frequency | <i>Hz</i> | 0,09 |
| Gain margin | <i>dB</i> | 20 |
| Phase margin | $^\circ$ | 81,9 |

Table 5.2: Simulated and calculated values for the SST at Åna-Sira HPP.

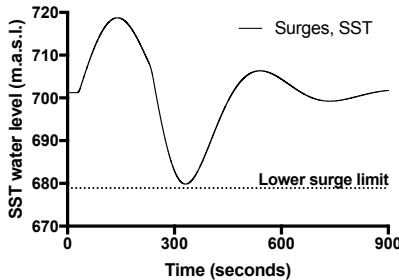
SST at Torpa HPP



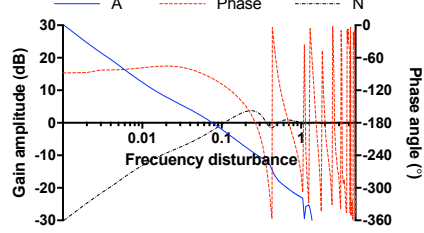
(a) Turbine pressure.



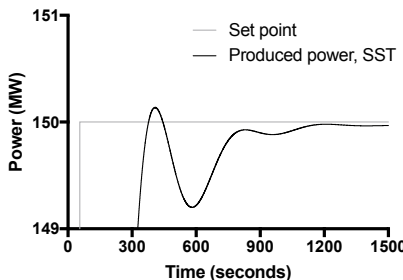
(b) Close up on turbine pressure.



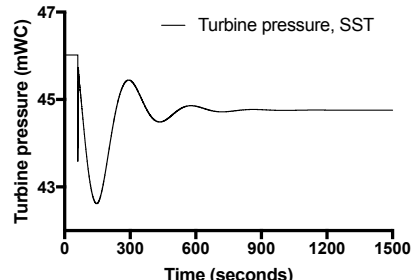
(c) Mass oscillations.



(d) Frequency-response plot.



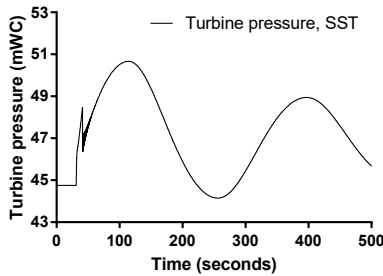
(e) Power step-response.



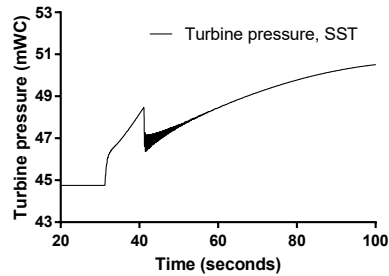
(f) Turbine pressure step-response.

Figure 5.2: LVTrans simulations for the SST at Torpa HPP.

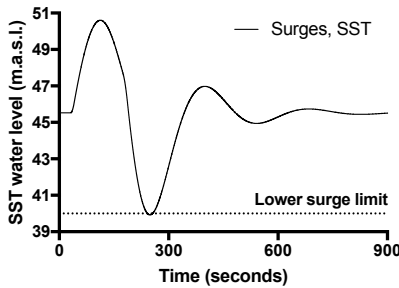
SST at Åna-Sira HPP



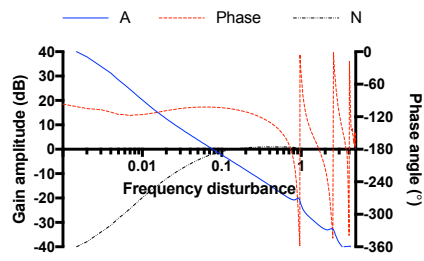
(a) Turbine pressure.



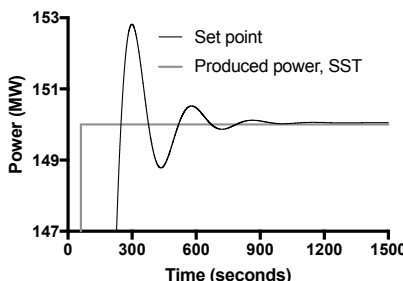
(b) Close up on turbine pressure.



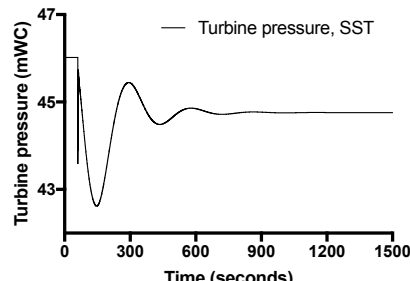
(c) Mass oscillations.



(d) Frequency-response plot.



(e) Power step-response.



(f) Turbine pressure step-response.

Figure 5.3: LVTrans simulations for the SST at Åna-Sira HPP.

5.2 The Two Chamber Surge Tank

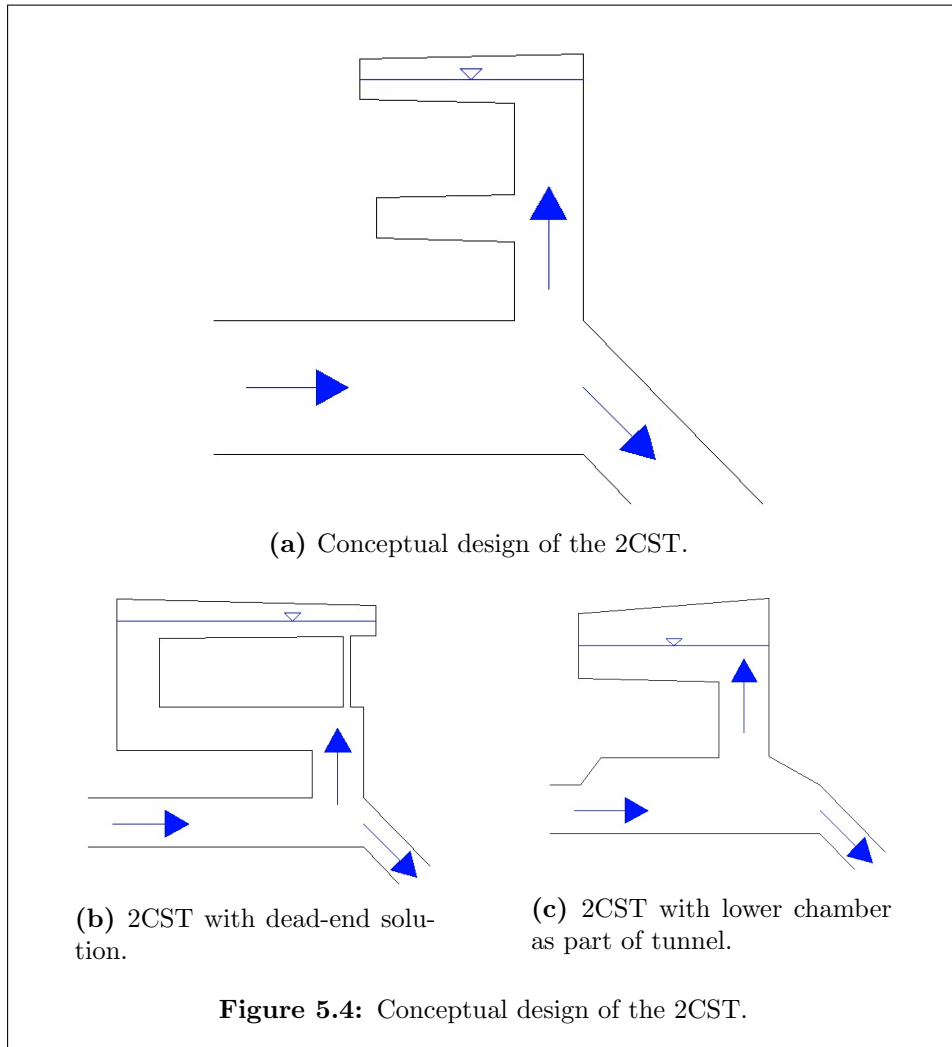


Figure 5.4: Conceptual design of the 2CST.

Description

The two chamber surge tank (2CST) consists of an upper and a lower surge chamber, with an inner riser shaft connecting the two chambers. It is an open surge tank solution, connected to atmospheric air through the upper chamber. The inner shaft, as well as the inlet of the 2CST, should have the Thoma-area to ensure stability in the surges. The design of the cham-

bers depend on the topography, and is in general very flexible as the most important is the total surface area and the flow patterns in the chambers, not the shape of the chambers. The 2CST can be easily visualized as a cylindrical shaft with a larger diameter in the lower and upper chamber, or the chambers can be visualized as longer tunnels with a large water surface area.

One possible solution is to construct the 2CST with the tunnel working as the lower chamber, increasing the tunnel volume in this part. These two different solutions, the conventional mentioned above, and the one with the tunnel as the lower chamber, are shown in Figures 5.4b and 5.4c.

Advantages

- Maintenance is relatively easy because the 2CST can be accessed from both the bottom and the top of the 2CST.
- Great flexibility on how to construct the 2CST, there exist almost an unlimited variety of ways of construction.
- Easily compatible with additional improvements, such as throttles (both in the connection tunnel and in the shaft between the lower and upper chamber), long chambers and aeration shafts.

Disadvantages

- The horizontal placement of the 2CST depends on the topography and is not very flexible.
- If the 2CST is large there may have to be constructed roads to access the 2CST from above.

Documentation**2CST at Torpa HPP**

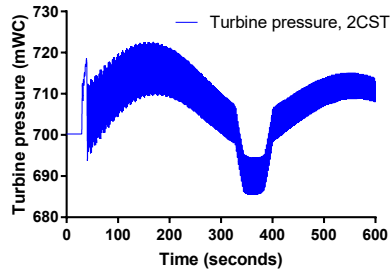
| Parameter | Unit | Value |
|-------------------------------|-----------------|-----------|
| Upsurge and downsurge | <i>m.a.s.l.</i> | 715 - 681 |
| Maximum turbine pressure | <i>mWc</i> | 723 |
| Water hammer amplitude | <i>mWc</i> | 719 |
| Mass oscillation amplitude | <i>mWc</i> | 715 |
| Water inertia time constant | <i>s</i> | 0,24 |
| Excavated volume - tunnels | $1000m^3$ | 710 |
| Excavated volume - surge tank | $1000m^3$ | 2,1 |
| Power overshoot | <i>MW</i> | 150,20 |
| Pressure undershoot | <i>mWc</i> | 688,5 |
| Cross frequency | <i>Hz</i> | 0,091 |
| Gain margin | <i>dB</i> | 10 |
| Phase margin | $^\circ$ | 85,1 |

Table 5.3: Simulated and calculated values for the 2CST at Torpa HPP.**2CST at Åna-Sira HPP**

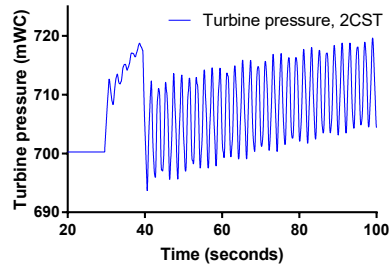
| Parameter | Unit | Value |
|-------------------------------|-----------------|-----------|
| Upsurge and downsurge | <i>m.a.s.l.</i> | 49,8 - 40 |
| Maximum turbine pressure | <i>mWc</i> | 49,8 |
| Water hammer amplitude | <i>mWc</i> | 49,1 |
| Mass oscillation amplitude | <i>mWc</i> | 49,8 |
| Water inertia time constant | <i>s</i> | 0,62 |
| Excavated volume - tunnels | $1000m^3$ | 407 |
| Excavated volume - surge tank | $1000m^3$ | 46,7 |
| Power overshoot | <i>MW</i> | 156,5 |
| Pressure undershoot | <i>mWc</i> | 42,4 |
| Cross frequency | <i>Hz</i> | 0,104 |
| Gain margin | <i>dB</i> | 21,5 |
| Phase margin | $^\circ$ | 78,9 |

Table 5.4: Simulated and calculated values for the 2CST at Åna-Sira HPP.

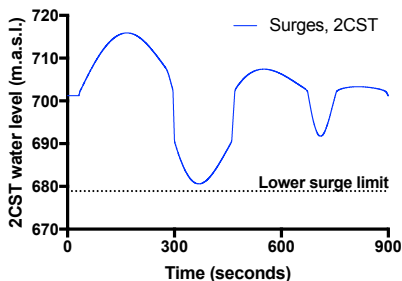
2CST at Torpa HPP



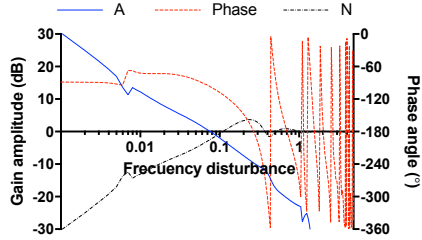
(a) Turbine pressure.



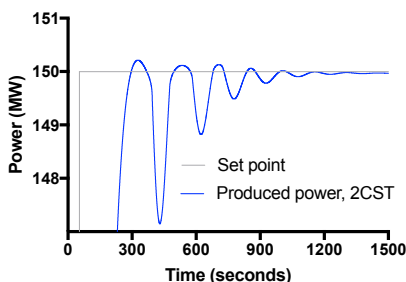
(b) Close up on turbine pressure.



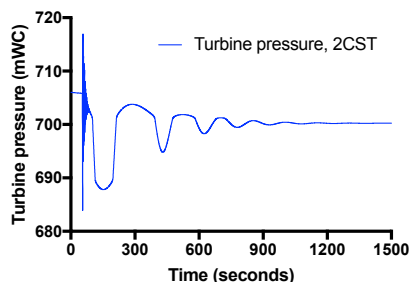
(c) Mass oscillations.



(d) Frequency-Response plot.



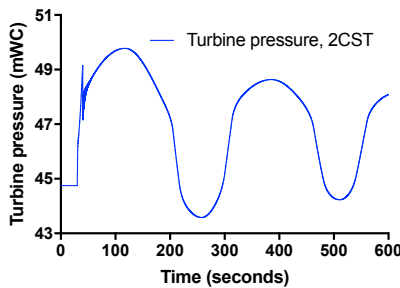
(e) Power Step-Response.



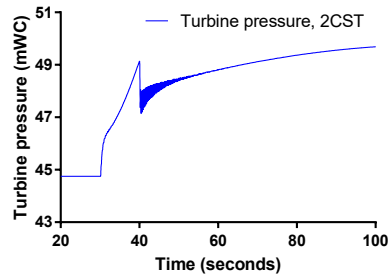
(f) Turbine pressure Step-Response.

Figure 5.5: LVTrans simulations for the 2CST at Torpa HPP.

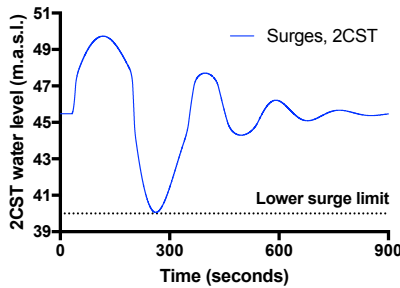
2CST at Åna-Sira HPP



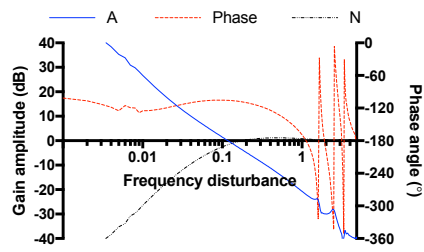
(a) Turbine pressure.



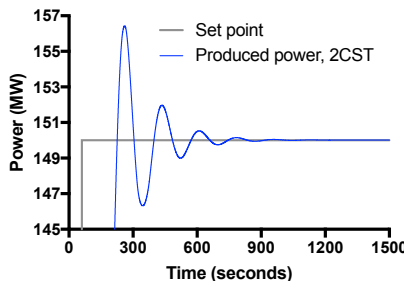
(b) Close up on turbine pressure.



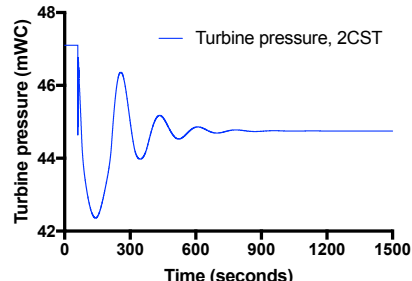
(c) Mass oscillations.



(d) Frequency-Response plot.



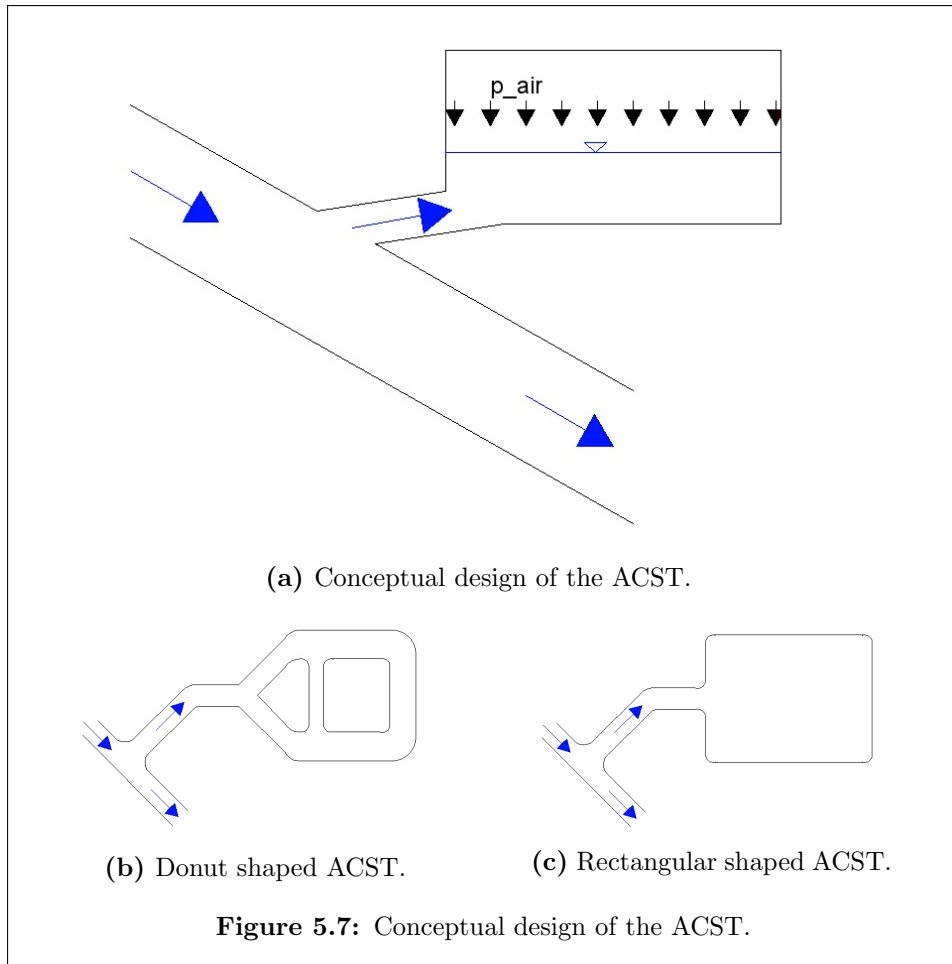
(e) Power Step-Response.



(f) Turbine pressure Step-Response.

Figure 5.6: LVTrans simulations for the 2CST at Åna-Sira HPP.

5.3 The Air Cushion Surge Tank



Description

The ACST is placed upstream the turbine, as close to the turbine as possible to make access to the construction area easier, and it is placed closer to the turbine compared to the open surge tank. The solution is a closed surge tank, without connection to the atmospheric air, and the function as well as the construction method is significantly different from the traditional open surge tank. The geological and topographical conditions, as well as the available knowledge of the technology decide whether it is suitable to

construct the ACST.

The ACST gives a great flexibility when to decide the shape and the placement of the excavated mountain cavern. The cavern can be a tunnel with a given cross-sectional area, for example shaped as a donut, or it can be a more traditional mountain cavern - the important parameters are the volume and the water surface area. The cavern is filled with pressurized air, making an air cushion that works as a damping unit. A thumb rule for the total volume for the cavern is 50 % larger than the necessary air volume (Broch, 2000). The amplitude of the surges in the ACST are very small compared to the surges in an open surge tank, but due to the compressed air the pressure amplitudes from the water hammer and the mass oscillations are comparable to the open surge tank solutions.

Advantages

- Cost savings - there might be no need for steel lined pressure tunnel or shaft, and the water way with an inclined pressure tunnel is shorter than the water way for the open surge tank solution.
- Flexibility in the placement of the cavern as long as it is not too close to the power house.
- Placement closer to the power house to reduce the inertia in the water masses and makes it possible to do construction from the downstream access tunnels.
- Great flexibility on how to construct the shape of the cavern.

Disadvantages

- Requires more surveillance and maintenance.
- Emptying and refilling the ACST is very time demanding, up till several months may be required.
- Requires a comprehensive study to map the geological conditions.
- May require additional constructions like hydraulic jacking and a water curtain.

Documentation**ACST Torpa HPP**

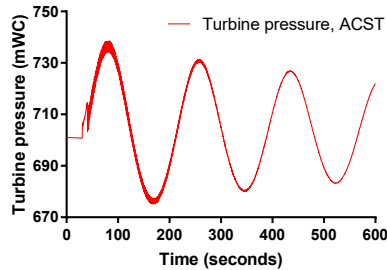
| Parameter | Unit | Value |
|-------------------------------|-----------------|--------------|
| Upsurge and downsurge | <i>m.a.s.l.</i> | 293 - 291,2 |
| Maximum turbine pressure | <i>mWc</i> | 738 |
| Water hammer amplitude | <i>mWc</i> | 714 |
| Mass oscillation amplitude | <i>mWc</i> | 736 |
| Water inertia time constant | <i>s</i> | 0,15 |
| Excavated volume - tunnels | $1000m^3$ | 696 |
| Excavated volume - surge tank | $1000m^3$ | 17 |
| Power overshoot | <i>MW</i> | 157 |
| Pressure undershoot | <i>mWc</i> | 673 |
| Cross frequency | <i>Hz</i> | 0,102 |
| Gain margin | <i>dB</i> | 12,1 |
| Phase margin | $^\circ$ | 80 |

Table 5.5: Simulated and calculated values for the ACST at Torpa HPP.**ACST Åna-Sira HPP**

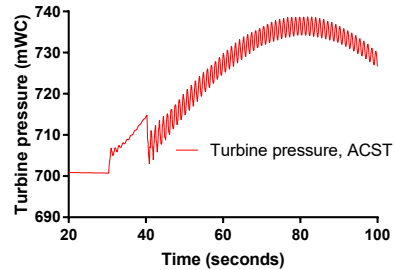
| Parameter | Unit | Value |
|-------------------------------|-----------------|--------------|
| Upsurge and downsurge | <i>m.a.s.l.</i> | 33,8 - 31,8 |
| Maximum turbine pressure | <i>mWc</i> | 54,9 |
| Water hammer amplitude | <i>mWc</i> | 51 |
| Mass oscillation amplitude | <i>mWc</i> | 54,9 |
| Water inertia time constant | <i>s</i> | 0,8 |
| Excavated volume - tunnels | $1000m^3$ | 286 |
| Excavated volume - surge tank | $1000m^3$ | 90 |
| Power overshoot | <i>MW</i> | 151,8 |
| Pressure undershoot | <i>mWc</i> | 42,7 |
| Cross frequency | <i>Hz</i> | 0,106 |
| Gain margin | <i>dB</i> | 14 |
| Phase margin | $^\circ$ | 75,6 |

Table 5.6: Simulated and calculated values for the ACST at Åna-Sira HPP.

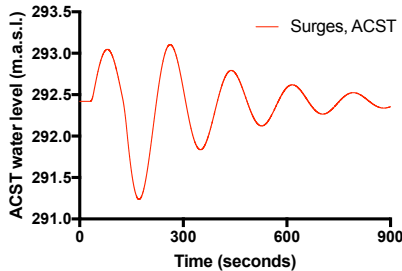
ACST at Torpa HPP



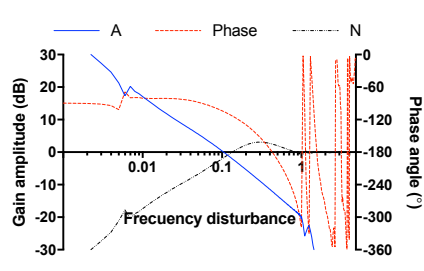
(a) Turbine pressure.



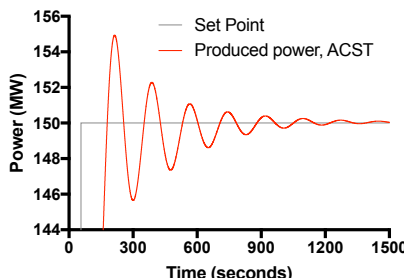
(b) Close up on turbine pressure.



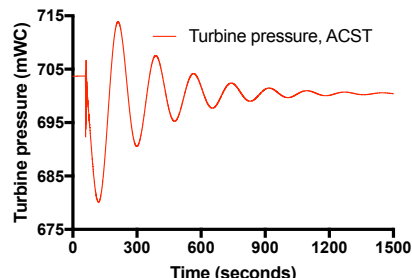
(c) Mass oscillations.



(d) Frequency-Response plot.



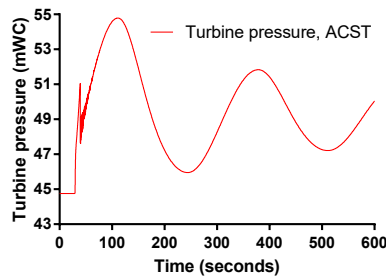
(e) Power Step-Response.



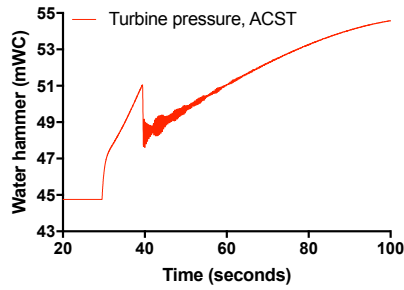
(f) Turbine pressure Step-Response.

Figure 5.8: LVTrans simulations for the ACST at Torpa HPP.

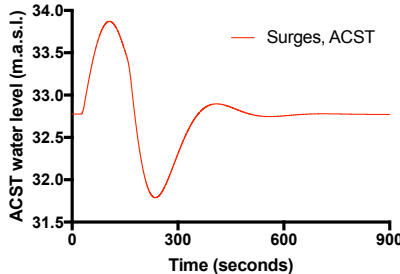
ACST at Åna-Sira HPP



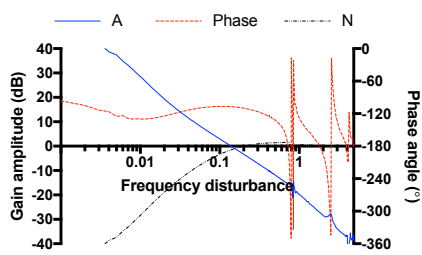
(a) Turbine pressure.



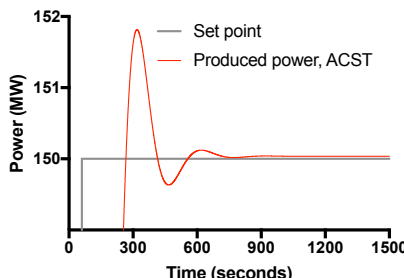
(b) Close up on turbine pressure.



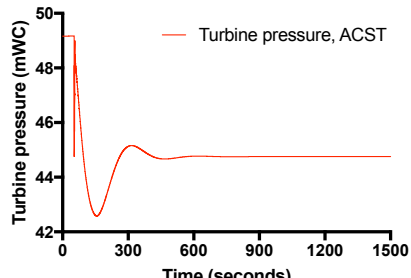
(c) Mass oscillations.



(d) Frequency-Response plot.



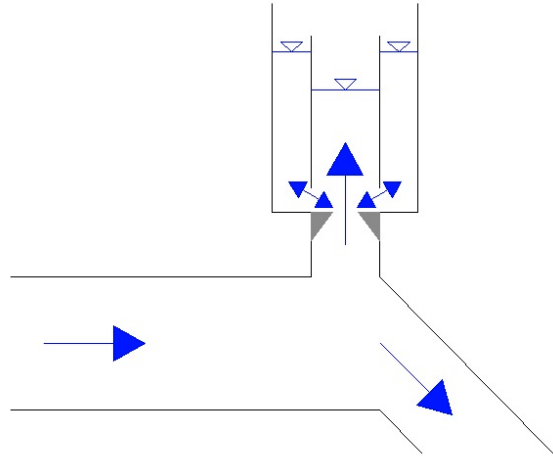
(e) Power Step-Response.



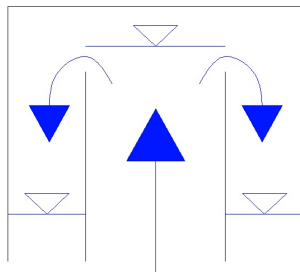
(f) Turbine pressure Step-Response.

Figure 5.9: LVTrans simulations for the ACST at Åna-Sira HPP.

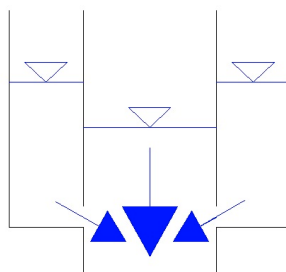
5.4 The Differential Surge Tank



(a) Conceptual design of the DST.



(b) Overflow of the DST.



(c) Throttling of the DST.

Figure 5.10: Conceptual design of the DST.

Description

The differential surge tank (DST) enhances a separation of the water so that a large water volume can be delayed. One way to create this effect is to construct a surge tank consisting of an inner riser where the water rises fast up the inner riser before it flows over the top, which functions like a weir into the outer chamber that has a larger area than the inner riser. The exit from the outer riser to the tunnel is then heavily throttled, thus delaying

the water even more. The difference in the water level in the inner riser and the outer chamber decides whether the water flows in or out the throttle mechanism.

Another solution for the DST is a combination of a SST and a throttled SST, placed close after each other. This is the solution that is the design for the simulations done in this Surge Tank Atlas.

On Figure 5.10 the DST is shaped as a vertical cylinder. The DST can also be shaped as a part of a chamber surge tank solution, for example in a 2CST, where the differential effect can be introduced by a throttle in the lower chamber, and by letting the water flow over a weir in the upper chamber.

Advantages

- The differential effects in the DST dampen the oscillations more efficiently compared to the SST.
- The throttling and the weir in the DST can reduce the excavated volume significantly by reducing the upsurge.

Disadvantages

- The design might give complex hydraulic conditions, and it has to be investigated in detail to find out how the weir and the throttle, or other installations, influence the hydraulic behavior in the DST.
- The construction of the chamber is potentially more expensive compared to a traditional open surge tank solution, both for simulating and modeling the solution, and to construct the throttle and the weir.

Documentation**DST at Torpa HPP**

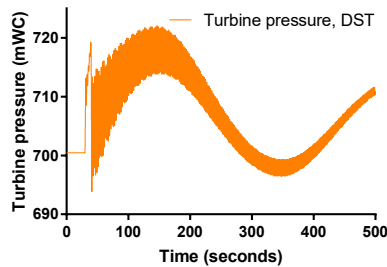
| Parameter | Unit | Value |
|---------------------------------|-----------------|-----------------------|
| Upsurge and downsurge - SST/DST | <i>m.a.s.l.</i> | 719 - 681 / 719 - 681 |
| Maximum turbine pressure | <i>mWc</i> | 721,5 |
| Water hammer amplitude | <i>mWc</i> | 719,5 |
| Mass oscillation amplitude | <i>mWc</i> | 718,5 |
| Water inertia time constant | <i>s</i> | 0,24 |
| Excavated volume - tunnels | $1000m^3$ | 710 |
| Excavated volume - surge tank | $1000m^3$ | 5,7 |
| Power overshoot | <i>MW</i> | 150,25 |
| Pressure undershoot | <i>mWc</i> | 691 |
| Cross frequency | <i>Hz</i> | 0,09 |
| Gain margin | <i>dB</i> | 9,9 |
| Phase margin | $^\circ$ | 81,9 |

Table 5.7: Simulated and calculated values for the DST at Torpa HPP.**DST at Åna-Sira HPP**

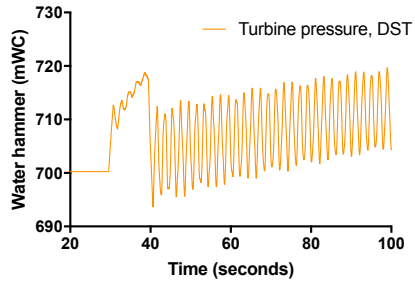
| Parameter | Unit | Value |
|---------------------------------|-----------------|-------------------------|
| Upsurge and downsurge - SST/DST | <i>m.a.s.l.</i> | 53,1 - 40,9 / 50,5 - 43 |
| Maximum turbine pressure | <i>mWc</i> | 53,1 |
| Water hammer amplitude | <i>mWc</i> | 50,7 |
| Mass oscillation amplitude | <i>mWc</i> | 53,1 |
| Water inertia time constant | <i>s</i> | 0,62 |
| Excavated volume - tunnels | $1000m^3$ | 407 |
| Excavated volume - surge tank | $1000m^3$ | 13,8 |
| Power overshoot | <i>MW</i> | 151,7 |
| Pressure undershoot | <i>mWc</i> | 42,4 |
| Cross frequency | <i>Hz</i> | 0,105 |
| Gain margin | <i>dB</i> | 20 |
| Phase margin | $^\circ$ | 79 |

Table 5.8: Simulated and calculated values for the DST at Åna-Sira HPP.

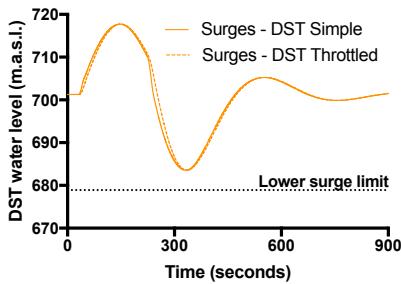
DST at Torpa HPP



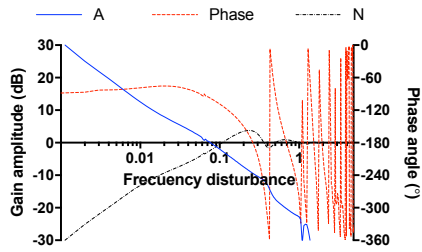
(a) Turbine pressure.



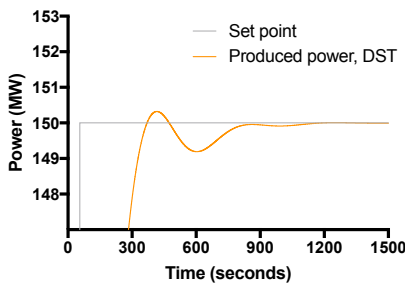
(b) Close up on turbine pressure.



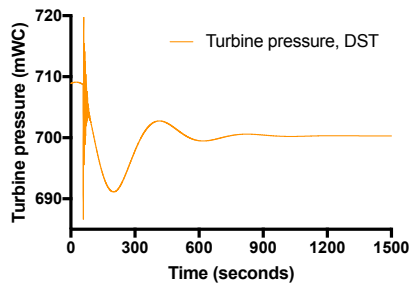
(c) Mass oscillations.



(d) Frequency-Response plot.



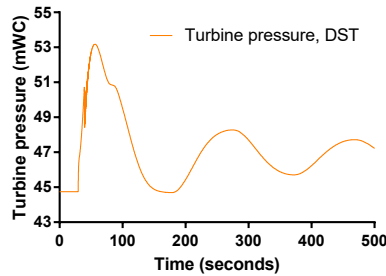
(e) Power Step-Response.



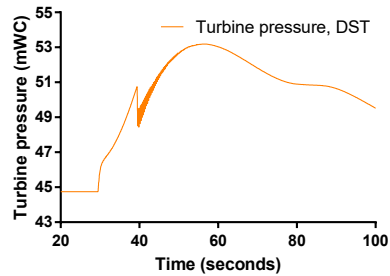
(f) Turbine pressure Step-Response.

Figure 5.11: LVTrans simulations for the DST at Torpa HPP.

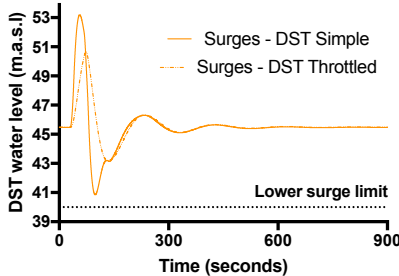
DST at Åna-Sira HPP



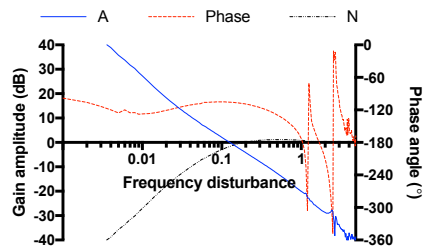
(a) Turbine pressure.



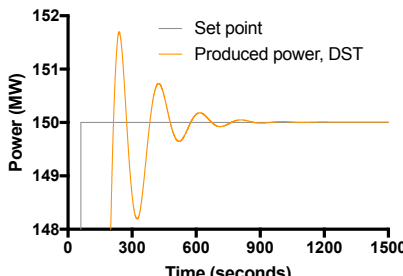
(b) Close up on turbine pressure.



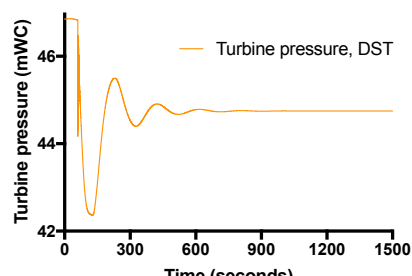
(c) Mass oscillations.



(d) Frequency-Response plot.



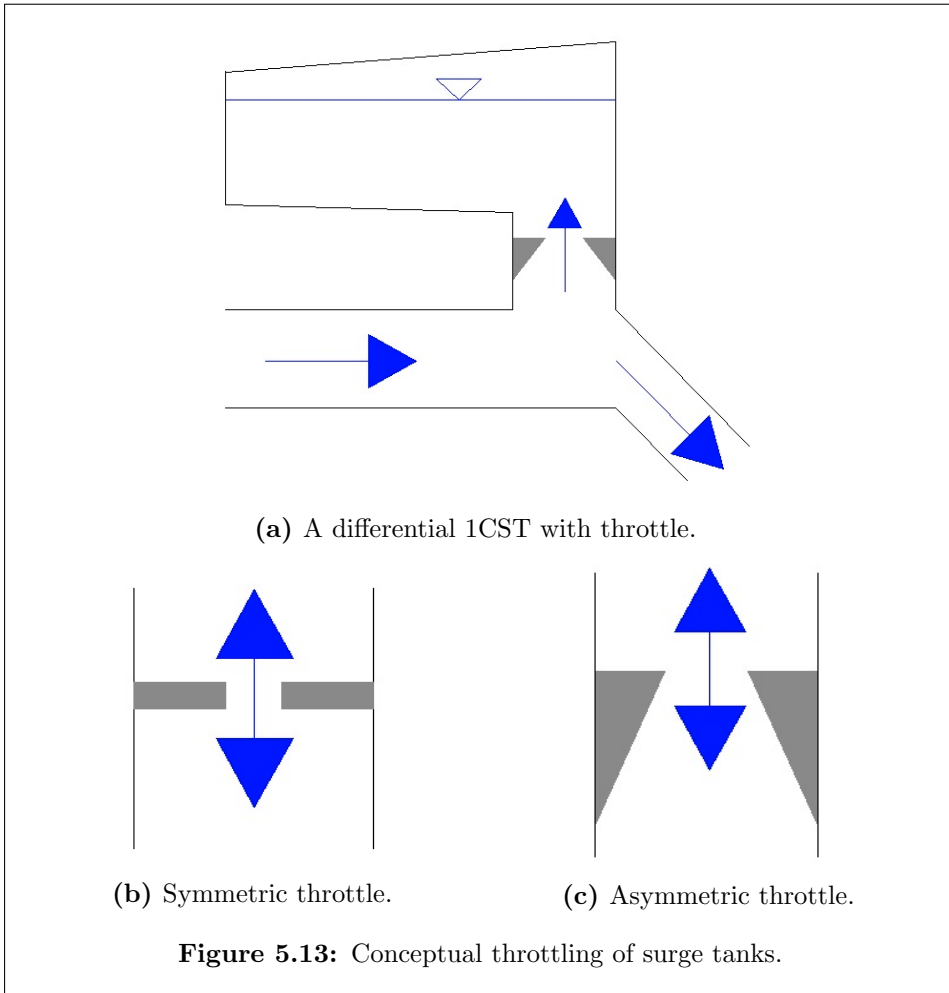
(e) Power Step-Response.



(f) Turbine pressure Step-Response.

Figure 5.12: LVTrans simulations for the DST at Åna-Sira HPP.

5.5 The Throttled Surge Tank



Description

A way to reduce the excavated volume in a surge tank, and to more efficiently optimize the hydraulic losses in the surge tank, is by installing a throttle in the surge tank. The singular loss will though have to be compared against the pressure amplitudes after a complete shutdown, as heavier throttling increases the water hammer and reduces the mass oscillation pressure amplitude. The throttle can be designed with symmetric or asymmetric

intended singular losses, or as a reverse-flow throttle - the vortex throttle. The asymmetric throttle is usually shaped as an orifice with increasing or decreasing diameter from the throttle inlet to the outlet.

The throttle itself, made by steel or concrete, is an expensive arrangement, but it might be worth the cost compared with the reduction of the total excavated volume. It is important to make sure, by simulation or modeling, that the throttle will work as planned, without a significant increase in the pressure amplitude from the water hammer.

Advantages

- Optimized loss coefficients.
- Less total excavated volume.
- Flexibility on how to construct the throttle and where to place it in the surge tank.
- Easy to combine with any kind of surge tank solution.

Disadvantages

- Increased water hammer pressure amplitude.
- More complex hydraulic behavior around the throttle.
- Difficult to modify after installation.

The C_v values used for the simulations for the 2CST and ACST at both Torpa HPP and Åna-Sira HPP are shown in Table 5.9.

| Surge tank solution | No throttling | Medium throttling | Strong throttling |
|----------------------|---------------|-------------------|-------------------|
| 2CST at Torpa HPP | 100000 | 1000 | 100 |
| ACST at Torpa HPP | 100000 | 30 | 8 |
| 2CST at Åna-Sira HPP | 100000 | 60000 | 15000 |
| ACST at Åna-Sira HPP | 100000 | 20000 | 5000 |

Table 5.9: Values for the singular losses for throttling of the 2CST and the ACST at Torpa and Åna-Sira HPP.

Documentation**Throttling of the 2CST at Torpa HPP**

| | | Throttling | | |
|-------------------------------------|-----------------|------------|--------|--------|
| Parameter | Unit | No | Medium | Strong |
| Upsurge | <i>m.a.s.l.</i> | 715 | 715 | 712 |
| Downsurge | <i>m.a.s.l.</i> | 681 | 680,8 | 686 |
| Water hammer pressure amplitude | <i>mWC</i> | 719 | 720 | 723 |
| Mass oscillation pressure amplitude | <i>mWC</i> | 715 | 715 | 713 |
| Power overshoot | <i>MW</i> | 150,20 | 150,15 | 149,8 |
| Pressure undershoot | <i>mWC</i> | 688,5 | 688,5 | 688 |
| Cross frequency | <i>Hz</i> | 0,091 | 0,091 | 0,091 |
| Gain margin | <i>dB</i> | 10 | 10 | 10 |
| Phase margin | ° | 85,1 | 85,1 | 85,1 |

Table 5.10: Simulated values for throttling of the 2CST at Torpa HPP.**Throttling of the ACST at Torpa HPP**

| | | Throttling | | |
|-------------------------------------|-----------------|------------|--------|--------|
| Parameter | Unit | No | Medium | Strong |
| Upsurge | <i>m.a.s.l.</i> | 293 | 292,8 | 292,6 |
| Downsurge | <i>m.a.s.l.</i> | 291,2 | 291,8 | 292,2 |
| Water hammer pressure amplitude | <i>mWC</i> | 714 | 729 | 748 |
| Mass oscillation pressure amplitude | <i>mWC</i> | 736 | 729 | 718 |
| Power overshoot | <i>MW</i> | 157 | 152,8 | 152 |
| Pressure undershoot | <i>mWC</i> | 673 | 683 | 686 |
| Cross frequency | <i>Hz</i> | 0,102 | 0,102 | 0,102 |
| Gain margin | <i>dB</i> | 12,1 | 12,1 | 12,1 |
| Phase margin | ° | 80 | 80 | 80 |

Table 5.11: Simulated values for throttling of the ACST at Torpa HPP

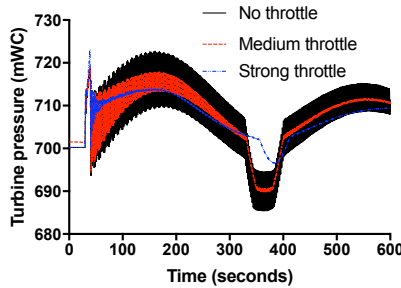
Throttling of the 2CST at Åna-Sira HPP

| | | Throttling | | |
|-------------------------------------|-----------------|------------|--------|--------|
| Parameter | Unit | No | Medium | Strong |
| Upsurge | <i>m.a.s.l.</i> | 49,8 | 49,7 | 49 |
| Downsurge | <i>m.a.s.l.</i> | 40 | 40,8 | 42,8 |
| Water hammer pressure amplitude | <i>mWC</i> | 49,1 | 49,5 | 52,5 |
| Mass oscillation pressure amplitude | <i>mWC</i> | 49,8 | 49,7 | 49,1 |
| Power overshoot | <i>MW</i> | 156,5 | 155,2 | 153,6 |
| Pressure undershoot | <i>mWC</i> | 42,4 | 42,8 | 43 |
| Cross frequency | <i>Hz</i> | 0,104 | 0,104 | 0,101 |
| Gain margin | <i>dB</i> | 21,5 | 21,5 | 20 |
| Phase margin | ° | 78,9 | 78,9 | 80 |

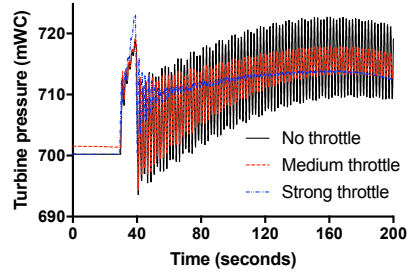
Table 5.12: Simulated values for throttling of the 2CST at Åna-Sira HPP.**Throttling of the ACST at Åna-Sira HPP**

| | | Throttling | | |
|-------------------------------------|-----------------|------------|--------|--------|
| Parameter | Unit | No | Medium | Strong |
| Upsurge | <i>m.a.s.l.</i> | 33,8 | 33,7 | 33,5 |
| Downsurge | <i>m.a.s.l.</i> | 31,8 | 32,2 | 32,6 |
| Water hammer pressure amplitude | <i>mWC</i> | 51 | 53,5 | 61 |
| Mass oscillation pressure amplitude | <i>mWC</i> | 54,9 | 53,5 | 51,6 |
| Power overshoot | <i>MW</i> | 151,8 | 151,4 | 150,6 |
| Pressure undershoot | <i>mWC</i> | 42,7 | 42,9 | 43,9 |
| Cross frequency | <i>Hz</i> | 0,106 | 0,106 | 0,104 |
| Gain margin | <i>dB</i> | 14 | 14 | 13,4 |
| Phase margin | ° | 75,6 | 75,6 | 77 |

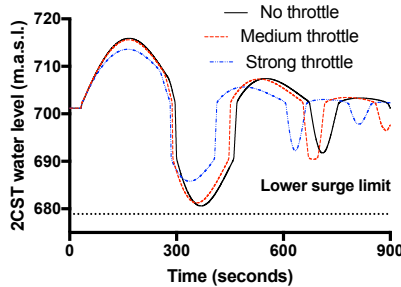
Table 5.13: Simulated values for throttling of the ACST at Åna-Sira HPP.

Throttling of the 2CST at Torpa HPP


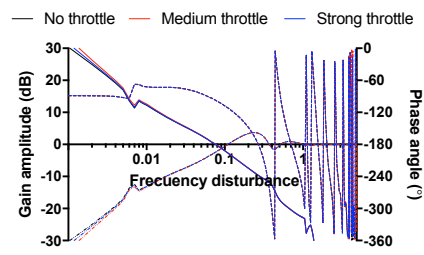
(a) Turbine pressure.



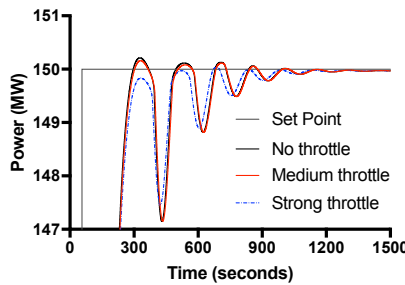
(b) Close up on turbine pressure.



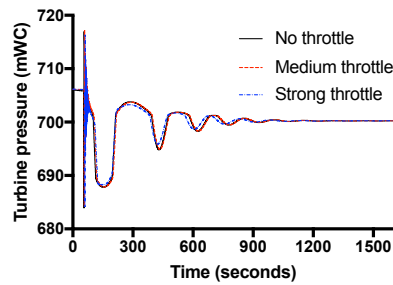
(c) Mass oscillations.



(d) Frequency-Response plot.



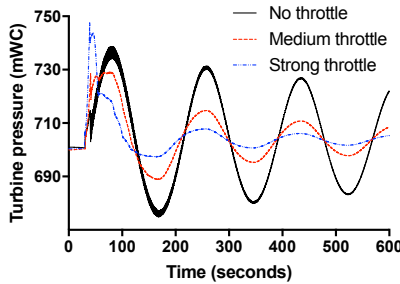
(e) Power Step-Response.



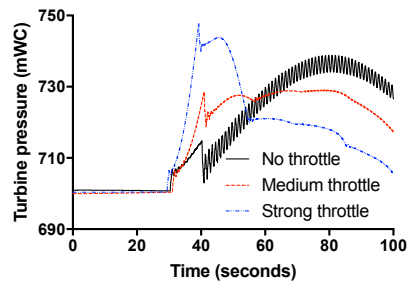
(f) Turbine pressure Step-Response.

Figure 5.14: LVTrans simulations for the throttling of the 2CST at Torpa HPP.

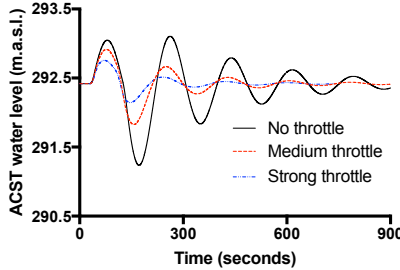
Throttling of the ACST at Torpa HPP



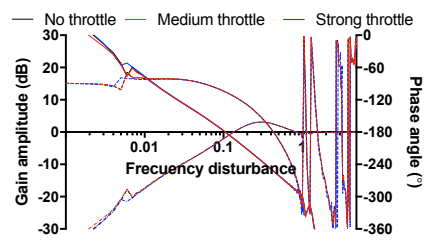
(a) Turbine pressure.



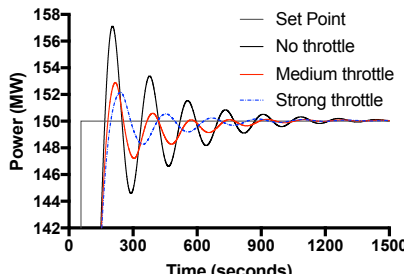
(b) Close up on turbine pressure.



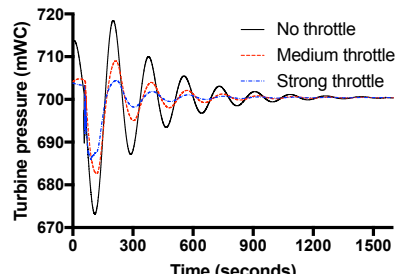
(c) Mass oscillations.



(d) Frequency-Response plot.



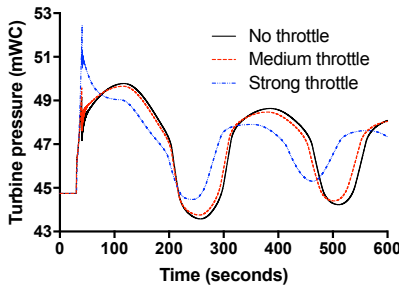
(e) Power Step-Response.



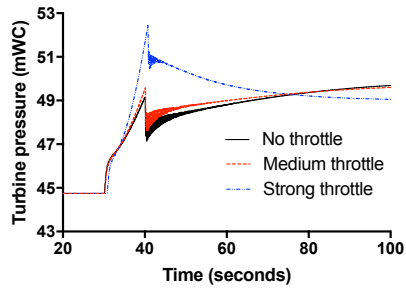
(f) Turbine pressure Step-Response.

Figure 5.15: LVTrans simulations for the throttling of the ACST at Torpa HPP.

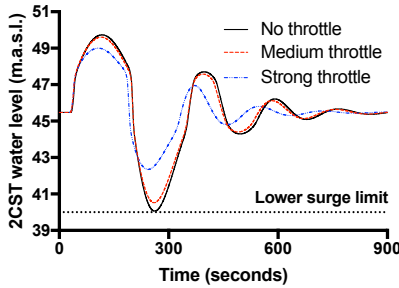
Throttling of the 2CST at Åna-Sira HPP



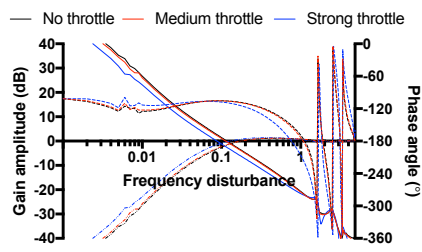
(a) Turbine pressure.



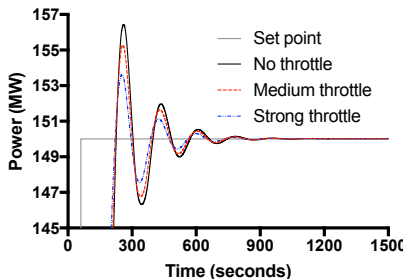
(b) Close up on turbine pressure.



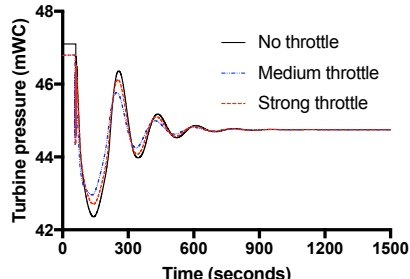
(c) Mass oscillations.



(d) Frequency-Response plot.



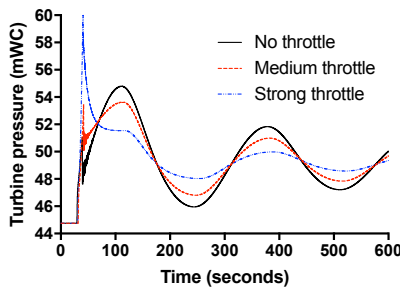
(e) Power Step-Response.



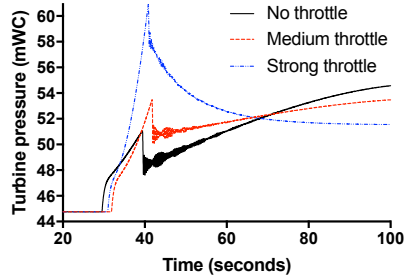
(f) Turbine pressure Step-Response.

Figure 5.16: LVTrans simulations for the throttling of the 2CST at Åna-Sira HPP.

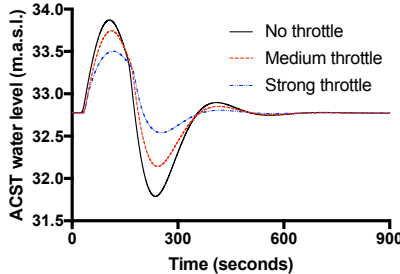
Throttling of the ACST at Åna-Sira HPP



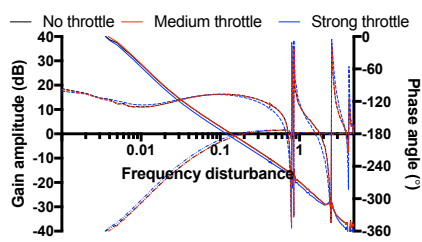
(a) Turbine pressure.



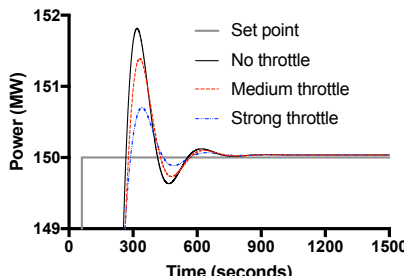
(b) Close up on turbine pressure.



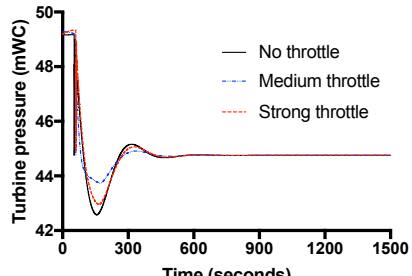
(c) Mass oscillations.



(d) Frequency-Response plot.



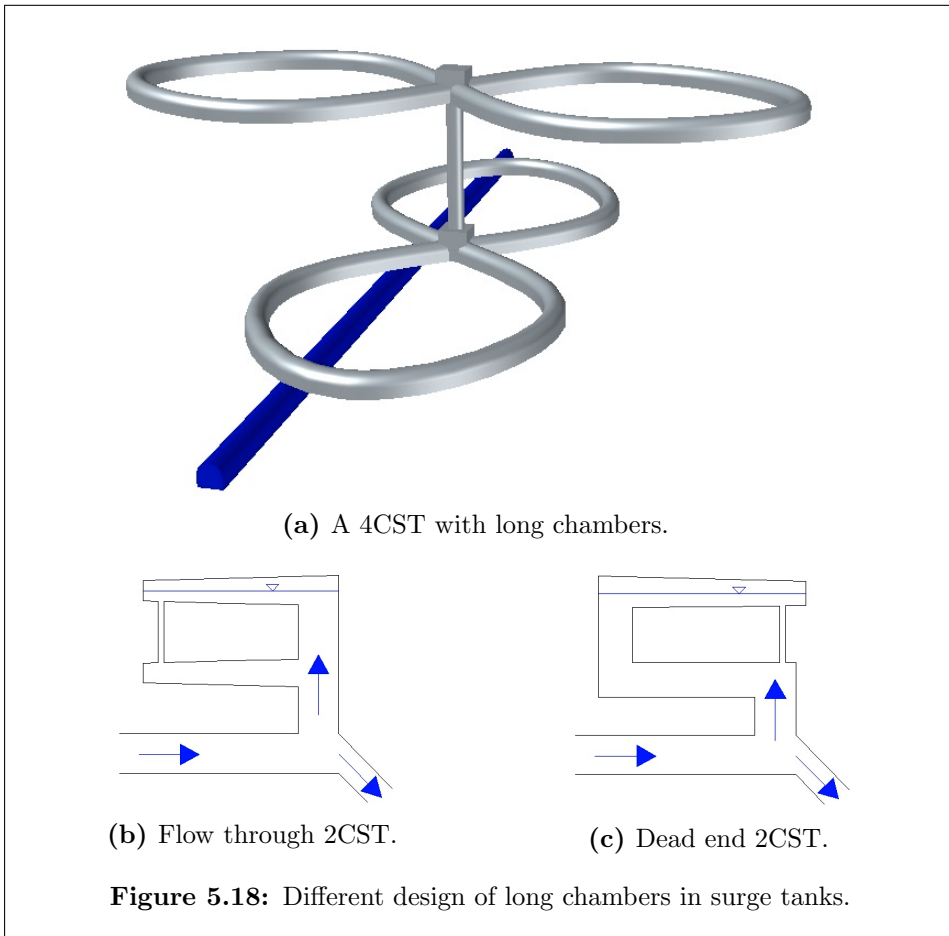
(e) Power Step-Response.



(f) Turbine pressure Step-Response.

Figure 5.17: LVTrans simulations for the throttling of the ACST at Åna-Sira HPP.

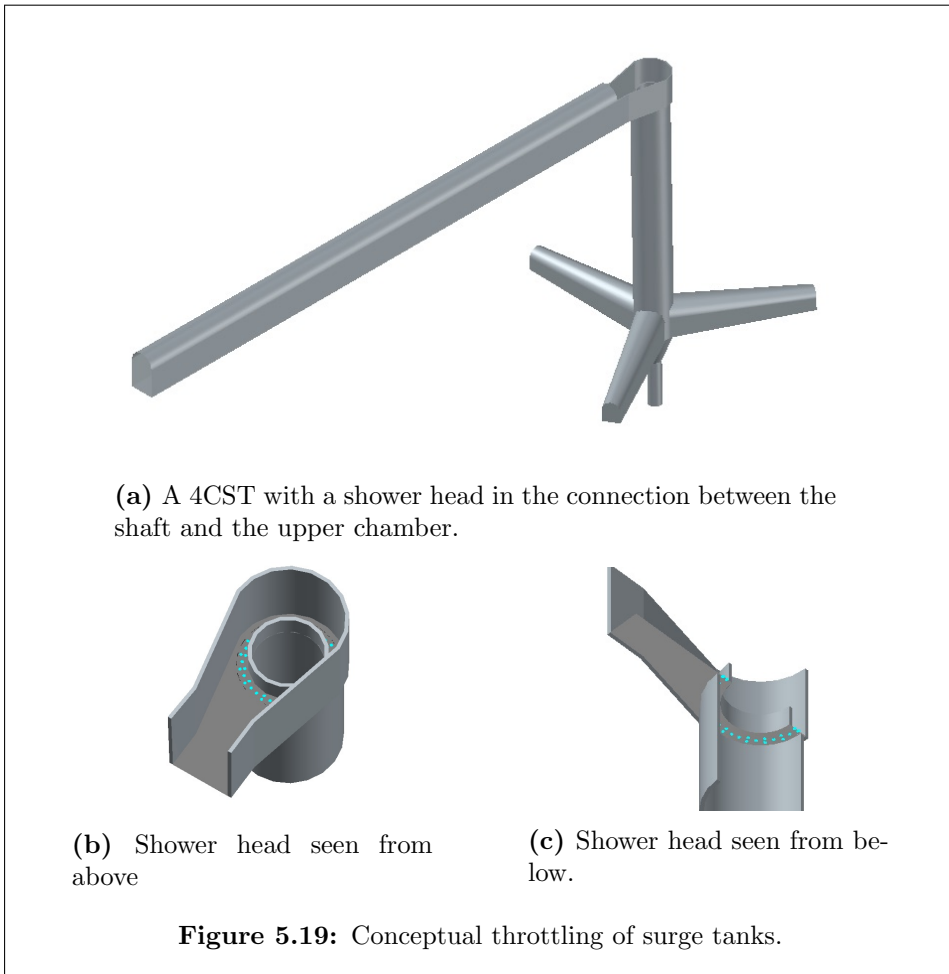
5.6 The Surge Tank with long chambers



Description

Long chambers as part of the surge tank introduces free surface flow, which gives a significantly different hydraulic behavior. To use these long chambers in the surge tank, as in the surge tank at Atdorf PSP in Germany (Richter et al., 2014), it is important to make sure that the flow in the chamber is not varying between pressurized flow and free surface flow, to maintain the system stable. Inclination of the chambers and control of the roughness, eventually with installments in the chamber to optimize the loss coefficients are ways to make sure the design criteria is met.

5.7 The Surge Tank with a "shower head"



Description

The "shower head" is an installation to reduce the massive waterfall in the connection between shaft and chamber. This waterfall can be damaging as it entrains air into the tunnel system. To dampen this waterfall, the "shower head" divides the water flow into several tiny water beams that hit the water surface in the shaft with less energy. The illustrations are based on the Krespa surge tank at the Obervermunt II PSP in Austria, from a model at TU Graz (Richter et al., 2012).

5.8 Parameter vulnerability analysis

As the results presented in the Surge Tank Atlas and in the section above are based on given designs of the hydropower plants, with fixed parameters, it is of interest to investigate how a variation of the parameters affects the behavior of the surge tanks. The performed simulations, and on what hydropower plant and surge tank solution they are performed on, are shown in the list below, and the values used for the simulations are shown in Table 5.14. The values are changed so that the simulations show sufficient differences to investigate how the behavior changes.

1. Placement of the surge tank for the 2CST solution at Torpa (1a) and Åna-Sira (1b), the water hammer is simulated. The distance from the surge tank to the turbine is increased and decreased.
2. Volume of the ACST at Torpa (2a) and Åna-Sira (2b), mass oscillations is simulated. The volume of the ACST is increased and decreased.
3. Volume of the ACST at Torpa (3a) and Åna-Sira (3b), mass oscillations is simulated. The volume of the ACST is increased and decreased.
4. PID-parameters of the ACST at Torpa (4a) and Åna-Sira (4b), power Step-Response test is simulated. P and T_i are turned more aggressive and more stable.
5. PID-parameters of the ACST at Torpa (5a) and Åna-Sira (5b), pressure Step-Response test is simulated. P and T_i are turned more aggressive and more stable.
6. Throttling of the SST at Åna-Sira, to find the optimal volume of the simple surge tank with throttling. A complete shutdown is simulated, and the turbine pressure is plotted.
7. Throttling of the SST at Åna-Sira, to find the optimal volume of the simple surge tank with throttling. A complete shutdown is simulated, and the mass oscillations is plotted.
8. Throttling of the SST at Åna-Sira, to find the optimal volume of the simple surge tank with throttling. The excavated surge tank volume is calculated.

9. Too strong throttling of the 2CST at Torpa (9a) and Åna-Sira (9b). A complete shutdown is simulated, and the turbine pressure is plotted.

10. Too strong throttling of the 2CST at Torpa (10a) and Åna-Sira (10b). A Step-Response test is simulated, and the produced power is plotted.

11. Too strong throttling of the 2CST at Torpa (11a) and Åna-Sira (11b). A Step-Response test is simulated, and the turbine pressure is plotted.

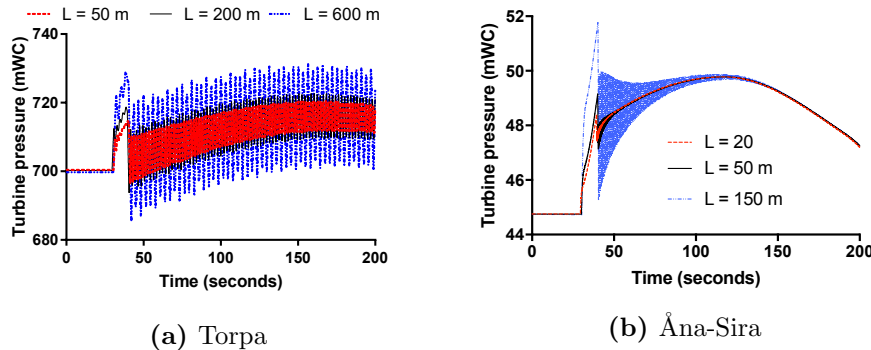


Figure 5.20: Complete shutdown simulation to investigate of how the placement of a 2CST affects the turbine pressure at Torpa and Åna-Sira.

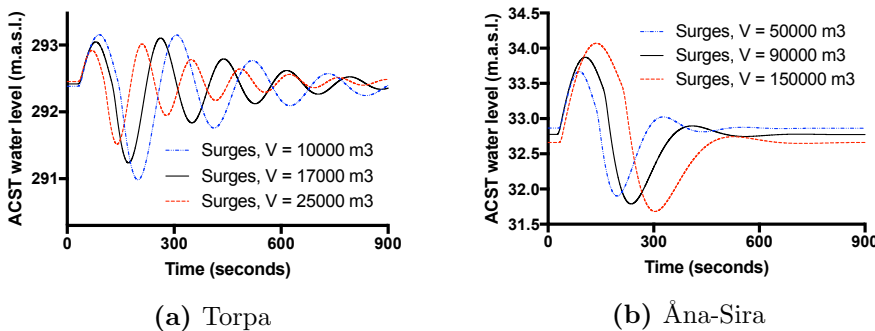


Figure 5.21: Worst case scenario simulation of how the mass oscillations change with the volume of the ACST at Torpa and Åna-Sira.

| Simulation | Minimum | Actual | Maximum | Figure |
|-------------------|----------------------|-------------------------------------|-----------------------|---------------|
| 1a - Torpa | 50 m | 200 m | 600 m | 5.20a |
| 1b - Åna-Sira | 20 m | 50 m | 150 m | 5.20b |
| 2a - Torpa | 10000 m ³ | 17000 m ³ | 25000 m ³ | 5.21a |
| 2b - Åna-Sira | 50000 m ³ | 90000 m ³ | 150000 m ³ | 5.21b |
| 3a - Torpa | 10000 m ³ | 17000 m ³ | 25000 m ³ | 5.22a |
| 3b - Åna-Sira | 50000 m ³ | 90000 m ³ | 150000 m ³ | 5.22b |
| 4a - Torpa | $P = 2, T_i = 8$ | $P = 4, T_i = 6$ | $P = 6, T_i = 4$ | 5.23a |
| 4b - Åna-Sira | $P = 2.5, T_i = 10$ | $P = 4.5, T_i = 8$ | $P = 6.5, T_i = 5$ | 5.23b |
| 5a - Torpa | $P = 2, T_i = 8$ | $P = 4, T_i = 6$ | $P = 6, T_i = 4$ | 5.24a |
| 5b - Åna-Sira | $P = 2.5, T_i = 10$ | $P = 4.5, T_i = 8$ | $P = 6.5, T_i = 5$ | 5.24b |
| 6 - Åna-Sira | - | $D = 65 \text{ m}, Cv = \text{Max}$ | $D = 48, Cv = 20000$ | 5.25a |
| 7 - Åna-Sira | - | $D = 65 \text{ m}, Cv = \text{Max}$ | $D = 48, Cv = 20000$ | 5.25b |
| 8- Åna-Sira | - | $D = 65 \text{ m}, Cv = \text{Max}$ | $D = 48, Cv = 20000$ | 5.26 |
| 9a - Torpa | - | $Cv = 100000$ | $Cv = 10$ | 5.27a |
| 9b - Åna-Sira | - | $Cv = 100000$ | $Cv = 1000$ | 5.27b |
| 10a - Torpa | - | $Cv = 100000$ | $Cv = 10$ | 5.28a |
| 10b - Åna-Sira | - | $Cv = 100000$ | $Cv = 1000$ | 5.28a |
| 11a - Torpa | - | $Cv = 100000$ | $Cv = 10$ | 5.29a |
| 11b - Åna-Sira | - | $Cv = 100000$ | $Cv = 1000$ | 5.29a |

Table 5.14: Values for the simulation in the parameter vulnerability analysis.

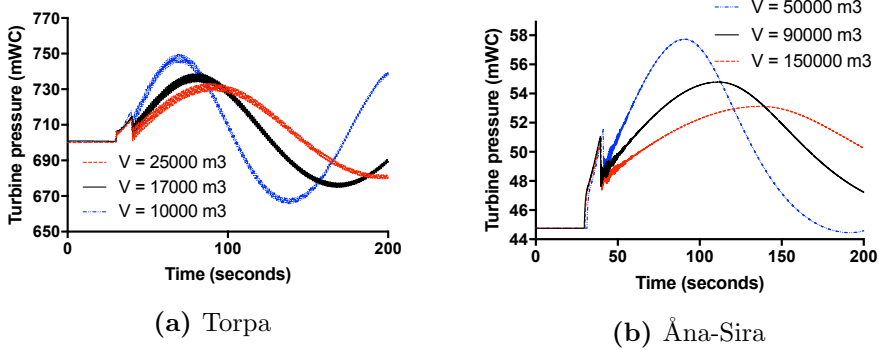


Figure 5.22: Complete shutdown simulation to investigate of how the volume of an ACST affects the turbine pressure at Torpa and Åna-Sira.

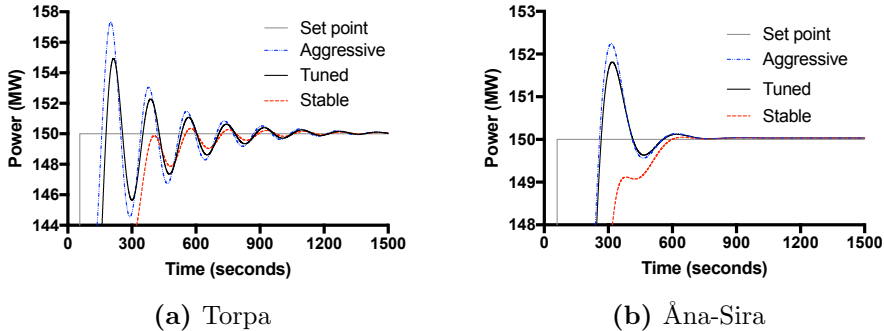


Figure 5.23: Step-Response test to investigate how the produced power changes with PID-parameters for the ACST at Torpa and Åna-Sira.

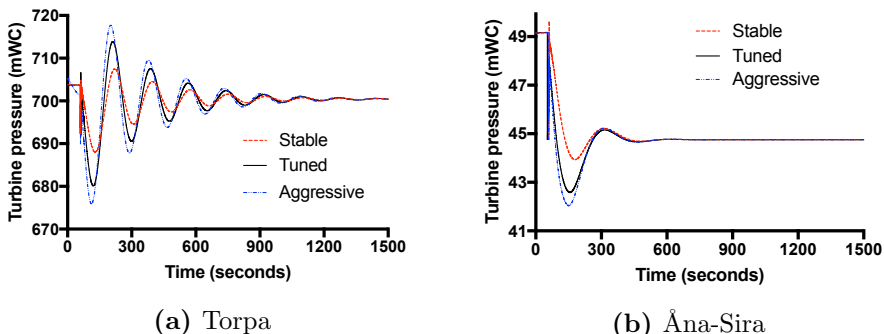


Figure 5.24: Step-Response test to investigate how the turbine pressure changes with PID-parameters for the ACST at Torpa and Åna-Sira.

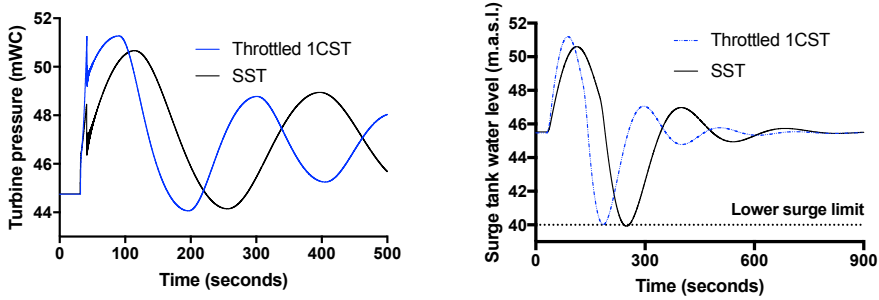


Figure 5.25: Complete shutdown to investigate how the turbine pressure changes with throttling, and worst case scenario simulation to investigate the mass oscillations with throttling of the SST at Åna-Sira.

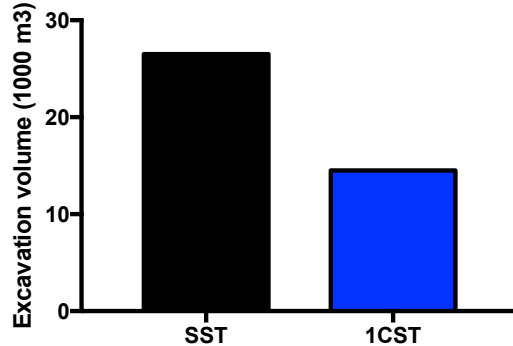


Figure 5.26: Calculation of excavated volume with throttling of the SST at Åna-Sira.

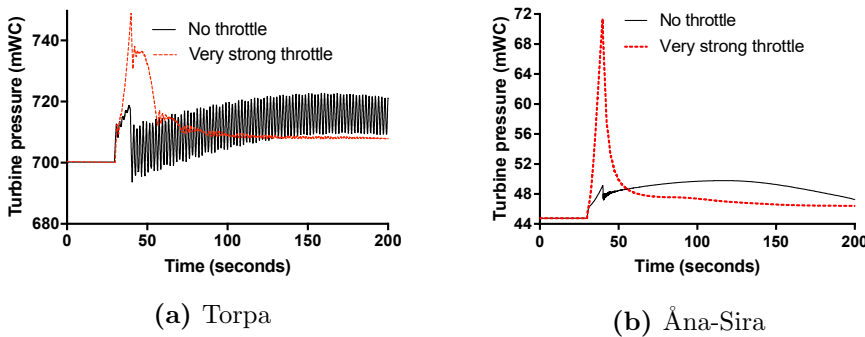


Figure 5.27: Complete shutdown simulated for very strong throttling of the 2CST at Torpa and Åna-Sira.

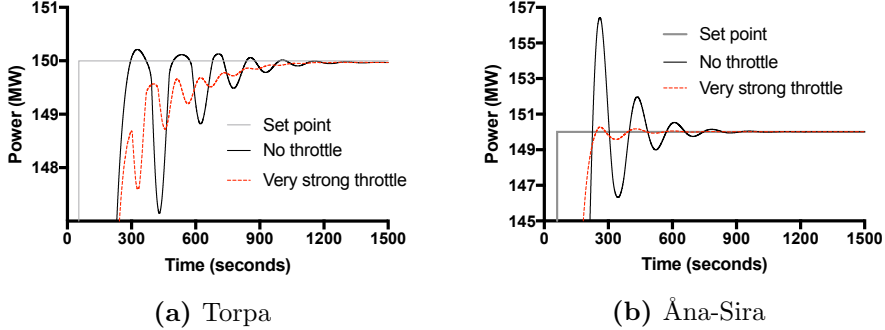


Figure 5.28: Step-Response test to investigate how the produced power changes with very strong throttling of the 2CST at Torpa and Åna-Sira.

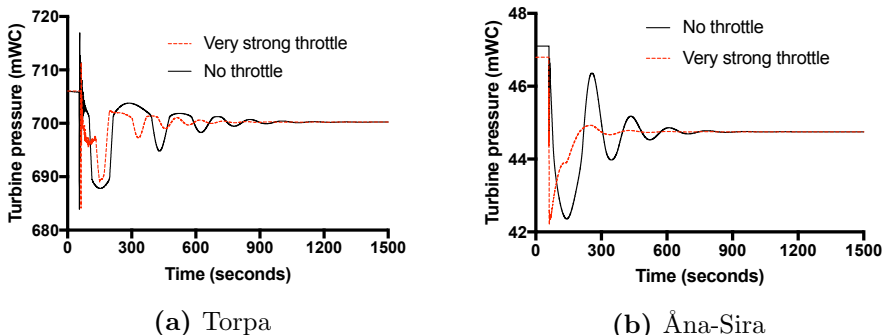


Figure 5.29: Step-Response test to investigate how the turbine pressure changes with very strong throttling of the 2CST at Torpa and Åna-Sira.

5.9 Comparison and discussion of results

In this section the results from the documentation sheets in the Surge Tank Atlas will be described and compared. The documentation in the Surge Tank Atlas could give some ideas on what surge tank solution is the most suitable for a given hydropower plant, but due to the complexity of these projects, a variation of the parameters will give more useful comparisons so that the Surge Tank Atlas will contain a wider variation of data. Hence it is important to read these results and comparisons with some precautions, as they depend on several parameters with a wide range of values. A change in one of these parameters can change the results from the simulations, and hence the conclusions drawn from the results presented in the Surge Tank Atlas.

5.9.1 Turbine pressure after complete shutdown

The first significant difference between the behavior of the turbine pressure at Torpa and Åna-Sira HPP, as shown in Figure 5.30, is that the water hammer oscillate with a very small period for Torpa HPP, especially for the SST and the 2CST. The turbine pressure for the DST follows the same curve as the SST and the 2CST, due to the mass oscillations, but due to the differential effect of the DST, the oscillating water hammer dampens faster. This throttling effect is also shown on Figure 5.14b, where it is clearly visible how the throttle increases the first maximum water hammer pressure amplitude, and reduces the following oscillating water hammer. These water hammer oscillations are damped faster for the ACST, and for all the surge tank solutions at the low head hydropower plant. It is also worth to mention that the turbine pressures, in percent above the static pressure, are significantly higher for the Åna-Sira HPP.

As shown in the parameter vulnerability analysis, the placement of the surge tank is a very important parameter for the behavior of the water hammer and the mass oscillation pressure amplitude, as a shorter distance between the surge tank and the turbine reduces the water hammer amplitude, while the changes for the mass oscillation amplitude are almost negligible. A consequence of this is that the open surge tank solutions in a high head hydropower plant may have the highest turbine pressure as a combination of the mass oscillation pressure amplitude and the water hammer pressure amplitude.

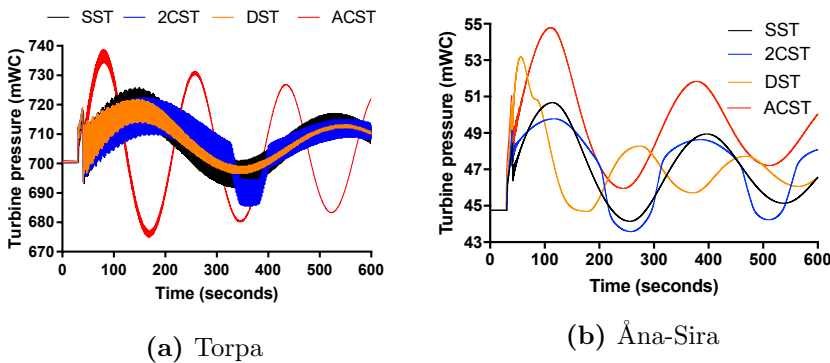


Figure 5.30: Comparison of turbine pressure after turbine shutdown.

The volume of the surge tank also plays an important role for the turbine pressure. Changes in the volume, in this case simulated for the ACST at Torpa and Åna-Sira HPP, does not affect the water hammer pressure amplitude significantly, as the water hammer reaches the free water surface in the surge tank, but the pressure amplitude from the mass oscillations and the frequency of the mass oscillations increase with smaller surge tank volume.

When the surge tank is throttled, the goal is to optimize the hydraulic losses. The throttling is optimal when the pressure amplitudes from the water hammer and the mass oscillation equal each other. It is easy to observe from the simulations that stronger throttling introduces a larger singular loss when water flows into the surge tank, hence the pressure amplitude from the water hammer increases significantly, and the mass oscillations decrease. Too strong throttling, as shown for the 2CST at Torpa and Åna-Sira HPP, will give water hammers far above the design pressure, which is best shown by the strong throttling of the 2CST at Åna-Sira as shown in Figure 5.29b, where the mass oscillations are almost gone, hence the surge tank has nearly lost its function.

5.9.2 Mass oscillations

For the mass oscillations in the surge tanks, which are the water masses that oscillate between the upper magazine and the reservoir inside the surge tank, there are a significant difference between the open and the closed surge tank, due to the different design and the air pressure in the closed

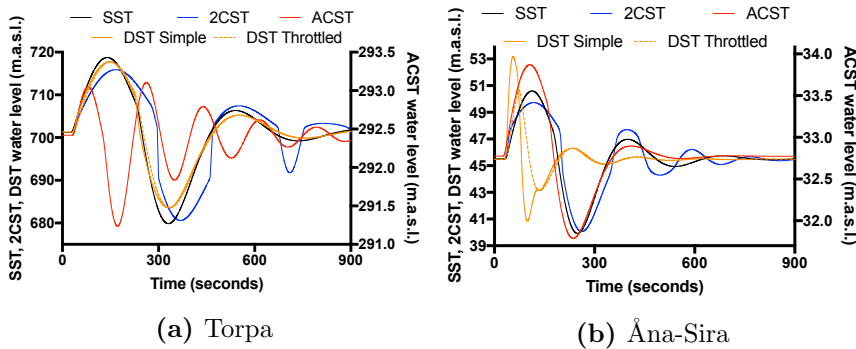


Figure 5.31: Comparison of water levels in the surge tanks.

ACST. For the open surge tank the water level oscillations in the surge can be of large amplitudes, while the closed air cushion surge tank have amplitudes significantly smaller than the open surge tank. The behavior and the frequency of the mass oscillations can be quite similar, as is the fact for the simulation for the ACST at Åna-Sira, and the ACST at Torpa could probable have yielded the same behavior with a larger surge tank volume, increasing the surge period of the ACST.

Smaller volume of the surge tank gives larger values of the upsurge and downsurge values and more frequent surges, a change in the distance between the surge tank and the turbine does not affect the mass oscillations significantly, throttling of the surge tank gives smaller values of the upsurge and downsurge, and too strong throttling almost removes the surges in the surge tank.

5.9.3 Turbine regulation

In the following sections the results from the Frequency-Response tests and the Step-Response tests will be described to evaluate the stability and the governing performance of the hydropower plants, and how the surge tanks affect these. The results from the simulations are shown in Tables 5.15 and 5.16.

| Frequency-Response parameters | | | | |
|--------------------------------------|------------|-------------|-------------|------------|
| Parameter | SST | 2CST | ACST | DST |
| Cross frequency (Hz) | 0,09 | 0,091 | 0,102 | 0,09 |
| Gain margin $\angle h$ (dB) | 10 | 10 | 12,1 | 9,9 |
| Phase margin Ψ ($^{\circ}$) | 81,8 | 85,1 | 80 | 81,9 |
| Step-Response parameters | | | | |
| Parameter | SST | 2CST | ACST | DST |
| Power overshoot (MW) | 150,15 | 150,2 | 157 | 150,25 |
| Pressure undershoot (mWc) | 693 | 688,5 | 673 | 691 |

Table 5.15: Simulated regulation parameters for the surge tank solutions at Torpa HPP.

| Frequency-Response parameters | | | | |
|--------------------------------------|------------|-------------|-------------|------------|
| Parameter | SST | 2CST | ACST | DST |
| Cross frequency (Hz) | 0,09 | 0,104 | 0,106 | 0,105 |
| Gain margin $\angle h$ (dB) | 20 | 21,5 | 14 | 20 |
| Phase margin Ψ ($^{\circ}$) | 81,9 | 78,9 | 75,6 | 79 |
| Step-Response parameters | | | | |
| Parameter | SST | 2CST | ACST | DST |
| Power overshoot (MW) | 152,8 | 156,5 | 151,2 | 151,7 |
| Pressure undershoot (mWc) | 42,6 | 42,4 | 42,7 | 42,4 |

Table 5.16: Simulated regulation parameters for the surge tank solutions at Åna-Sira.

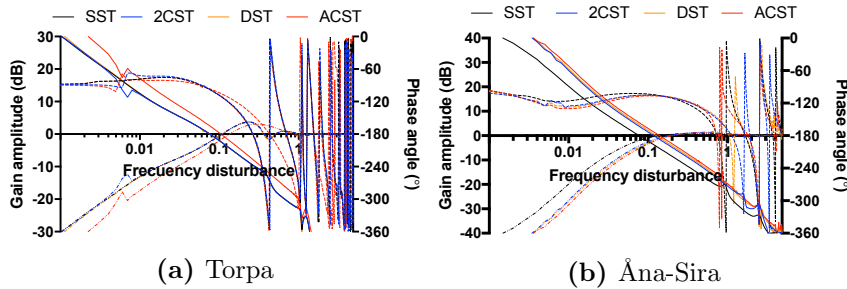


Figure 5.32: Comparison of Bode plots.

Frequency-Response test

As shown in Figure 5.32, the behavior of the Bode plots are different for the hydropower plants, but all of the values for the gain margin and the phase margin are within the acceptable limits, as they state that the phase margins are more than 45° and the gain margin more than 6 dB , hence the Bode plots confirm that all of the solutions are stable, and all of them with good margins, giving an opportunity to run the power plants more aggressively, for example by changing the PID-parameters to improve the governor performance, or to reduce the size of the surge tanks.

When acceptable throttling values are used, meaning that the turbine pressure after a shutdown maintains within the design pressure, the Bode plots all show that the changes in the cross frequency, gain margin and phase margin are quite small. Hence both medium and strong throttling of both Torpa and Åna-Sira HPP give acceptable values from the Frequency-Response test.

Power Step-Response test

For the power Step-Response, the results for the Åna-Sira HPP show a similarity between the closed surge tank and the open surge tank solutions, while the behavior for the open surge tank solutions for Torpa HPP show a different governor performance compared to the closed surge tank, with lower power overshoot values, and hence a slower operation of the hydropower plant. More aggressive PID-parameters increase the power overshoot values, and stronger throttling decreases the power overshoot.

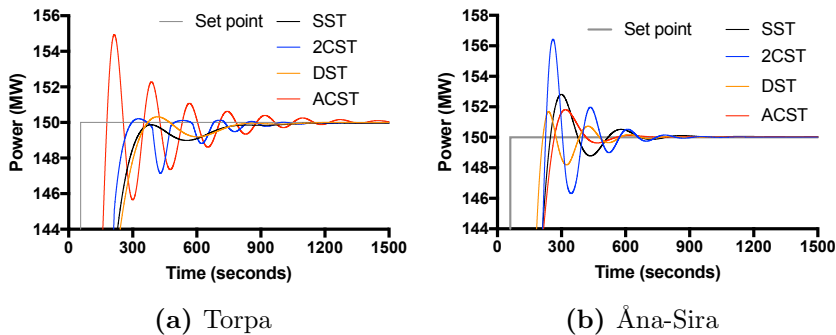


Figure 5.33: Comparison of power Step-Response.

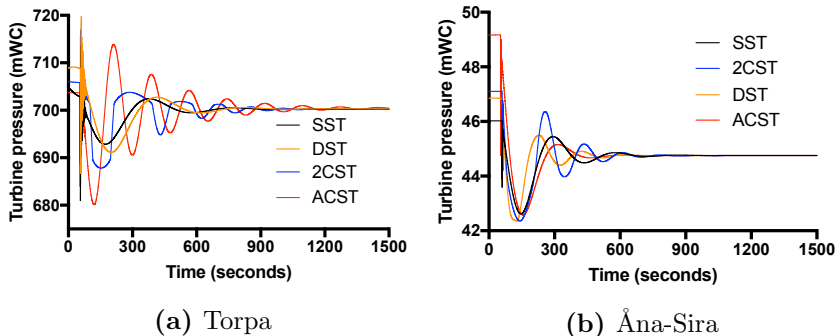


Figure 5.34: Comparison of pressure Step-Response.

Pressure Step-Response test

The pressure Step-Response show that the pressure undershoot is bigger for the ACST at Torpa, as it is the solution that reaches the highest power overshoot. The open surge tank solutions at Torpa have quite similar behavior, but one can see, as is also the case for the power Step-Response, that the response for the 2CST is delayed a little bit before it drops more suddenly, due to the storage capacity in the chambers and the connection shaft between the chambers with a much smaller diameter compared to the chambers. More aggressive PID-parameters give a higher pressure undershoot, while too strong throttling increases the pressure undershoot slightly, and almost removes the turbine pressure oscillations.

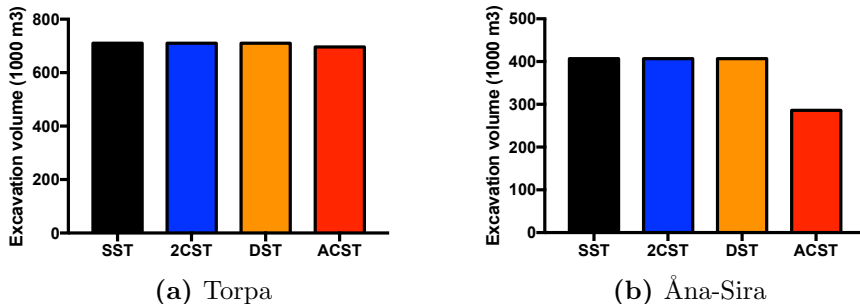


Figure 5.35: Excavation volumes of the tunnels at Torpa and Åna-Sira.

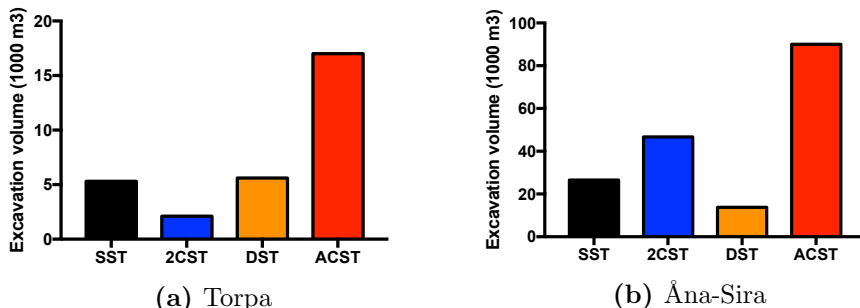


Figure 5.36: Excavation volumes of the surge tanks at Torpa and Åna-Sira.

5.9.4 Excavations

In Figures 5.35 and 5.36 the total excavation volumes for the solutions are shown, one for the tunnels and one for the surge tanks. As one can see, in general the water way for the closed air cushion surge tank requires smaller volume than the open surge tank solutions, but on the other side the surge tank itself requires more excavation volume. The surge tank excavation volumes are larger for the Åna-Sira HPP.

The changes in the necessary excavation volume for a SST and a throttled SST, in this case the 1CST at Åna-Sira, the excavation volume for the 1CST is almost half the excavation volume of the SST, hence the throttle itself can save a significant amount of excavation. The mass oscillations in both of the solutions are quite similar, when the diameter of the surge shaft is reduced from 65 to 48 meters.

Chapter 6

Conclusion and suggestions for future work

In this chapter conclusions will be drawn from the results presented in the Surge Tank Atlas, and some suggestions for future work will be presented.

6.1 Conclusion

Based on the results presented in Section 5.9, the following conclusions can be drawn:

6.1.1 Turbine pressure after complete shutdown

The most important conclusions from the results of the turbine pressure after a complete shutdown are:

- There is a significant difference in the turbine pressure after a turbine shutdown, as the closed surge tank dampens the water hammer more efficient than the open surge tank. For both the open and the close surge tank, closer placement of the surge tank reduces the water hammer pressure amplitude, while the mass oscillation pressure amplitude remains unchanged. Smaller volume of the surge tank increases the water hammer, and increase both the amplitude and the frequency of the mass oscillations.
- The difference in the behavior of the open and the closed surge tank solutions are bigger for a high head than a low head hydropower plant, due to the frequent water hammer oscillations that follows the mass oscillations for the open surge tank in the high head hydropower plant.

- Throttling of the surge tank increases the water hammer pressure amplitude significantly, and decreases the mass oscillation pressure amplitude, thus giving a more efficient dampening of the turbine pressure. If the throttle is too strong the surge tank loses its function, as the pressure amplitude from the water hammer increases drastically and the mass oscillations almost disappear. It is important that a strong throttling of the surge tank is tested good enough during various load situations to be sure that the throttle is not too strong.

6.1.2 Mass oscillations

The above mentioned turbine pressure from the mass oscillations depends, and are directly connected to, the mass oscillation between the surge tank and the upper reservoir, hence the behavior of the surges in the surge tank serve to describe how the turbine pressure will evolve after a complete shutdown. The most important conclusions are:

- The water level in the surge tank has a higher amplitude for an open surge tank compared to the closed surge tank, but the behavior and period of the surges can be similar. As the closed surge tank is pressurized, a lower amplitude in meters and a closer placement to the turbine do not necessarily mean that the turbine pressures are lower than for the open surge tank, as this is a combination of several factor, especially the placement and volume of the surge tank.
- Throttling of the surge tank reduces the mass oscillations and the amplitude of the surges in the surge tank, while too strong throttling almost removes the surges completely, and hence the function of the surge tank.

6.1.3 Turbine regulation

Regulation of the hydropower plant is essential, as the reason for the existence of the hydropower plant is to deliver power to the grid. As the author master's thesis had limited knowledge to turbine regulation the approach has been of a more general approach, but some conclusions can be drawn, and the most important are:

- The tuned PID-parameters for all of the simulated surge tank solutions, both at the high and low head hydropower plant, are not very different, hence the values of P and T_i could have been the same for all the solutions.
- The Bode plots are similar for the open and the close surge tank, while there are some differences from the high and the low head hydropower plant. Still the used PID-parameters prove that the simulated hydropower plants are able to perform a stable operation, also with medium and strong throttling of the surge tanks.
- The Step-Response tests show more changes than the Bode plots, as throttling of the surge tank limits the power overshoot and the pressure undershoot. Too strong throttling of the surge tank gives a much slower regulation compared to the situation with no throttle as the power overshoot decreases drastically, meaning that the hydropower plant uses longer time to reach the wanted Set point of 150 MW.

6.1.4 Other conclusions

Some other conclusions are also drawn from the simulations in the Surge Tank Atlas:

- There is a significant difference between the high and the low head hydropower plant regarding the water time inertia constant, with higher values of t_a for the low head hydropower plant, hence the water masses in the low head hydropower plant are significantly slower than in the high head plant. This leads to the conclusion that the water masses at the high head hydropower plant are more vulnerable for disturbances and singular losses in the water way, as shown in Table 5.9, where it is proved that the ACST can be throttled stronger than the 2CST, for both hydropower plants.
- Throttling of the surge tank reduces the necessary volume significantly, which for a SST compared with a throttled 1CST could mean a significant saving in excavation volume. As the surge tanks are bigger for the low head hydropower plant, both absolutely and relatively to the excavated tunnel volume, this would have a bigger effect for the low head hydropower plant.

- The PID-parameters are of great importance for the other simulations to be correct, and it is very difficult to draw conclusion based on bad tuned PID-parameters. For example the open surge tanks at the high head hydropower plant at Torpa acts a little bit slower than the open surge tanks at Åna-Sira, probably due to PID-parameters that could have been more aggressive.

6.2 Suggestions for future work

As future work within the same subject, the following is proposed:

- A Surge Tank Atlas like this could have been systematized further, where one can imagine a more interactive Surge Tank Atlas with the possibility of given parameters as input, and actual surge tank solutions as output. It would also been interesting to use the same method to investigate a high head hydropower plant with larger discharge, and a low head hydropower plant with lower discharge, to widen the simulations scenarios further.
- The programming of the DST should be finished, to be able to use the DST as an integrated solution in LVTrans. The simulations performed in this Surge Tank Atlas are based on a combined solution with a SST and a throttled SST, hence the behavior is comparable to a throttled open surge tank, that dampens the water hammer more efficient compared to the unthrottled open surge tank. A DST with a weir allowing water to flow from the inner to the outer chamber, and a throttle unit between the inner and outer riser would have been of interest in the Surge Tank Atlas.
- To be able to simulate long chambers in LVTrans, with free surface flow, a programming of a unit allowing this would have been interesting. As LVTrans already has a unit for free surface flow, the process of connecting this unit, through a connection shaft, would have made it possible to widen the surge tank basis significantly in a Surge Tank Atlas.

Bibliography

- Balchen, J. G., Trond Andresen and Bjarne A. Foss (2003), *Reguleringssteknikk*, Institutt for teknisk kybernetikk, NTNU, Trondheim.
- Bode, H. W. (1945), *Network Analysis and Feedback Amplifier Design*, D. Van Nostrand Company, New York.
- Broch, E. (2000), Unlined High Pressure Tunnels and Air Cushion Surge Chambers, in ‘AITES-ITA World Tunnel Congress’, South African Institute of Mining and Metallurgy, Durban, South Africa.
- Dahlø, T. (1988), ‘Experience from Air Cushion Surge Chambers’, *Norwegian Tunneling Today* (5).
- Edvardsen, S. and Broch, E. (2002), *Underground Powerhouses and High Pressure Tunnels*, Vol. 14 of *Hydropower Development*, Department of Hydraulic and Environmental Engineering, NTNU, Trondheim, Norway.
- Gomsrud, D. (2015), Design of a Surge Tank Throttle for Tonstad Hydropower Plant, PhD thesis, Department of Hydraulic and Environmental Engineering, Norwegian University of Science and Technology.
- Guttormsen, O. (2006), *TVM4165 Vannkraftverk og Vassdragsteknikk. Vassdragsteknikk II*, Tapir Akademiske Forlag, Trondheim, Norway.
- Hu, J., Zhang, J., Suo, L. and Fang, J. (2007), Advance in Research on Air Cushion Surge Chamber in Hydropower Plan, in ‘International Mechanical Engineering Congress and Exposition’, ASME, Seattle, Washington, USA.
- Jaeger, C. (1954), *Present Trends in Surge Tank Design*, Institution of Mechanical Engineers.
- Johnson, R. D. (1908), *The Surge Tank in Water Power Plants*, American Society of Mechanical Engineers Transactions, Niagara Falls, New York.
- National Instruments (2016), ‘PID Theory Explained’, <http://www.ni.com/white-paper/3782/en/> (Accessed June 1st 2016).
- Nielsen, T. (1990), *Dynamisk Dimensjonering av Vannkraftverk*, Vannkraftlaboratoriet, NTNU, Trondheim, Norway.

BIBLIOGRAPHY

- Nielsen, T. (2015), *Dynamic Dimensioning of Hydro Power Plants*, Vannkraftlaboratiet, NTNU.
- Oppland Energi AS (2016), ‘Torpa kraftverk’, <http://www.opplandenergi.no/Kraftverksoversikt/Torpa/> (Accessed March 7th 2016).
- Richter, W., Dobler, W. and Knoblauch, H. (2012), Hydraulic and Numerical Modelling of an Asymmetric Orifice Within a Surge Tank, in ‘4th IAHR International Symposium on Hydraulic Structures’, Porto, Portugal.
- Richter, W., Schneider, J., Knoblauch, H. and Zenz, G. (2014), Behaviour of Long Chambers in Surge Tanks, Technical report, Institute of Hydraulic Engineering and Water Resources Management, TU Graz, Austria.
- Sandvåg, S. U. (2015), Surge Tank Design for Pumped Storage Plants in Norway, Project thesis, Department of Hydraulic and Environmental Engineering, Norwegian University of Science and Technology, Trondheim, Norway.
- Statnett (2016), ‘Nettdrift er en balansekonst’, <http://statnett.no/Samfunnsoppdrag/vart-samfunnsoppdrag/Nettdrift-er-en-balansekunst/> (Accessed June 4th 2016).
- Steyrer, P. (1999), Economic Surge Tank Design by Sophisticated Hydraulic Throttling, in ‘28th IAHR Congress’, Graz, Austria.
- Svee, R. (1972), Surge Chamber with an Enclosed, Compressed Air-Cushion, in ‘International Conference of Pressure Surges’, BHRA Fluid Engineering, Canterbury, England.
- Svingen, B. (2015), Lvtrans manual 18.05.2015, Technical report, Trondheim, Norway.
- Thoma, D. I. D. (1910), *Zur Theorie des Wasserschlusses bei selbsttätig geregelten Turbinenanlagen*, Technischen Hochschule München, München, Germany.
- Vereide, K., Lia, L., Richter, W. and Zenz, G. (2015), ‘Surge Tank Research in Austria and Norway’, *WasserWirtschaft Extra* 1, 58 – 62.
- Vereide, K., Svingen, B., Nielsen, T. and Lia, L. (2016), ‘Effect of Surge Tank Throttling on Governor stability and Performance in Hydropower Plants’, *IEEE Transactions on Energy Conversion*.

- Vereide, K. V., Tekle, T. and Nielsen, T. K. (2015), ‘Thermodynamic Behavior and Heat Transfer in Closed Surge Tanks for Hydropower Plants’, *Journal of Hydraulic Engineering* **141**(6).
- Wylie, E. B. and Streeter, V. L. (1993), *Fluid Transients in Systems*, Prentice Hall, Englewood Cliffs, NJ.

BIBLIOGRAPHY

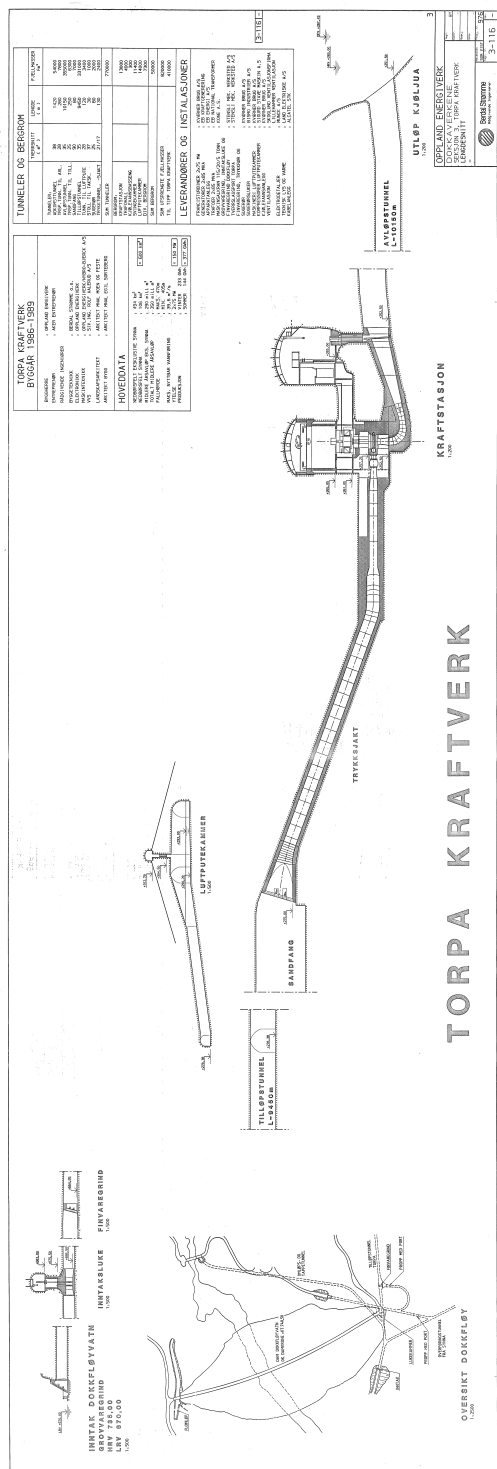
Appendix A

Construction drawings

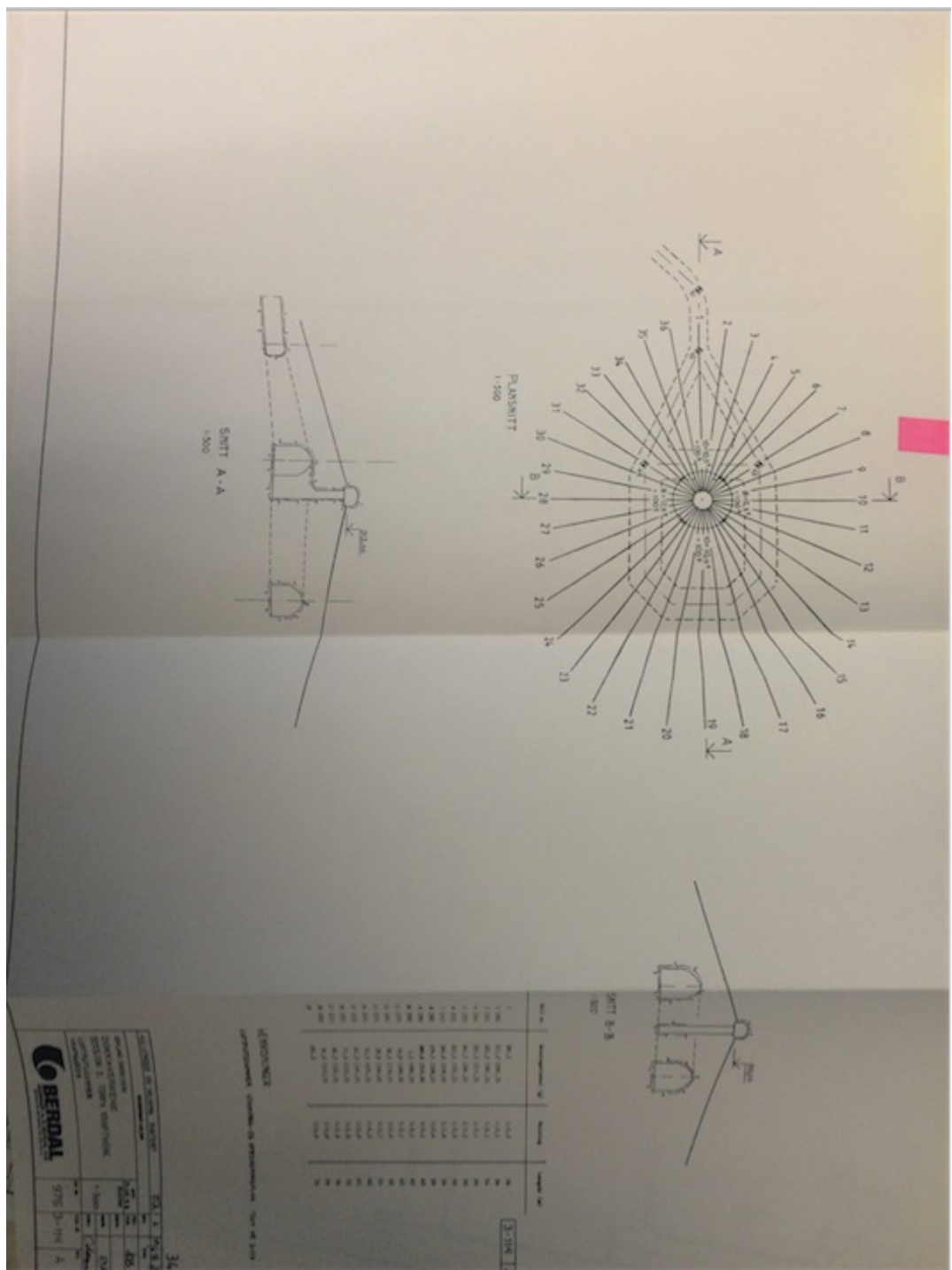
A.1 Torpa

| Name | Number | From |
|--|---------|---|
| Seksjon 3 Torpa Kraftverk, Lengdesnitt | 3-116 | Berdal Strømme Rådgivende Ingeniører |
| Seksjon 3 Torpa Kraftverk, Luftputekammer, Vanngardin | 3-114 A | Ingeniør A.B. Berdal A/S |
| Seksjon 3 Torpa Kraftverk, Luftputekammer, Stiknings- og sprengningsplan | 3-113 E | Ingeniør A.B. Berdal A/S |

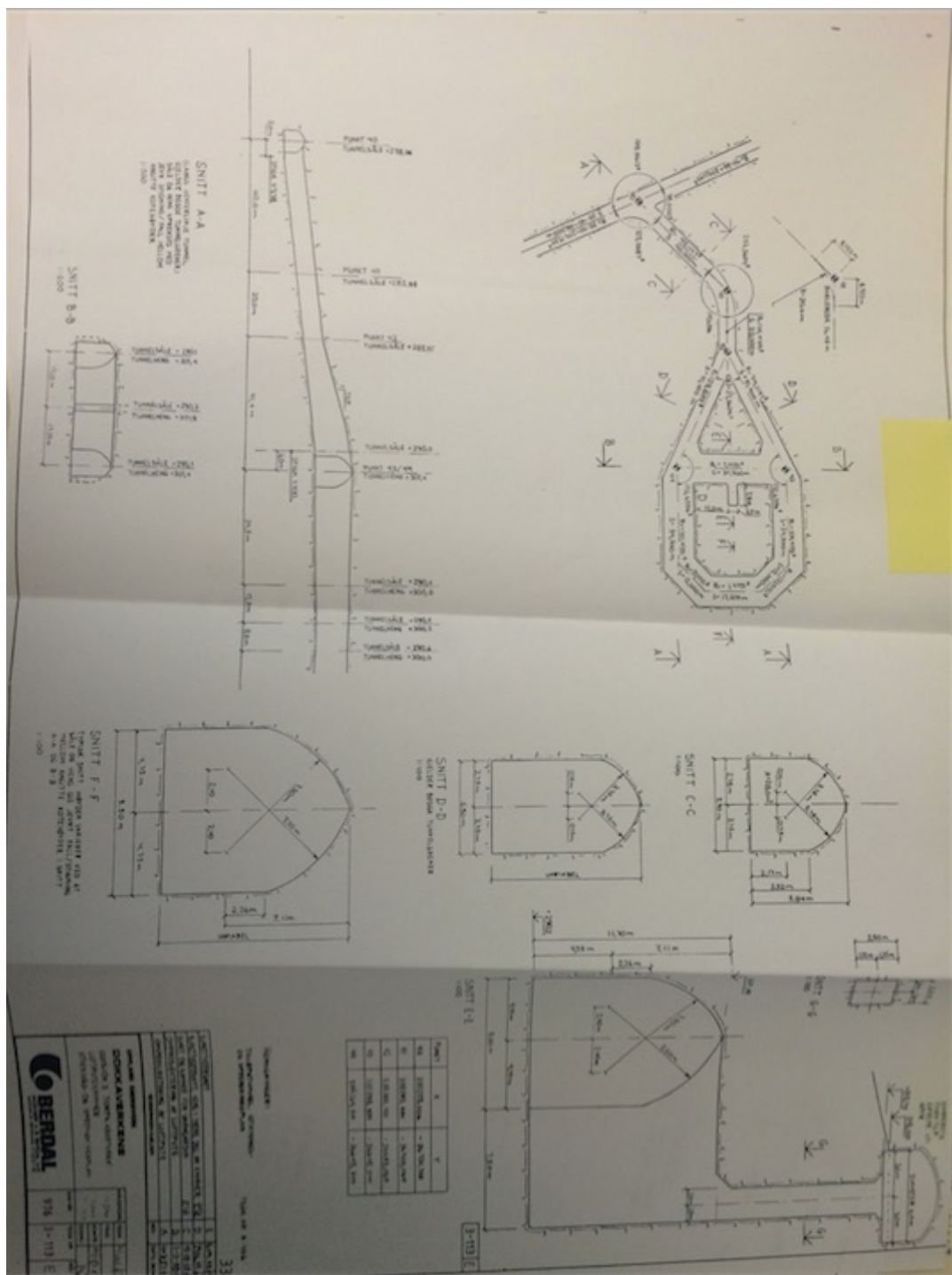
Chapter A. Construction drawings



A.1 Torpa



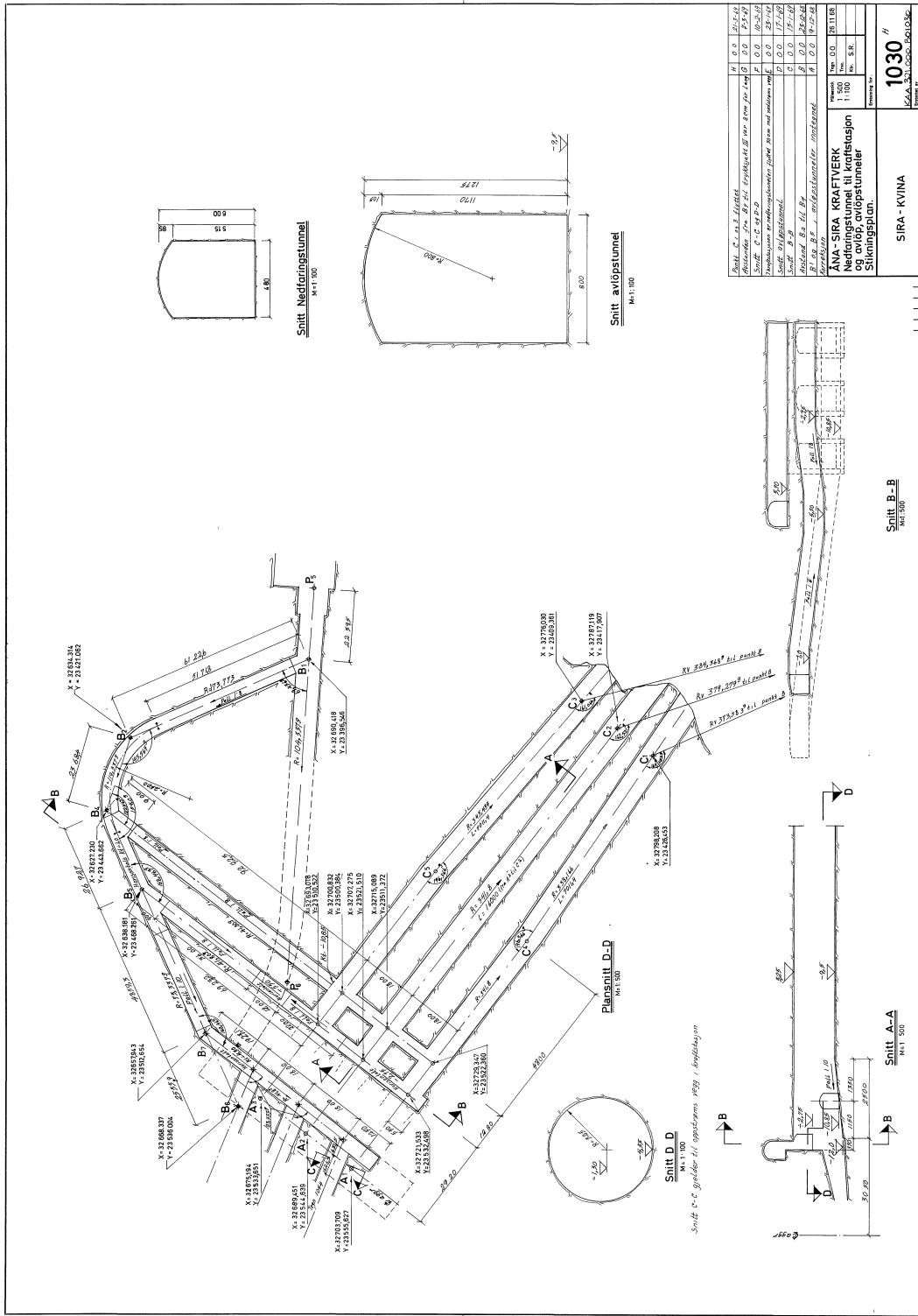
Chapter A. Construction drawings



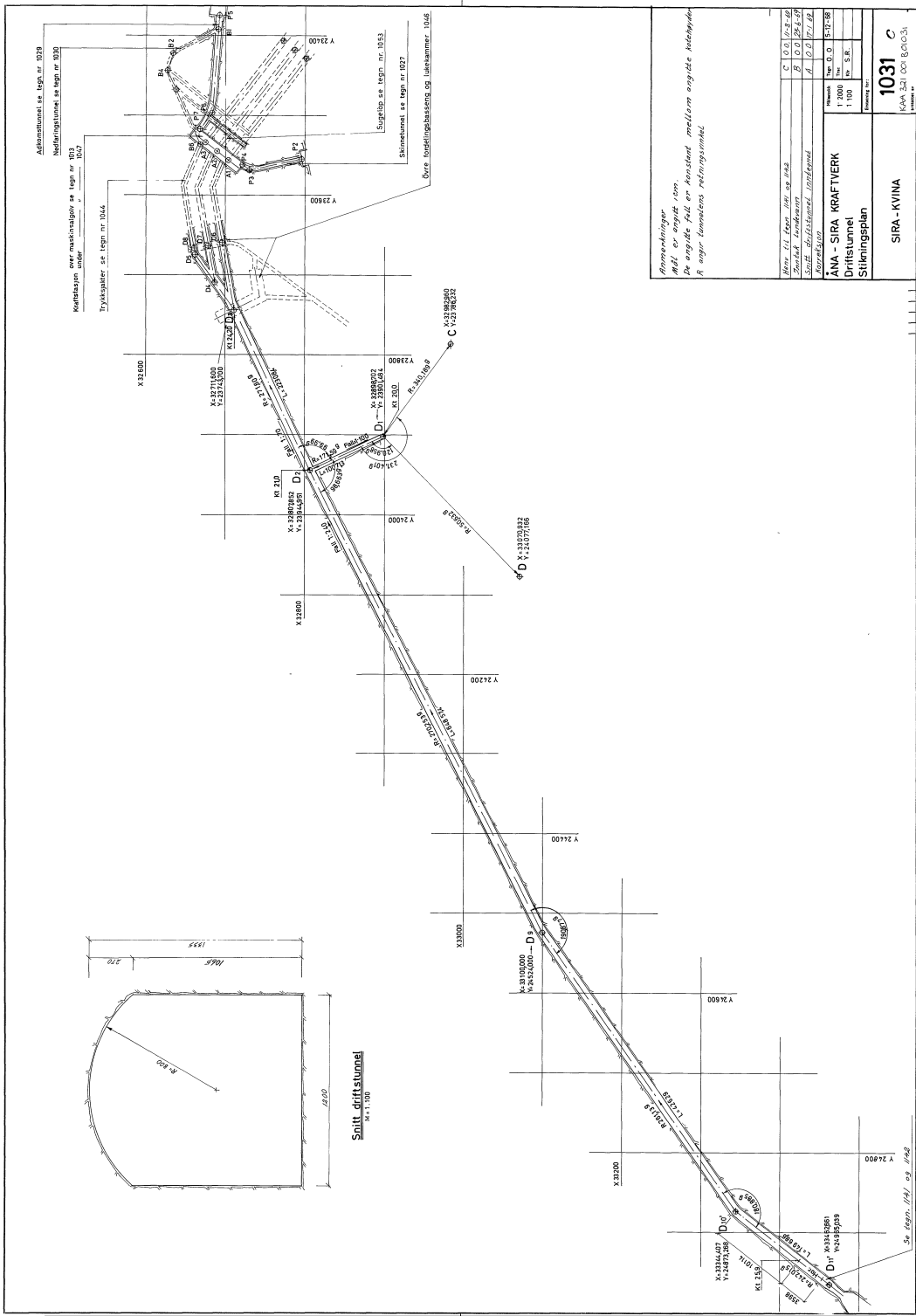
A.2 Åna-Sira

| Name | Number | From |
|---|----------------------------------|---------------------------------|
| Nedfaringstunnel til kraftstasjon og avløp, avløpstunneler, Stikningsplan | 1030H, KAA.321.000 .B01030 | Sira-Kvina Kraftsel- skap |
| Driftstunnel, Stikningsplan | 1031C, KAA.321.000 .B01031 | Sira-Kvina Kraftsel- skap |
| TRYKKSJAKTER, Stikning, sprengning | 1044B, KAA.323.000. B01044 | Sira-Kvina Kraftsel- skap |
| Øvre fordelingsbasseng, lukekammer. Stikning, sprengning. | 1046D, KAA.322.001. B01046 | Sira-Kvina Kraftsel- skap |
| Øvre fordelingsbasseng, Hvelv over driftstunnel, Forskaling, armering | 1116, KAA.322.001. B01116 | Sira-Kvina Kraftsel- skap |
| Driftstunnel, Inntak Lundevann, Sprengning - snitt | 1142C, KAA.321.001. B01142 | Sira-Kvina Kraftsel- skap |
| Betongdekke i adkomsttunnel til lukekammer topp trykksjakter, Propper mot øvre svingekammer | 1453, KAA.321.021. B01453 | Sira-Kvina Kraftsel- skap |

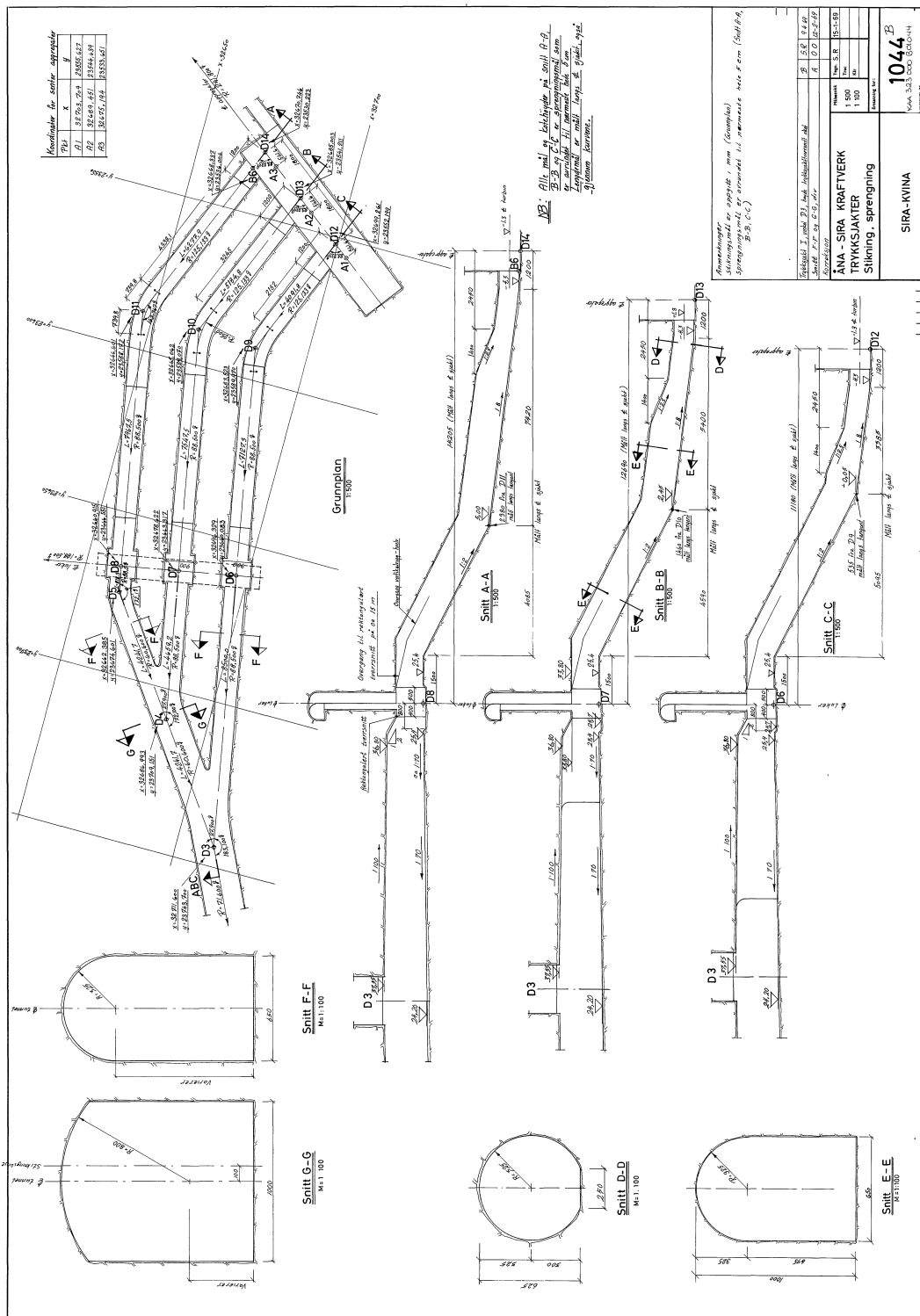
Chapter A. Construction drawings



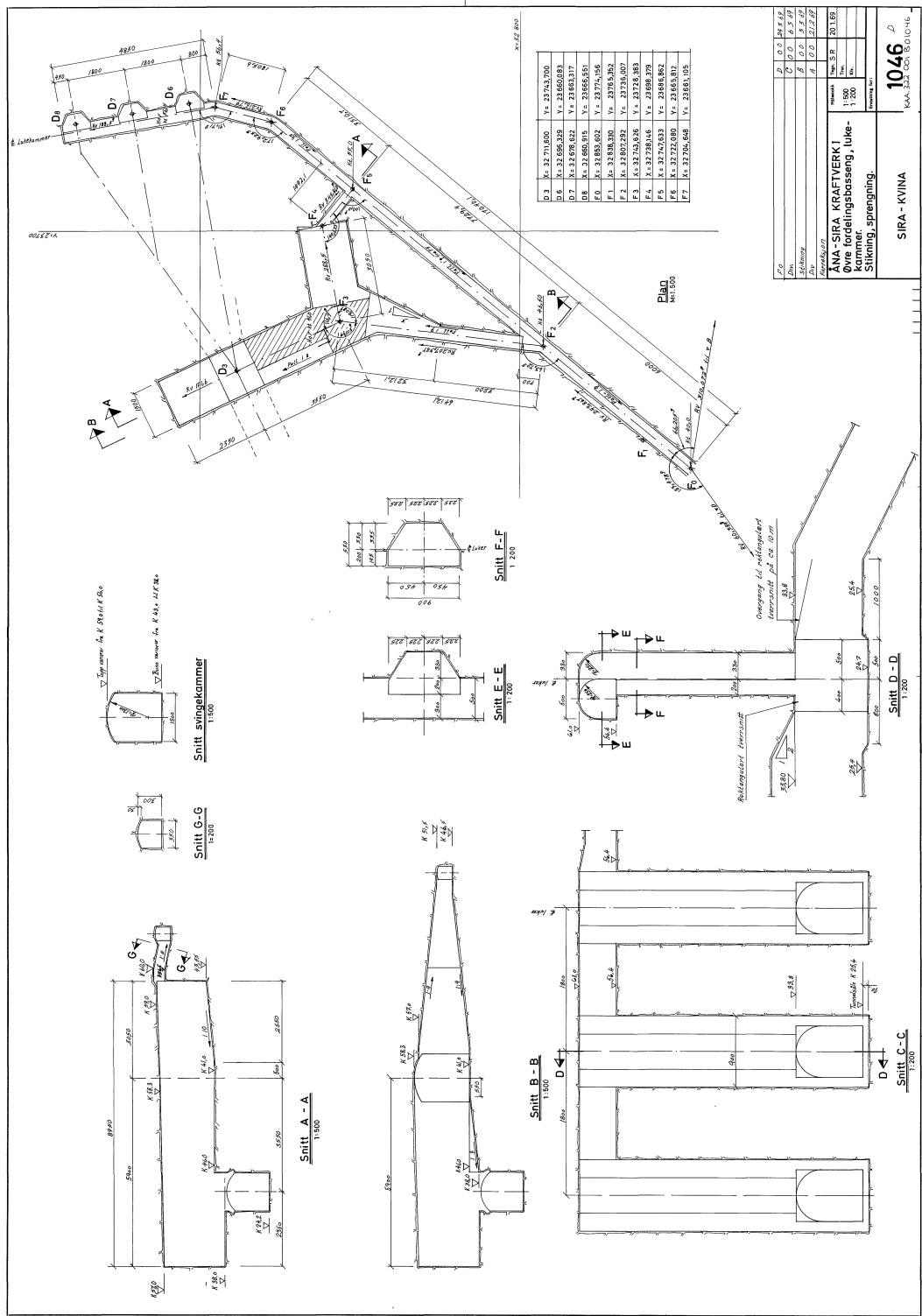
A.2 Åna-Sira



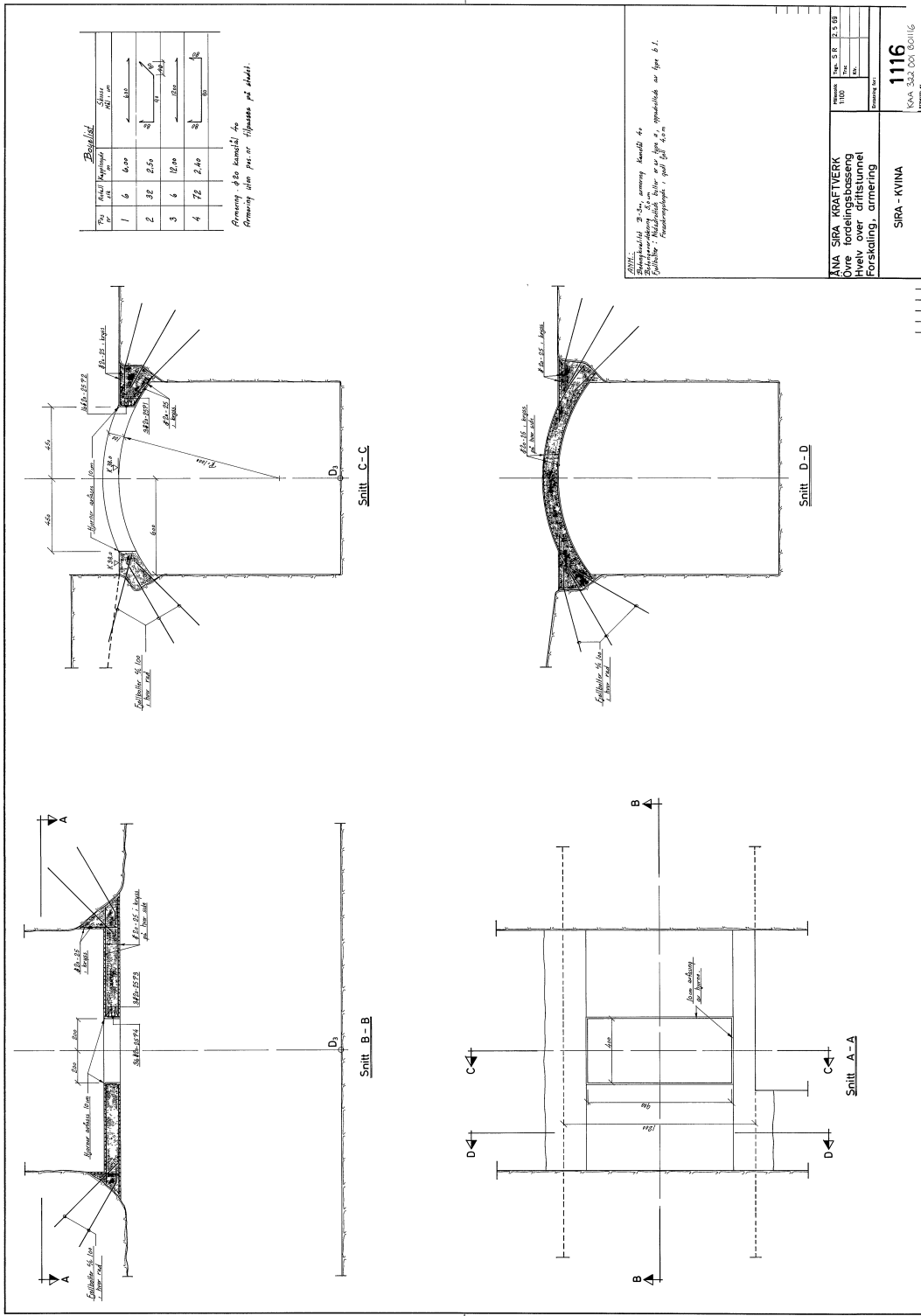
Chapter A. Construction drawings

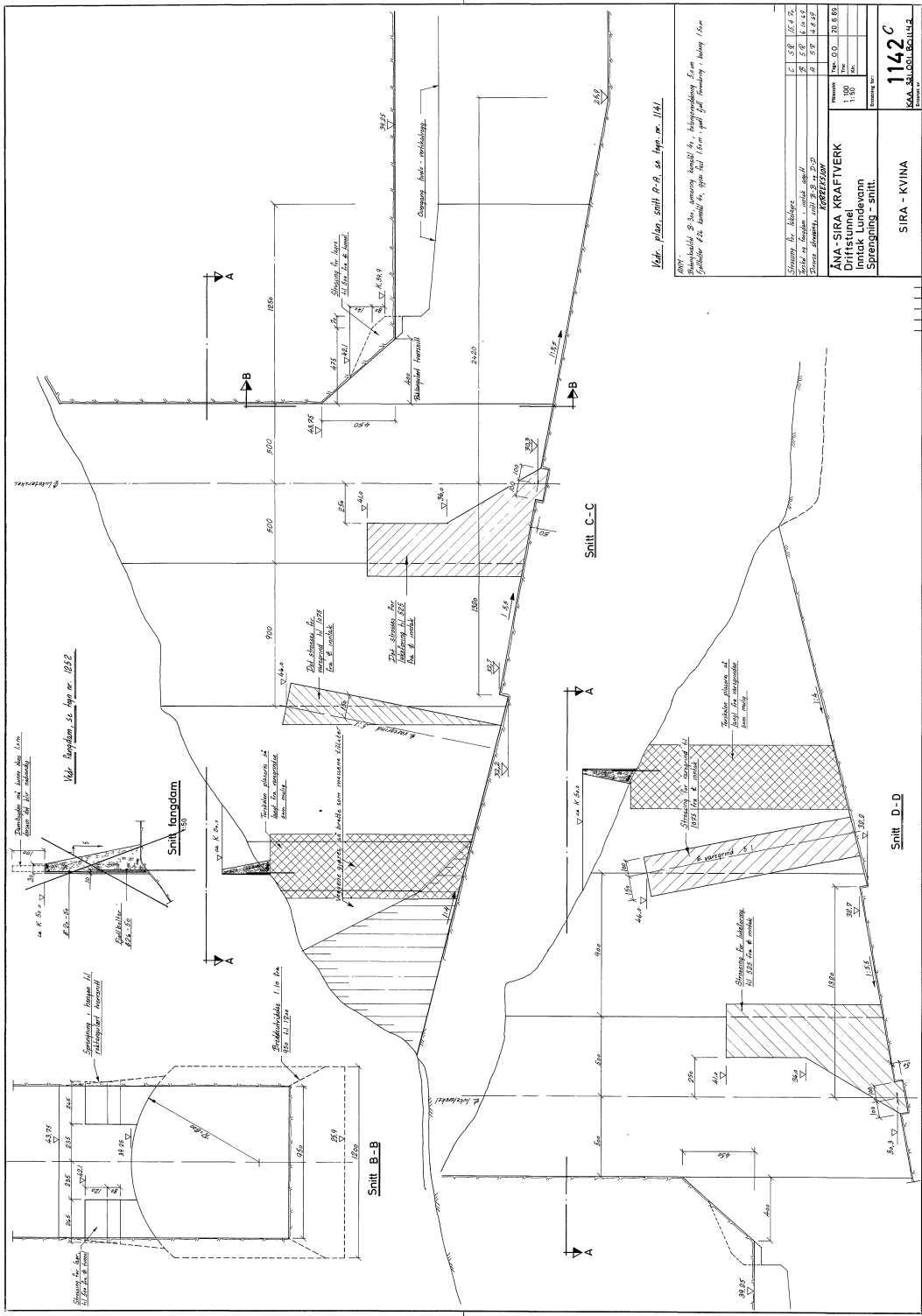


A.2 Åna-Sira

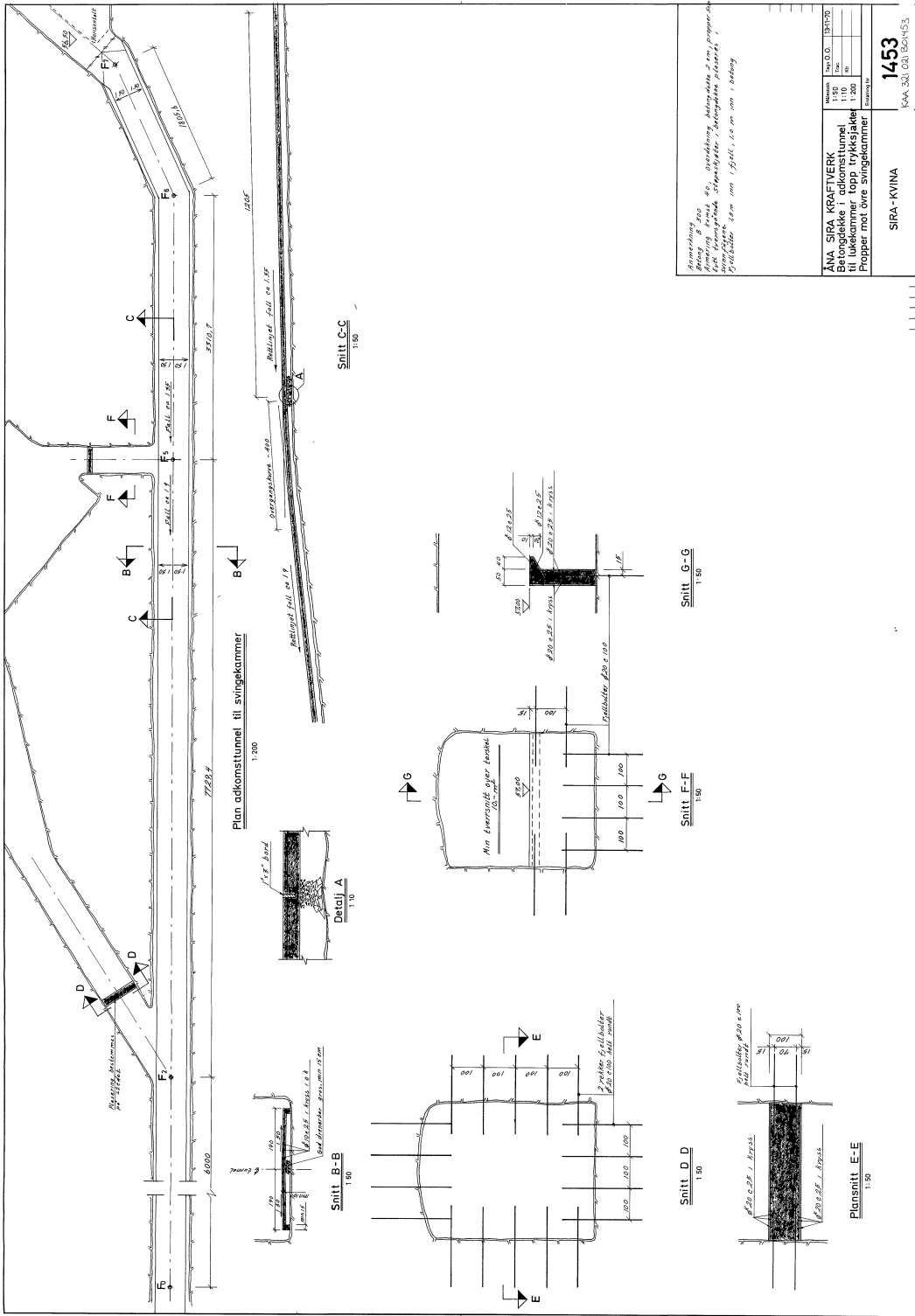


Chapter A. Construction drawings





Chapter A. Construction drawings



Appendix B

LVTrans script for differential surge tank

Note: The script was tried in LVTrans, but it did not succeed. This is how far the code was written.

```

float64 Cv, L0, A, A0, dA, dQ, dL, Ba, Ca, Sb, Sc, dF, F, Ha, dHa, Q0, Q_outer, Qdiff0, D, Hb0, dHb;
float64 g = 9.82;
float64 eps = 0.00001;
float64 epsL = 0.01;
int32 N = 0;
Sc = Cp1/Bp1 + Cm2/Bm2;
Sb = 1.0/Bp1 + 1.0/Bm2;
Ca = Sc/Sb;
Ba = 1.0/Sb;

Q0 = Q;
L0 = L;
Qdiff0 = Qdiff;
Hb0 = Hb;
L = 2.0*L - L00;
if (Lout <= Llim) Lout=Llim;
if (Lout < 1.000001*Llim) Lout=Llim;
Lout_0 = Lout;

// Finner A(L0)
if (L0 <= L_h[0]) A0 = A_h[0];
else if ((L0 >= L_h[0]) && (L0 < L_h[1])) A0 = dA_h[1]*(L0 - L_h[0]) + A_h[0];
else if ((L0 >= L_h[1]) && (L0 < L_h[2])) A0 = dA_h[2]*(L0 - L_h[1]) + A_h[1];
else if ((L0 >= L_h[2]) && (L0 < L_h[3])) A0 = dA_h[3]*(L0 - L_h[2]) + A_h[2];
else if ((L0 >= L_h[3]) && (L0 < L_h[4])) A0 = dA_h[4]*(L0 - L_h[3]) + A_h[3];
else if ((L0 >= L_h[4]) && (L0 < L_h[5])) A0 = dA_h[5]*(L0 - L_h[4]) + A_h[4];
else if ((L0 >= L_h[5]) && (L0 < L_h[6])) A0 = dA_h[6]*(L0 - L_h[5]) + A_h[5];
else if ((L0 >= L_h[6]) && (L0 < L_h[7])) A0 = dA_h[7]*(L0 - L_h[6]) + A_h[6];
else if ((L0 >= L_h[7]) && (L0 < L_h[8])) A0 = dA_h[8]*(L0 - L_h[7]) + A_h[7];
else if ((L0 >= L_h[8]) && (L0 < L_h[9])) A0 = dA_h[9]*(L0 - L_h[8]) + A_h[8];
else if (L0 >= L_h[9]) A0 = A_h[9];

```

```

do {
    // Finner A(L) og dA
    if (L <= L_h[0]) {A = A_h[0]; dA = dA_h[0];}
    else if ((L >= L_h[0]) && (L < L_h[1])) {A = dA_h[1]*(L - L_h[0]) + A_h[0]; dA = dA_h[1];}
    else if ((L >= L_h[1]) && (L < L_h[2])) {A = dA_h[2]*(L - L_h[1]) + A_h[1]; dA = dA_h[2];}
    else if ((L >= L_h[2]) && (L < L_h[3])) {A = dA_h[3]*(L - L_h[2]) + A_h[2]; dA = dA_h[3];}
    else if ((L >= L_h[3]) && (L < L_h[4])) {A = dA_h[4]*(L - L_h[3]) + A_h[3]; dA = dA_h[4];}
    else if ((L >= L_h[4]) && (L < L_h[5])) {A = dA_h[5]*(L - L_h[4]) + A_h[4]; dA = dA_h[5];}
    else if ((L >= L_h[5]) && (L < L_h[6])) {A = dA_h[6]*(L - L_h[5]) + A_h[5]; dA = dA_h[6];}
    else if ((L >= L_h[6]) && (L < L_h[7])) {A = dA_h[7]*(L - L_h[6]) + A_h[6]; dA = dA_h[7];}
    else if ((L >= L_h[7]) && (L < L_h[8])) {A = dA_h[8]*(L - L_h[7]) + A_h[7]; dA = dA_h[8];}
    else if ((L >= L_h[8]) && (L < L_h[9])) {A = dA_h[9]*(L - L_h[8]) + A_h[8]; dA = dA_h[9];}
    else if (L >= L_h[9]) {A = A_h[9]; dA = dA_h[10];}

    // Indre sjakt, L under Llim
    if (L <= Llim && Lout <= Llim) {
        dQ = (dA*(L - L0) + A + A0)/dt;
        Q = (A + A0)*(L - L0)/dt - Q0;
        if (Q < 0.0) Cv = Cvm; else Cv = Cvp;
        F = L + Z0 + Q*abs(Q)/(2.0*Cv) - Ca + Ba*Q;
        dF = 1.0 + dQ*(Ba + abs(Q)/Cv);
    };

    // Indre sjakt, L under Llim, når Lout > Llim
    if (L <= Llim && Lout > Llim) {
        dQ = Adiff*0.5*pow((2*g*(Lout-Llim)/kdiff),-0.5) + (dA*(L - L0) + A + A0)/dt;
        Q = Adiff*sqrt(2*g*(Lout-Llim)/kdiff) + Adiff*sqrt(2*g*(Lout_0-Llim)/kdiff) + (A + A0)*(L - L0)/dt - Q0;
        if (Q < 0.0) Cv = Cvm; else Cv = Cvp;
        F = L + Z0 + Q*abs(Q)/(2.0*Cv) - Ca + Ba*Q;
        dF = 1.0 + dQ*(Ba + abs(Q)/Cv);
    };
}

```

```

// Indre sjakt. L over Llim
if (L > Llim) {
    dQ = Adiff*0.5*pow((2*g*abs(L - Lout)/kdiff),-0.5) + (dA*(L - L0) + A + A0)/dt;
    Q = Adiff*sqrt(2*g*abs(Lout - L)/kdiff)*(Lout - L)/(abs(Lout - L)) + Adiff*sqrt(2*g*abs(Lout_0 - L0)/kdiff)*(Lout_0 - L0)/(abs(Lout_0 - L0)) + (A + A0)*(L - L0)/dt - Q0;
    if (Q < 0.0) Cv = Cvm; else Cv = Cvp;
    F = L + Z0 + Q*abs(Q)/(2.0*Cv) - Ca + Ba*Q;
    dF = 1.0 + dQ*(Ba + abs(Q)/Cv);
};

// Vann i ytre sjakt, tomt i indre
if (L < Llim && Lout > Llim) {
    Q = 2.0*A*(L-L0)/dt - Q0 - Qdiff - Qdiff0;
    if (Q >= 0.0) Cv = Cvp; else Cv = Cvm;
    if (L > epsL)
        Hb = (L + L0)*(Q - Q0)/(A*g*dt) + L + L0 + 2.0*Z0 + L0*Q0*abs(Q0)/(2*g*D*A*A) - Hb0;
    else Hb = L + Z0;
    Ha = Hb + Q*abs(Q)/(2.0*Cv);
    F = Ha - Ca + Ba*Q;

    dQ = 2.0*A/dt;
    if (L > epsL)
        dHb = (Q - Q0 + (L + L0)*dQ)/(A*g*dt) + 1.0 + L*2.0*abs(Q)*dQ/(2*g*D*A*A);
    else dHb = 1.0;
    dHa = dHb + abs(Q)*dQ/Cv;
    dF = dHa + Ba*dQ;
};

dL = -F/dF;
L = L + dL;
Qdiff = Adiff*sqrt(2*g*abs(Lout - L)/kdiff)*(Lout - L)/(abs(Lout - L));
Lout = max(Lout_0 - Qdiff/Aout, Llim);

```

```

N++;
}

while (abs(dL) > eps && N < 100);

// Finner A(L) og dA

if (L <= L_h[0]) A = A_h[0];
else if ((L >= L_h[0]) && (L < L_h[1])) A = dA_h[1]*(L - L_h[0]) + A_h[0];
else if ((L >= L_h[1]) && (L < L_h[2])) A = dA_h[2]*(L - L_h[1]) + A_h[1];
else if ((L >= L_h[2]) && (L < L_h[3])) A = dA_h[3]*(L - L_h[2]) + A_h[2];
else if ((L >= L_h[3]) && (L < L_h[4])) A = dA_h[4]*(L - L_h[3]) + A_h[3];
else if ((L >= L_h[4]) && (L < L_h[5])) A = dA_h[5]*(L - L_h[4]) + A_h[4];
else if ((L >= L_h[5]) && (L < L_h[6])) A = dA_h[6]*(L - L_h[5]) + A_h[5];
else if ((L >= L_h[6]) && (L < L_h[7])) A = dA_h[7]*(L - L_h[6]) + A_h[6];
else if ((L >= L_h[7]) && (L < L_h[8])) A = dA_h[8]*(L - L_h[7]) + A_h[7];
else if ((L >= L_h[8]) && (L < L_h[9])) A = dA_h[9]*(L - L_h[8]) + A_h[8];
else if (L >= L_h[9]) A = A_h[9];

// Indre sjakt, L under Llim
if (L <= Llim && Lout <= Llim) {
    Q = (A + A0)*(L - L0)/dt - Q0;
    if (Q < 0.0) Cv = Cvm; else Cv = Cvp;
};

// Indre sjakt, L under Llim, når Lout > Llim
if (L <= Llim && Lout > Llim) {
    Q = Adiff*sqrt(2*g*(Lout-Llim)/kdiff) + Adiff*sqrt(2*g*(Lout_0-Llim)/kdiff) + (A + A0)*(L - L0)/dt - Q0;
    if (Q < 0.0) Cv = Cvm; else Cv = Cvp;
};

// Indre sjakt. L over Llim
if (L > Llim) {

```

```

Q = Adiff*sqrt(2*g*abs(Lout - L)/kdiff)*(Lout - L)/(abs(Lout - L)) + Adiff*sqrt(2*g*abs(Lout_0
- L0)/kdiff)*(Lout_0 - L0)/(abs(Lout_0 - L0)) + (A + A0)*(L - L0)/dt - Q0;
if (Q < 0.0) Cv = Cvm; else Cv = Cvp;
};

// Vann i ytre sjakt, tomt i indre
if (L < Llim && Lout > Llim) {
    Q = 2.0*A*(L - L0)/dt - Q0 - Qdiff - Qdiff0;
    if (Q >= 0.0) Cv = Cvp; else Cv = Cvm;
    if (L > epsL) Hb = (L + L0)*(Q - Q0)/(A*g*dt) + L + L0 + 2.0*Z0 + L0*Q0*abs(Q0)/(2*g*D*A*A) -
Hb0;
    else Hb = L + Z0;
};

Hb = Z0 + L;
Ha = Hb + Q*abs(Q)/(2.0*Cv);
HPin = Ha;
HPup = Ha;
HPout = Ha;
QPin = (Cp1 - Ha)/Bp1;
QPout = (-Cm2 + Ha)/Bm2;
QPup = Q;
LP = L;
HLiqKote = Z0 + LP;
Qdiff = Adiff*sqrt(2*g*abs(Lout - L)/kdiff)*(Lout - L)/(abs(Lout - L));
Lout = Lout_0 - Qdiff/Aout;

```

Appendix C

Design and parameters in LV- Trans

| | | Simple Surge Tank, Torpa HPP | | | | | | | | | | |
|-------------------|--------|------------------------------|--------|-------------------|--------|----------------|--------|-------------------|---------|------------|------|-------------|
| Upper Magazine | | Headrace tunnel | | Simple surge tank | | Pressure shaft | | Pressure tunnel 1 | | Turbine | PID | |
| H0 | 706,1 | L | 9320 | H0 | 708 | L | 452 | L | 200 | Or | 35 | Pr |
| Cvp | 100000 | D | 6,7 | D | 13 | D | 6 | D | 5 | Hr | 430 | Nr |
| Cvm | 100000 | f | 0,07 | f | 0,07 | f | 0,04 | f | 0,04 | Hr_design | 430 | SP_Power |
| Lambda | 500000 | Cvp | 100000 | Lambda | 100000 | Lambda | 500000 | Lambda | 375 | P_n_grid | 150 | Td_n_grid |
| rho | 1000 | Cvm | 100000 | rho | 1000 | rho | 1000 | rho | 3564003 | Tl_n_grid | 8 | P_n_island |
| a | 1200 | | a | a | 1200 | a | 1200 | a | 3564003 | Tl_n_grid | 0 | P_n_island |
| DH? | FALSE | | DH? | FALSE | DH? | FALSE | DH? | FALSE | 9,2 | P_n_island | 3 | Tl_n_island |
| Areal | 0 | | Areal | 0 | Areal | 0 | Areal | 0 | 55,6 | P_n_island | 8 | P_n_island |
| P | 0 | | P | 0 | P | 0 | P | 0 | 1,708 | P_n_island | 0 | P_n_island |
| Z0 | 670 | | Z0 | 670 | Z0 | 670 | Z0 | 670 | 1,019 | Tl_power | 100 | Tl_power |
| Z1 | 670 | | Z1 | 256 | Z1 | 256 | Z1 | 256 | 6 | T_ramp | 60 | T_ramp |
| Q0 | 35 | | Q0 | 35 | Q0 | 35 | Q0 | 35 | 0,1 | Rp_droop | 0,06 | Rp_droop |
| H0 | 708 | | H0 | 708 | H0 | 708 | H0 | 708 | 0 | T_close_hi | 10 | T_close_low |
| Pressure tunnel 2 | | Outlet 1 | | Lower Surge Tank | | Outlet 2 | | Lower Magazine | | Rm | | |
| L | 30 | L | 200 | H0 | 265 | L | 9950 | H0 | 265 | Rd | 0,04 | T_open_hi |
| D | 2,5 | D | 6,7 | D | 33 | D | 6,7 | Cvp | 100000 | eta_h | 0,93 | T_open_hi |
| f | 0,015 | f | 0,07 | f | 0,07 | f | 0,07 | Cvm | 100000 | eta_r | 0,92 | kap_change |
| Lambda | 500000 | Lambda | 500000 | Cvp | 100000 | Lambda | 500000 | Lambda | Nturb | 1 | a | 0,5 |
| rho | 1000 | rho | 1000 | Cvm | 100000 | rho | 1000 | rho | Poles | 16 | b | 1 |
| a | 1200 | a | 1200 | Cvm | 100000 | a | 1200 | a | D_grid | 0 | c | 0 |
| DH? | FALSE | DH? | FALSE | DH? | FALSE | DH? | FALSE | DH? | delta_r | 0,7854 | | |
| Areal | 0 | Areal | 0 | Areal | 0 | Areal | 0 | Areal | F_grid | 50 | | |
| P | 0 | P | 0 | P | 0 | P | 0 | P | eve_mod | 0,2 | | |
| Z0 | 256 | Z1 | 251,5 | Z1 | 251,5 | Z1 | 251,5 | Z1 | | | | |
| Z1 | 256 | Z1 | 35 | Z0 | 35 | Z0 | 35 | Z0 | | | | |
| Q0 | 35 | Q0 | 265 | H0 | 265 | H0 | 265 | H0 | | | | |
| H0 | 708 | H0 | | | | | | | | | | |

Table C.1: LVTrans data for the SST at Torpa HPP.

| Two Chamber Surge Tank, Torpa HPP | | | | | | | | | | | |
|-----------------------------------|-------------------------|------------------|----------------|-------------------|-------------------|---------------------|-----------------------|------|--|--|--|
| Upper Magazine | Headrace tunnel | Two chamber | Pressure shaft | Pressure tunnel 1 | Pressure tunnel 2 | Turbine | | PID | | | |
| H_0 | 706,1 L | 9320 Cv_p | 100000 L | 452 L | 200 L | 30 Q_f | 430 N_r | 150 | | | |
| Cv_p | 100000 D | 6,7 Cvn | 100000 D | 6 D | 5 D | 2,5 H_r | 430 SP_Power | | | | |
| Cvn | 100000 f | 0,07 H_0 | 708 f | 0,04 f | 0,04 f | 0,015 H_r_design | 430 P_n_grid | 150 | | | |
| Λ | Λ | 500000 B_with | 10 Λ | 500000 Λ | 500000 Λ | 500000 N_r | 375 Tl_n_grid | 3 | | | |
| ρ_h | 10000 C_cnst | 1,8 ρ_h | 10000 ρ_h | 1000 ρ_h | 1000 ρ_h | 1000 Tr | 3564003 Td_n_grid | 8 | | | |
| a | 1200 L_weir | 10000 a | 1200 a | 1200 a | 1200 a | 1200 Fr | 3564003 Td_n_grid | 0 | | | |
| $DH?$ | FALSE LO | 0 $DH?$ | 0 $DH?$ | 0 $DH?$ | 0 $DH?$ | 0 $b1r(deg)$ | 9,2 P_n_island | 3 | | | |
| $Areal$ | 0 L_1 | 6,6 $Areal$ | 0 $Areal$ | 0 $Areal$ | 0 $Areal$ | 0 $r1$ | 55,6 P_n_island | 8 | | | |
| P | 0 L_2 | 6,7 P | 0 P | 0 P | 0 P | 0 $r1$ | 1,708 P_n_island | 0 | | | |
| 20 | 670 L_3 | 21 Z_1 | 670 Z_1 | 256 Z_1 | 256 Z_1 | 256 Tq | 1,019 Tl_power | 100 | | | |
| Z_1 | 670 L_4 | 22 Z_1 | 256 Z_1 | 256 Z_1 | 256 Z_1 | 256 Tq | 6 T_ramp | 60 | | | |
| Q_0 | 35 L_5 | 26 Q_0 | 35 Q_0 | 35 Q_0 | 35 Q_0 | 35 Twt | 0,1 Rp_droop | 0,06 | | | |
| H_0 | 708 L_6 | 27 H_0 | 708 H_0 | 708 H_0 | 708 H_0 | 708 Rq | 0 T_close_hi | 10 | | | |
| Outlet 1 | | | | | | | | | | | |
| L | Lower Surge Tank | | | | | | | | | | |
| D | 200 H_0 | 265 L_8 | 36 L | 9950 H_0 | 265 L | Rm | 0,05 T_close_lo | 10 | | | |
| f | 6,7 D | 33 L_9 | 40 D | 6,7 Cv_p | 100000 Cv_m | Rd | 0,04 T_open_hi | 10 | | | |
| Λ | 0,07 f | 0,07 A_0 | 5000 f | 0,07 Cv_m | 100000 Cv_m | eta_h | 0,93 T_open_hi | 10 | | | |
| ρ_h | 500000 Cvn | 100000 A_1 | 5000 Λ | 500000 Λ | 500000 Λ | eta_r | 0,92 kap_chang | 0,5 | | | |
| a | 1200 Cvn | 10000 A_2 | 10 ρ_h | 1000 ρ_h | 1000 ρ_h | $Nurb$ | 1 a | 0 | | | |
| $DH?$ | FALSE | A3 | 10 a | 1200 a | 1200 a | $Poles$ | 16 b | 1 | | | |
| $Areal$ | 0 | A4 | 200 $DH?$ | 200 $DH?$ | 200 $DH?$ | D_grid | 0 c | 0 | | | |
| P | 0 | A5 | 200 $Areal$ | 0 $Areal$ | 0 $Areal$ | $delta_r$ | 0,7854 | | | | |
| 20 | 256 | A6 | 10 P | 0 P | 0 P | F_grid | 50 | | | | |
| Z_1 | 251,5 | A7 | 10 Z_0 | 251,5 | 251,5 | eve_mod | 0,2 | | | | |
| Q_0 | 35 | A8 | 200 Z_1 | 251,5 | 35 | | | | | | |
| H_0 | 265 | A9 | 200 Q_0 | 708 H_0 | 265 H_0 | | | | | | |
| Outlet 2 | | | | | | | | | | | |
| Lower Magazine | | | | | | | | | | | |

Table C.2: LVTrans data for the 2CST at Torpa HPP.

| Differential Surge Tank, Torpa HPP | | | | | | | | | |
|------------------------------------|-----------------|--------------------------|-------------------|-------------------|----------------|-------------------------|--------|---------------------|---------------|
| Upper Magazine | Headrace tunnel | Differential Tank | Connection tunnel | Simple surge tank | Pressure shaft | Turbine | | PID | |
| H_0 | 708,2 | L | 9320 | H_0 | 708 | L | 452 | Q_r | 35 |
| C_{vp} | 100000 | D | 6,7 | D | 12 | D | 4 | H_r | 430 |
| C_{vm} | 100000 | f | 0,07 | f | 0,07 | f | 0,04 | H_r _design | SP_Power |
| ρ_m | | Lambda | 500000 | C_{vp} | 250 | Lambda | 500000 | N_r | 150 |
| ρ_a | | ρ_m | 1000 | C_{vm} | 1000 | ρ_m | 100000 | T_r | 375 |
| a | | a | 1200 | | ρ_m | a | 1200 | E_r | 3 |
| $DH?$ | FALSE | | | | $DH?$ | | FALSE | $\alpha_1(r/\deg)$ | 3564003 |
| $Areal$ | 0 | | | | $Areal$ | | 0 | $\theta_{bir}(deg)$ | T_d,n_grid |
| P | 0 | | | | P | | 0 | r_1 | 9,2 |
| Z_0 | 670 | Z1 | 670 | Z_1 | 670 | Z1 | 20 | P_{n_island} | 5,6 |
| Q_0 | 35 | Q0 | 35 | Q_0 | 35 | Q0 | 35 | P_{n_island} | 1,708 |
| H_0 | 708 | H_0 | 708 | H_0 | 708 | R_q | 0,1 | $T_{l,power}$ | 1,019 |
| Pressure tunnel 1 | | Pressure tunnel 2 | | Outlet 1 | | Lower Surge Tank | | Outlet 2 | |
| L | 200 | L | 30 | H_0 | 200 | L | 9950 | R_m | 0,05 |
| D | 5 | D | 2,5 | D | 6,7 | D | 6,7 | η_d | 10 |
| f | 0,04 | f | 0,015 | f | 0,07 | f | 0,07 | η_a,h | 0,93 |
| λ | 500000 | Lambda | 500000 | Lambda | 500000 | C_{vp} | 100000 | $\eta_{eta,r}$ | 0,92 |
| ρ_h | 1000 | ρ_m | 1000 | ρ_m | 1000 | C_{vm} | 100000 | Nurb | 0,5 |
| a | 1200 | a | 1200 | a | 1200 | | 1000 | Poles | 1 |
| $DH?$ | FALSE | $DH?$ | FALSE | $DH?$ | FALSE | $DH?$ | 1200 | D_{grid} | b |
| $Areal$ | 0 | $Areal$ | 0 | $Areal$ | 0 | $Areal$ | 0 | $\delta_{eta,r}$ | c |
| P | 0 | P | 0 | P | 0 | P | 0 | F_{grid} | 0,7854 |
| Z_0 | 256 | Z0 | 256 | Z0 | 251,5 | Z1 | 251,5 | e_{ve_mod} | 50 |
| Z_1 | 256 | Z1 | 256 | Z1 | 251,5 | Z1 | 251,5 | | 0,2 |
| Q_0 | 35 | Q0 | 35 | Q0 | 35 | Q0 | 35 | | |
| H_0 | 708 | H_0 | 708 | H_0 | 708 | R_q | 0,2 | | |

Table C.3: LVTrans data for the DST at Torpa HPP.

| Air Cushion Surge Tank, Torpa HPP | | | | | | | | | | | |
|-----------------------------------|--------|----------------------|------|-------------|----------------|-------------------|----------------|-------------------|-----------------|-----------------|---------|
| Upper Magazine | | Pressure tunnel 1 | | Air cushion | | Pressure tunnel 2 | | Pressure tunnel 3 | | Turbine | |
| H_0 | 706,1 | L | 9120 | P_{init} | 423 | L | 280 | Q_r | 70 | Q_r | PID |
| C_{vp} | 100000 | D | | 6,7 | P_{atm} | 10,3 | D | | 3 | H_r | 430 |
| C_{vm} | 100000 | f | | 0,04 | V_{init} | 17000 | f | | 0,015 | H_r | 430 |
| Λ | 500000 | Liq_kote_i | | 292,5 | \Lambdaambda | 500000 | \Lambdaambda | | 500000 | N_r | 375 |
| ρ_h | 1000 | A_W | | 1500 | ρ_h | 1000 | ρ_h | | 1000 | T_r | 150 |
| a | 1200 | A_f | | 2250 | a | 1200 | a | | 1200 | E_r | 375 |
| $DH?$ | FALSE | C_{vp} | | 100000 | $DH?$ | | | FALSE | $\alpha1r(deg)$ | 3564003 | 3 |
| $Areal$ | 0 | C_{vm} | | 100000 | $Areal$ | 0 | $Areal$ | | 0 | $b1r(deg)$ | 3564003 |
| P | 0 | TW_{init} | | 275 | P | 0 | P | | 0 | $r1$ | 3564003 |
| Z_0 | 670 | $T{A}_{init}$ | | 275 | Z_0 | 278 | Z_0 | | 259 | r^2 | 3564003 |
| Z_1 | 278 | TR_{init} | | 275 | Z_1 | 259 | Z_1 | | 256 | T_a | 3564003 |
| Q_0 | 35 | C | | 1,4 | Q_0 | 35 | Q_0 | | 35 | T_{wt} | 3564003 |
| H_0 | 708 | a | | 0,01 | H_0 | 708 | H_0 | | 708 | R_q | 3564003 |
| | b | | | 0,01 | | 2600 | | | | T_{close_hi} | 3564003 |
| | | ρ_{hof} | | | | 2600 | | | | T_{close_lo} | 3564003 |
| | | c_{pf} | | 800 | | | | | | T_{open_hi} | 3564003 |
| | | \Lambdaambda_{daf} | | 3 | | | | | | T_{open_lo} | 3564003 |
| Outlet 1 | | Lower Surge Tank | | Outlet 2 | | Lower Magazine | | Nturb | | | |
| L | 200 | H_0 | | 265 | L | 9950 | H_0 | 265 | | 1 | q |
| D | 6,7 | D | | 33 | D | 6,7 | C_{vp} | 100000 | | 16 | b |
| f | 0,07 | f | | 0,07 | f | 0,07 | C_{vm} | 100000 | | 0 | c |
| \Lambdaambda | 500000 | C_{vp} | | 100000 | \Lambdaambda | 500000 | | | | 0,7854 | |
| ρ_h | 1000 | C_{vm} | | 100000 | ρ_h | 1000 | | | | 50 | |
| a | 1200 | | | a | $DH?$ | | | 1200 | | 0,2 | |
| $DH?$ | FALSE | | | | $Areal$ | | FALSE | | | | |
| $Areal$ | 0 | | | | P | 0 | | | | | |
| P | 0 | | | | | 20 | | 251,5 | | | |
| Z_0 | 256 | | | | | Z_1 | | 251,5 | | | |
| Z_1 | 251,5 | | | | | Q_0 | | 35 | | | |
| Q_0 | 35 | | | | | | | | | | |
| H_0 | 265 | | | | | | | | | | |

Table C.4: LVTrans data for the ACST at Torpa HPP.

| Simple Surge Tank, Åna-Sira HPP | | | | | | | | | | |
|---------------------------------|--------|-----------------|--------|-----------------------|--------|-----------------|--------|----------------|----------|----------------|
| Upper Magazine | | Headrace tunnel | | Simple surge tank | | Pressure tunnel | | Turbine | | PID |
| H_0 | 46,85 | L | 1450 | H_0 | 48 | L | 50 | Q_r | 375 | Pr |
| C_{vp} | 100000 | D | 18 | D | 65 | D | 15 | H_r | 44 | Nr |
| C_{vm} | 100000 | f | 0,07 | f | 0,07 | f | 0,04 | H_r_desig | 44 | SP_Power |
| ρ_m | | λ_m | 500000 | C_{vp} | 100000 | λ_m | 500000 | N_r | 50 | P_n_grid |
| a | | ρ_m | 1000 | C_{vm} | 100000 | ρ_m | 1000 | T_r | 4,5 | 4,5 |
| $DH?$ | FALSE | | 1200 | | | a | 1200 | E_r | 29305342 | $T_d_n_grid$ |
| $Areal'$ | 0 | | | | | $DH?$ | FALSE | $a1r(deg)$ | 16,8 | P_n_island |
| P | 0 | | | | | $Areal'$ | 0 | $b1r(deg)$ | 69,9 | P_n_island |
| Z_0 | 20 | | 20 | | | P | 0 | r_1 | 4,098 | P_n_island |
| Z_1 | 21 | | 20 | | | Z_0 | -1 | r_2 | 4,323 | T_L_power |
| Q_0 | 375 | | | | | Z_1 | -1 | T_a | 6 | T_ramp |
| H_0 | 46 | | | | | Q_0 | 375 | Twt | 0,1 | R_p_droop |
| Pressure shaft | | Outlet 1 | | Lower Magazine | | Turbine | | PID | | |
| L | 21 | L | 100 | H_0 | 0 | R_m | 0,05 | T_close_lc | 10 | |
| D_f | 16 | D | 18 | C_{vp} | 100000 | R_d | 0,04 | T_open_h | 10 | |
| λ_m | 0,04 | f | 0,07 | C_{vm} | 100000 | η_{turb} | 0,93 | T_open_h | 10 | |
| ρ_m | 500000 | λ_m | 500000 | | | η_{turb} | 0,92 | kap_chan | 0,5 | |
| a | 1000 | ρ_m | 1000 | | | N_{turb} | 1 | a | 0 | |
| $DH?$ | 1200 | a | 1200 | | | $Poles$ | 120 | b | 1 | |
| $Areal'$ | FALSE | $DH?$ | FALSE | | | D_grid | 0 | c | 0 | |
| P | 0 | $Areal'$ | 0 | | | δ_{grid} | 0,7854 | | 50 | |
| Z_0 | 20 | P | 0 | | | F_grid | 0,2 | | | |
| Z_1 | -1 | Z_1 | -1 | | | eve_mod | | | | |
| Q_0 | 375 | Q_0 | -9,5 | | | | | | | |
| H_0 | 46 | H_0 | 0 | | | | | | | |

Table C.5: LVTrans data for the SST at Åna-Sira HPP.

| Two Chamber Surge Tank, Åna-Sira HPP | | | | | | | | | | | |
|--------------------------------------|--------|------------------|-------|-------------|----------|----------------|----------|-------------------|--------|----------------|-----------|
| Upper Magazine | | HeadTrace tunnel | | Two chamber | | Pressure shaft | | Pressure tunnel 1 | | Turbine | |
| H_0 | 46,8 | L | 1450 | Cup | 100000 | L | 21 | Q_f | 50 | P_f | 150 |
| Cup | 100000 | D | 18 | Cvm | 100000 | D | 16 | H_f | 15 | N_f | 50 |
| Cvm | 100000 | f | 0,07 | H_0 | 46 | f | 0,04 | H_f | 0,04 | S_f | 150 |
| $Lambda$ | 500000 | B_with | | 10 | $Lambda$ | 500000 | $Lambda$ | 500000 | N_f | 44 | n_grid |
| rho | 1000 | C_cnst | | 1,8 | rho | 1000 | rho | 1000 | Tr | 29305342 | T_f |
| a | 1200 | L_weir | | 100000 | a | 1200 | a | 1200 | Er | 29305342 | T_d |
| $DH?$ | FALSE | L_0 | 0 | $DH?$ | 0 | $DH?$ | FALSE | $a1r(deg)$ | 16,8 | P_n_island | 4,5 |
| $Areal$ | 0 | L_1 | 17,9 | $Areal$ | 0 | $Areal$ | 0 | $b1r(deg)$ | 69,9 | P_n_island | 8 |
| P | 0 | L_2 | 18 | P | 0 | P | 0 | $r1$ | 4,098 | P_n_island | 0 |
| 20 | 20 | L_3 | 19 | Z_0 | 20 | Z_0 | -1 | $r2$ | 4,323 | T_f | 10 |
| Z_1 | 20 | L_4 | 20 | Z_1 | -1 | Z_1 | -1 | T_a | 6 | T_ramp | 60 |
| Q_0 | 375 | L_5 | 24 | Q_0 | 375 | Q_0 | 375 | Twt | 0,1 | R_p_droop | 0,06 |
| H_0 | 46 | L_6 | 25 | H_0 | 46 | H_0 | 46 | Rq | 0 | T_close_hi | 10 |
| Pressure tunnel 2 | | Outlet 1 | | L7 | | Lower Magazine | | Rm | | T_close_lo | |
| L | 50 | L | 100 | L_8 | 28 | H_0 | 0 | Rd | 0,04 | T_open_hi | 10 |
| D | 15 | D | 18 | L_9 | 31 | Cvp | 100000 | eta_h | 0,93 | T_open_hi | 10 |
| f | 0,015 | f | 0,07 | A_0 | 50000 | Cvm | 100000 | eta_r | 0,92 | kap_chang | 0,5 |
| $Lambda$ | 500000 | B_with | | 500000 | A_1 | 5000 | | $Nturb$ | 1 | q | 0 |
| rho | 1000 | rho | 1000 | A_2 | 1300 | | | $Poles$ | 120 | b | 1 |
| a | 1200 | a | 1200 | A_3 | 1300 | | | D_grid | 0 | c | 0 |
| $DH?$ | FALSE | $DH?$ | FALSE | A_4 | 4000 | | | $delta_r$ | 0,7854 | | |
| $Areal$ | 0 | $Areal$ | 0 | A_5 | 4000 | | | F_grid | 50 | | |
| P | 0 | P | 0 | A_6 | 1300 | | | eve_mod | 0,2 | | |
| 20 | -1 | Z_0 | -1 | A_7 | 1300 | | | | | | |
| Z_1 | -1 | Z_1 | -9,5 | A_8 | 6000 | | | | | | |
| Q_0 | 375 | Q_0 | 375 | A_9 | 6000 | | | | | | |
| H_0 | 46 | H_0 | 0 | | | | | | | | |

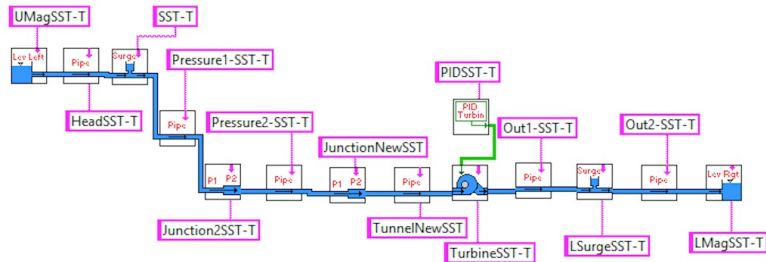
Table C.6: LVTrans data for the 2CST at Åna-Sira HPP.

| Upper Magazine | Headrace tunnel | Differential Tank | Differential Surge Tank, Ana-Sira HPP | Connection tunnel | Simple surge tank | Turbine | PID |
|----------------|-----------------|-------------------|---------------------------------------|-------------------|-------------------|-----------|-------------|
| H0 | 46,82 | L | 1450 | H0 | 48 | 708 | 375 |
| Cvp | 100000 | D | 18 | D | 50 | Or | Pr |
| Cvm | 100000 | f | 0,07 | f | 18 | 20 | 150 |
| | | Lambda | 500000 | Cvp | D | Hr | Nr |
| | | rho | 1000 | Cvm | 0,07 | 0,07 | SP_Power |
| a | 1200 | FALSE | rho | 5000 | Lambda | Hr_design | 150 |
| DH? | | | a | 500000 | Cvp | 50 | P_n_grid |
| Areal | 0 | | DH? | 100000 | Cvm | 100000 | 4,5 |
| P | 0 | | Areal | 100000 | Tr | Tr | 8 |
| Z0 | 20 | | P | 1200 | Er | 29305342 | Td_n_grid |
| Z1 | 20 | | Z0 | 20 | air(deg) | 29305342 | Td_n_grid |
| Q0 | 375 | | Z1 | 20 | b1r(deg) | 16,8 | P_n_island |
| H0 | 46 | | Q0 | 35 | r1 | 69,9 | P_n_island |
| | | | H0 | 708 | r2 | 4,098 | P_n_island |
| | | | | | Ta | 4,323 | Tl_power |
| | | | | | Twt | 6 | T_ramp |
| | | | | | Rq | 0,1 | Rp_droop |
| | | | | | Rm | 0 | T_close_hi |
| Pressure shaft | Pressure tunnel | Outlet 1 | Lower Magazine | | Rd | 0,05 | T_close_low |
| L | 21 | L | 100 | H0 | eta_h | 0,04 | T_open_hi |
| D | 16 | D | 50 | D | eta_r | 0,93 | T_open_hi |
| f | 0,04 | f | 15 | Cvp | Nturb | 0,93 | T_open_hi |
| Lambda | 500000 | Lambda | 0,015 | Cvm | Poles | 1 | a |
| rho | 1000 | rho | 0,07 | 100000 | D_grid | 120 | b |
| a | 1200 | a | 0,07 | 500000 | delta_r | 0 | c |
| DH? | FALSE | DH? | 1200 | 1000 | F_grid | 0,7854 | eve_mod |
| Areal | 0 | Areal | 1200 | 1200 | | 50 | |
| P | 0 | P | FALSE | 0 | | 0,2 | |
| Z0 | 20 | Z0 | 0 | 0 | | | |
| Z1 | -1 | Z1 | -1 | 0 | | | |
| Q0 | 375 | Q0 | -1 | -1 | | | |
| H0 | 46 | H0 | -9,5 | 375 | | | |
| | | | 375 | 0 | | | |
| | | | 0 | 0 | | | |

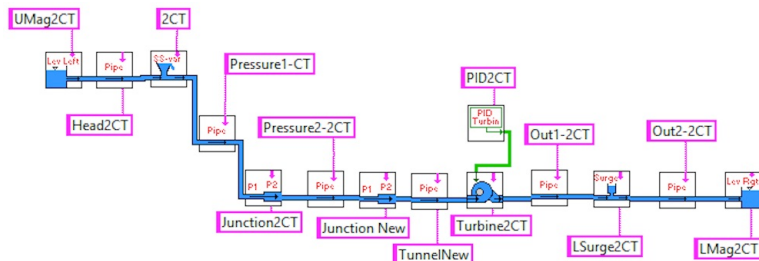
Table C.7: LVTrans data for the DST at Åna-Sira HPP.

| Air cushion surge tank, Åna-Sira HPP | | | | | | | | | |
|--------------------------------------|--------|-------------------|--------|-------------|--------|-------------------|----------|-------------|------|
| Upper Magazine | | Pressure tunnel 1 | | Air cushion | | Pressure tunnel 2 | | Turbine | |
| HO | 49,18 | L | 1450 | P_init | 25 | L | 60 | Qr | 375 |
| Cvp | 100000 | D | 15 | Parm | 10,3 | D | 14 | Nr | 44 |
| Cvm | 100000 | f | 0,07 | V_init | 90000 | f | 0,04 | SP_Power | 50 |
| Lambda | 500000 | Liq_kote_i | 33 | Lambda | 500000 | Nr | 50 | P_n_grid | 150 |
| rho | 1000 | Aw | 15000 | rho | 1000 | Tr | 29305342 | Tl_n_grid | 4,5 |
| a | 1200 | Af | 22500 | a | 1200 | Er | 29305342 | Td_n_grid | 0 |
| DH? | FALSE | Cvp | 100000 | DH? | FALSE | air(deg) | 16,8 | P_n_island | 4,5 |
| Areal | 0 | Cvm | 100000 | Areal | 0 | b1r(deg) | 69,9 | P_n_island | 8 |
| P | 0 | TWinit | 275 | P | 0 | r1 | 4,098 | P_n_island | 0 |
| Z0 | 24 | TAinit | 275 | Z0 | 3 | r2 | 4,323 | Tl_power | 10 |
| Z1 | 3 | TRinit | 275 | Z1 | 1 | Ta | 6 | T_ramp | 60 |
| Q0 | 375 | C | 1,4 | Q0 | 375 | Twt | 0,1 | Rp_droop | 0,06 |
| HO | 48 | a | 0,01 | HO | 48 | Rq | 0 | T_close_hi | 10 |
| b | b | rhof | 0,01 | | | Rm | 0,05 | T_close_low | 10 |
| cpf | 2600 | cpf | 2600 | | | Rd | 0,04 | T_open_hi | 10 |
| lambda | 800 | lambda | 3 | | | eta_h | 0,93 | T_open_hi | 10 |
| eta_r | | | | | | eta_r | 0,92 | kap_change | 0,5 |
| Nturb | | | | | | | 1 | a | 0 |
| Pressure tunnel 3 | | | | | | | | | |
| Outlet 1 | | Lower Magazine | | | | | | | |
| L | 120 | L | 20 | HO | 0 | | | | |
| D | 13 | D | 13 | Cvp | 100000 | | | | |
| f | 0,015 | f | 0,015 | Cvm | 100000 | | | | |
| Lambda | 500000 | Lambda | 500000 | | | | | | |
| rho | 1000 | rho | 1000 | | | | | | |
| a | 1200 | a | 1200 | | | | | | |
| DH? | FALSE | DH? | FALSE | | | | | | |
| Areal | 0 | Areal | 0 | | | | | | |
| P | 0 | P | 0 | | | | | | |
| Z0 | -1 | Z0 | 1 | | | | | | |
| Z1 | -9,5 | Z1 | -1 | | | | | | |
| Q0 | 375 | | | | | | | | |
| HO | 46 | | | | | | | | |
| Poles | 120 | b | | | | | | | |
| D_grid | | c | | | | | | | |
| delta_r | | 0 | | | | | | | |
| F_grid | | 0,7854 | | | | | | | |
| eve_mod | | 50 | | | | | | | |
| | | 0,2 | | | | | | | |

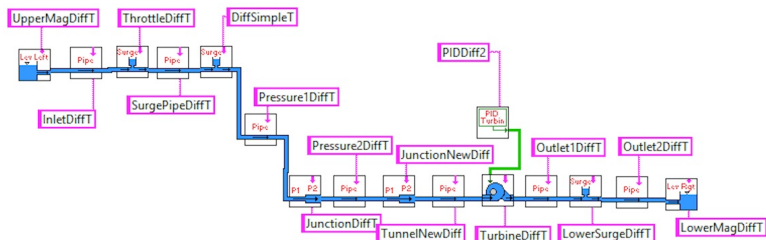
Table C.8: LVTrans data for the ACST at Åna-Sira HPP.



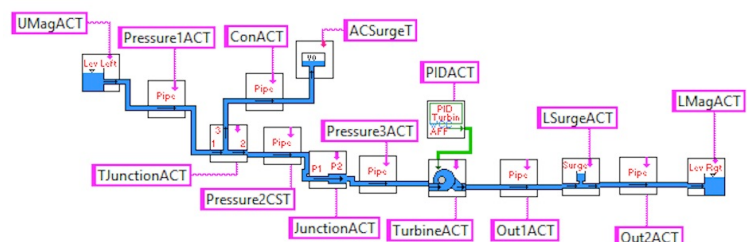
(a) SST at Torpa



(b) 2CST at Torpa



(c) DST at Torpa



(d) ACST at Torpa

Figure C.1: LVTrans designs for the surge tanks at Torpa HPP.

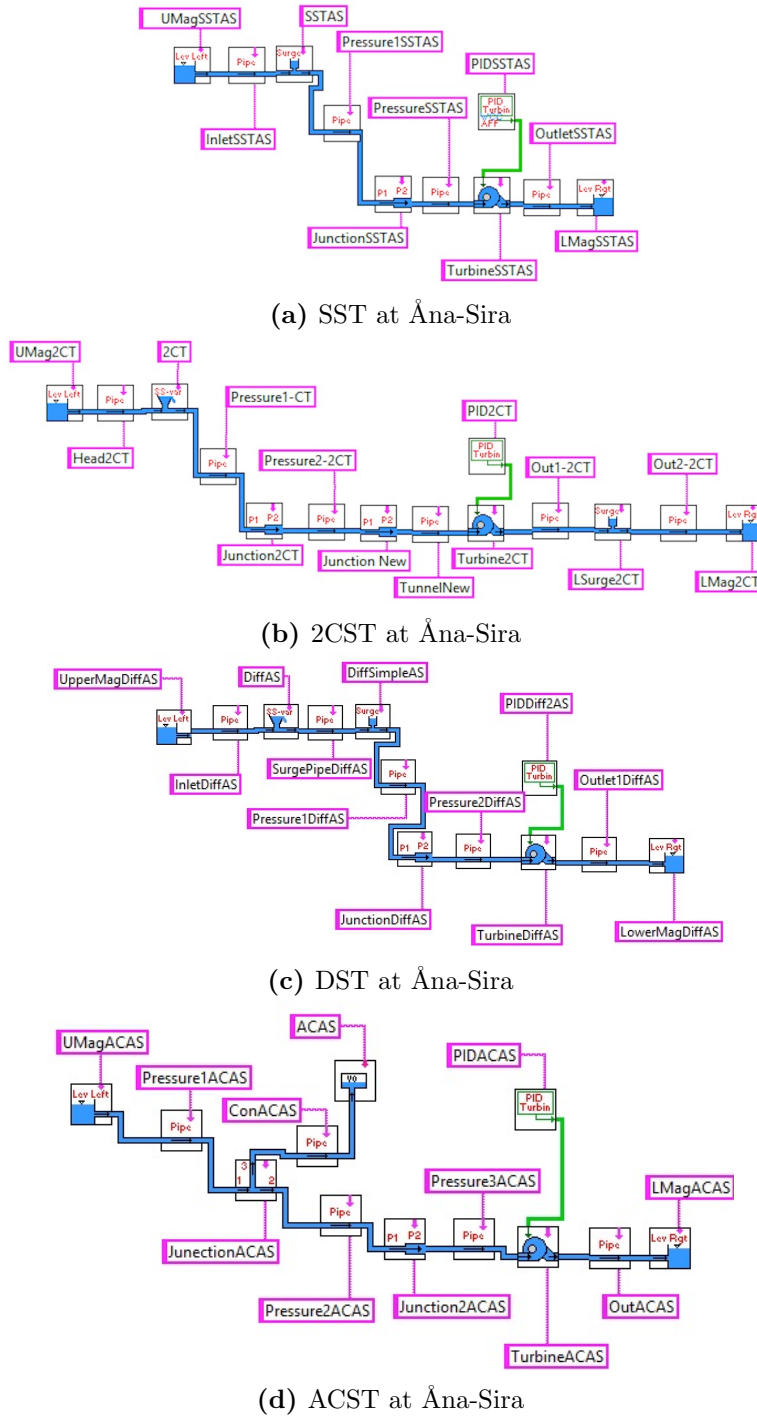


Figure C.2: LVTrans designs for the surge tanks at Åna-Sira HPP.